Spring 2021

The Drier Dryer

Daniel Anderson

Justin Lee

Thomas Morey

Josh Sunada

SANTA CLARA UNIVERSITY

Department of Mechanical Engineering

I HEREBY RECOMMEND THAT THE THESIS PREPARED
UNDER MY SUPERVISION BY

Daniel Anderson, Justin Lee, Thomas Morey, and Josh Sunada

ENTITLED

THE DRIER DRYER

BE ACCEPTED IN PARTIAL FULFILLMENT OF THE REQUIREMENTS
FOR THE DEGREE OF

BACHELORS OF SCIENCE

IN

MECHANICAL ENGINEERING

05/28/2021

Thesis Advisor: Dr. Hohyun Lee Date

6/10/21

Department Chair: Dr. Drazen Fabris Date

The Drier Dryer

By

Daniel Anderson, Justin Lee, Thomas Morey, and Josh Sunada

SENIOR DESIGN PROJECT REPORT

Submitted to

the Department of Mechanical Engineering

of

SANTA CLARA UNIVERSITY

in Partial Fulfillment of the Requirements

for the degree of

Bachelor of Science in Mechanical Engineering

Santa Clara, California

Spring 2021

The Drier Dryer

Daniel Anderson, Justin Lee, Thomas Morey, and Josh Sunada

Department of Mechanical Engineering
Santa Clara University
2021

ABSTRACT

With our product, The Drier Dryer, we aim to increase the efficiency of clothing dryers. This report contains an indepth look at the design approach we are taking to create our product. Our design utilizes a thermoelectric cooler combined with heat sinks and heat pipes to efficiently cool air to its dew point temperature and then reheat the air prior to sending it into a clothes dryer intake. Cooling the air to dew point temperature allows moisture to be removed from the air consequently decreasing the relative humidity. Throughout our design process we obtained simulation results providing a theoretical temperature the air needs to be cooled down to in order to remove moisture based on various design conditions. Our results showed that for conditions of 27 °C (80 °F) and 80% relative humidity, based on a design state of Hawaii, we require at least a 4 °C temperature difference across the cold side heat sink. Results from experimental testing in Santa Clara, CA on our two iterations of prototypes yielded a maximum temperature difference of approximately 2 °C. After applying our future plans to further idealize our prototype design as well as incorporating design conditions based on our simulation results, we aim to further increase our temperature difference allowing us to prove our theoretical results experimentally.

Keywords: Clothes Dryer, Dehumidify, Thermoelectric Module

Acknowledgements

The Dry Guys would like to thank Santa Clara University for funding our project and providing us with the education and inspiration necessary to bring our project to fruition. We would like to thank Professor Rodney Broome for allowing us to use his machine shop and for personally assisting our project's construction. Thank you to Matthew Blanco and Beverly Dutra for organizing purchases and reimbursement transfers for us. Thank you to Anne Hunter for coordinating the fulfillment of our maker lab projects. Finally, we would like to thank Dr. Timothy Hight, Dr. Tony Restivo, and Dr. Vlad Ivashyn for guiding us through our senior design journey with progress checks, milestone submissions, and constructive feedback.

Table of Contents

Table of Figures

Table of Tables

Chapter 1: Introduction

The objective of this project is to increase dryer efficiency. This thesis will therefore explore the motivation behind this endeavor, the research and technical equations that support the project's feasibility, the methods used to design and construct a system capable of increasing dryer efficiency, and an analysis of and response to the collected data. This introductory chapter examines the background of this project detailing the team's motivation and inspiration. It then reviews existing literature on the topic of thermoelectric module technology. Finally, it provides a high level overview of the project's objectives and goals.

1.1 Background

Clothes dryers consistently rank in the top three energy consuming household appliances, along with washing machines and refrigerators [1]. As depicted in Figure 1.1, one year of drying clothes with an electric dryer can cost an average of $250. At the same time, refrigerators, which operate around the clock, cost around $200 a year to run. Therefore, although using a clothes dryer is very convenient, it is also costly, even if it is used only a few times a week.

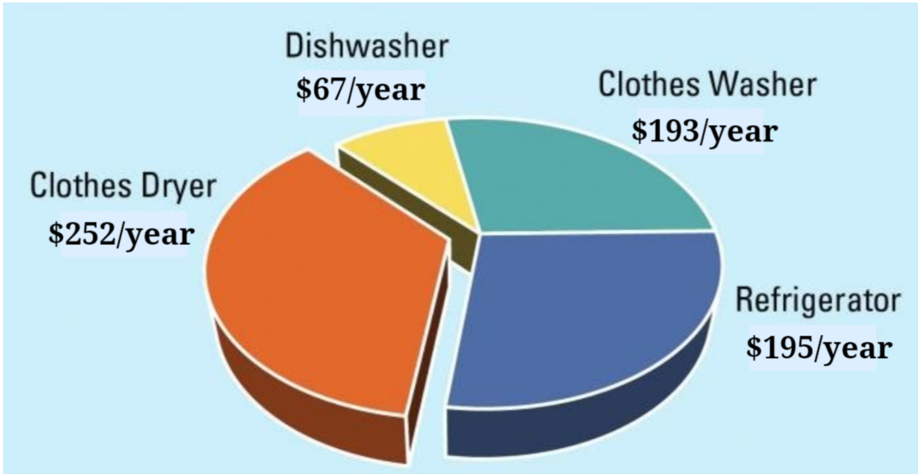

Figure 1.1: Cost of typical household appliances per year to operate based on the average HI electricity rate in 2020 of $0.3276/kWh [2]. Clothes dryers account for around 35% of the cost across all appliances listed.

There are many different makes and models of dryers, all with varying efficiencies. However, even running the same dryer in different weather conditions can drastically affect its cycle time [3]. Compared to drier climates, clothes-drying has always been inefficient in humid areas, from hanging clothes on a clothesline to using a mechanical clothes dryer. Our project, the Drier Dryer, stemmed from our team's interest in solving this problem. Having one member who lives in Honolulu, we understood first-hand how long clothes-drying can take, especially during rainy or hot, humid weather. Upon performing dryer performance tests in varying Honolulu temperatures and humidities, it was found that drying only five cotton t-shirts took at least 30 minutes to dry; on occasion this value exceeded 40 minutes (see Figure 1.2). Our team unanimously agreed that this was much too long to dry a few shirts and wanted to find a solution to aid others who are forced to dry clothes in similar conditions.

Figure 1.2: Five cotton t-shirts used in dryer tests. Drying these shirts in Honolulu consistently took 30-40 minutes.

After recalling knowledge from our thermodynamics and heat transfer classes, as well as from articles cited above, we found that there were two main factors that determined the time it took clothes dryers to dry clothes: temperature and relative humidity of the dryer intake air. We theorized that if we were able to decrease the intake air's relative humidity (since the dryer always increases its temperature), it would be able to remove more moisture from the wet clothes and shorten the overall cycle time. This makes sense intuitively as well. Figure 1.3 shows the relative humidity of air above some wet clothes. Evidently, the 95% humid air simply can't hold nearly as much water as the 10% air.

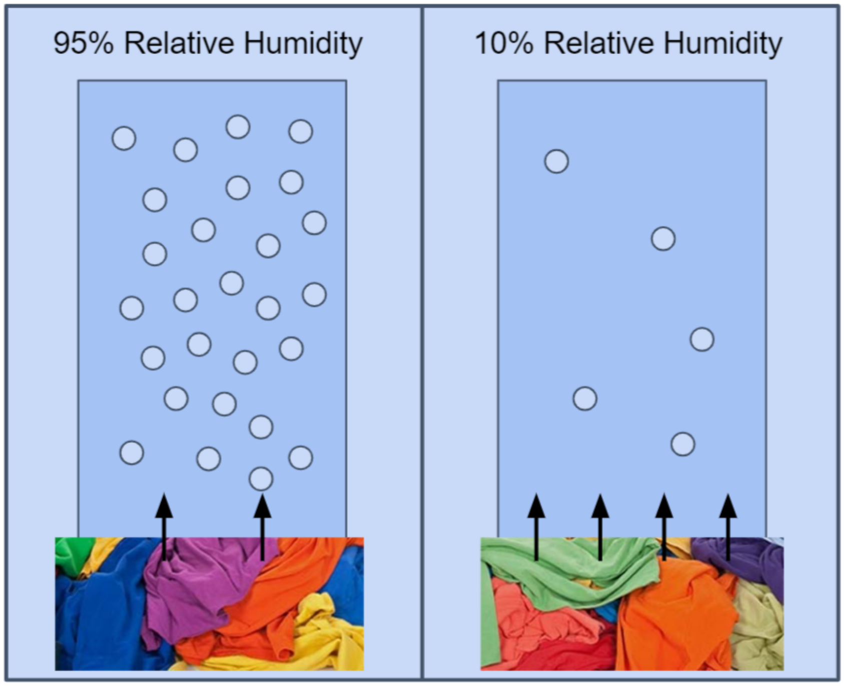

Figure 1.3: Air of 95% and 10% relative humidity above wet clothes, where the circles represent moisture content. The 95% air can not hold nearly as much water as the 10% air, because the 95% air is almost completely saturated.

To remove moisture from the air, it must first be cooled to its dew point temperature. As air temperature decreases, the amount of moisture it can hold also decreases. Thus, lowering air temperature while overall moisture content is held constant results in an increase in percent relative humidity, or how close air is to reaching its maximum moisture capacity. When air is cooled past its dew point, condensation forms. An example of this phenomenon is the formation of dew on grass early in the morning. Since air temperature is below its dew point temperature at this time, the excess moisture that the air can no longer hold forms water droplets on blades of grass. This act of removing moisture is imperative for the Drier Dryer to effectively increase dryer efficiency.

At first glance, cooling dryer intake air may seem counterintuitive; why would we cool air only for the dryer to heat it back up? Mitigating this is one reason why we chose to implement Peltier coolers, a thermoelectric module that is able to heat one side while simultaneously cooling the other by facilitating heat transfer across the module. They do this through a direct energy conversion between electricity and heat. Therefore, they can consecutively cool and then heat the incoming air, decreasing the heating load on the dryer. In addition, these modules are relatively simple, as they lack moving mechanical parts, are small, and produce negligible vibrations and noise.

To give more background on these coolers, their cooling capacity depends on the amount of voltage applied to the module and how well the module can dissipate the heat on its hot side. If the heat is properly ventilated and an optimal voltage is found, these coolers can achieve below freezing and above boiling point temperatures on the cold and hot sides, respectively. This process is called the Peltier Effect, and our design uses the Peltier cooler in a way that can cool down incoming air to reduce its relative humidity, and subsequently heat up the air as it goes into a dryer so that it can absorb more moisture. The following sections elaborate on our plans to do so in greater detail.

1.2 Review of Field Literature

Thermoelectric coolers (TECs) are ideal for our project because of their ability to produce both hot and cold temperatures without any moving mechanical equipment like condensers or compressors. A typical TEC is made of two different semiconducting materials. When a voltage of proper polarity is applied through the connected junction within the TEC, the Peltier effect occurs. This effect is described by the heat absorption from the cold junction being pumped to the hot junction at a rate proportional to the current passing through the circuit. Thus, each TEC has an optimal current and optimal voltage that results in its maximum coefficient of performance, or COP. In addition to their ability to produce both a hot and cold side, the TECs are sometimes equipped with fans and heat sinks in order to enhance their heat transfer and overall performance [4]. Figure 1.4 shows the typical design of a TEC.

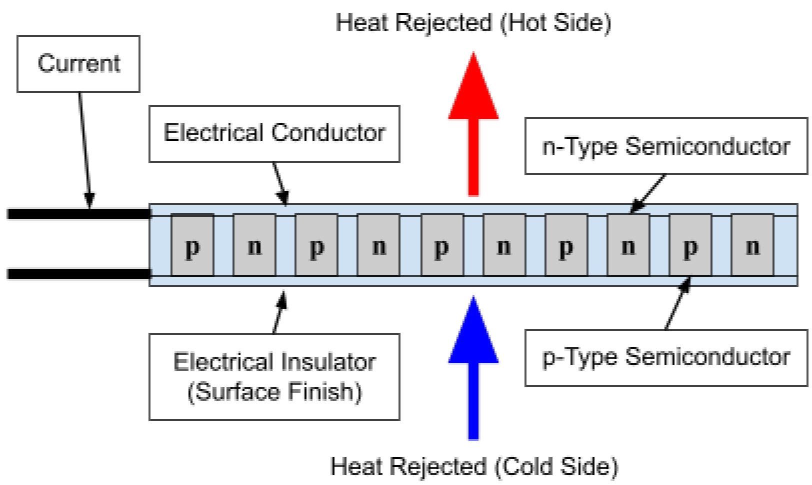

Figure 1.4: TEC design elements include p-type and n-type semiconductors generating a temperature difference with a current passed through the module.

There are numerous models of TECs that could have been used in our project. Initially, the two that seemed most practical belong to the MS Series and UltraTEC Series. The former series can produce the highest temperature differentials amongst TEC factors, which would make them ideal for both cooling intake air to remove moisture and reheating it before it enters the dryer drum. Unfortunately, these modules are typically designed for low heat transfer applications, so they proved to be too weak for our design. UltraTEC series modules are known for their high density of heat pumping capacity, which can reach up to 14 W/cm^2. This number is twice as high as standard modules. UltraTEC modules can have a cooling capacity of 100-300 W, but have low temperature differentials and high coefficients of performance, or COPs. COP is defined as the ratio of thermal output power to the electrical input power of the TEC. The low temperature differential is unfavorable for the opposite reason a high value is, but the high COP is also unfavorable. Although the higher COP makes the cooler slightly more cost-efficient when used over a long period of time, the initial investment cost for the module was deemed too expensive, typically at least twice the cost of an MS Series module [5]. Ultimately, the cons of both TEC series outweighed the pros, so we decided to select a TEC from the standard CP Series.

CP Series TECs are reliable and can be used in many different settings (Figure 1.5). They offer cooling capacity in the range of 10-100 watts and they come in numerous shapes and sizes. They are generally designed for high-current applications, but for the scope of our project, we determined they would prove to be the most adaptable and cost-effective due to their numerous models and their simple, low-cost designs [6]. In addition, it was found that determining the B-factor of these TECs was easier than doing so for other series. The significance of a TEC's B-factor will be discussed later in this section.

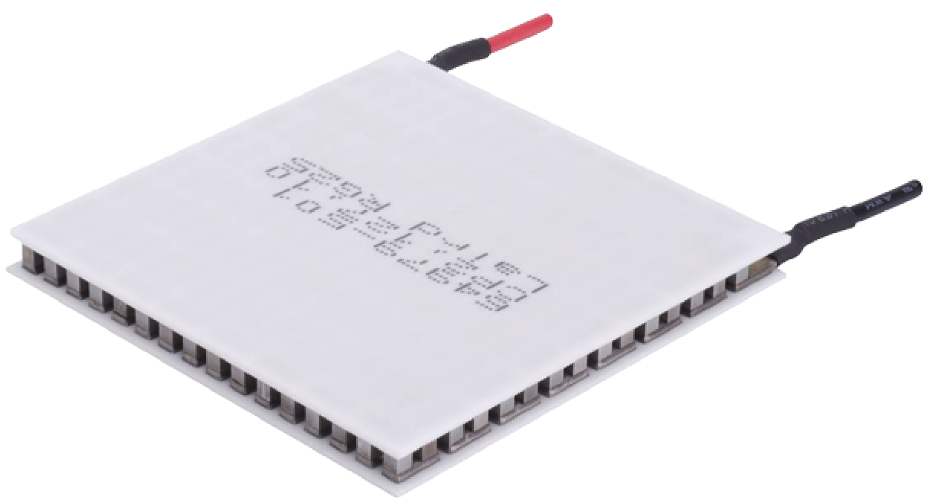

Figure 1.5: Laird CP series TEC capable of achieving a 70.5 °C temperature differential and a max heat transfer of 76.9 W. (Used without owner's permission) [17]

A previous Santa Clara University senior design team designed a device that cooled ambient air using four model TEC1-12706 TECs. Their goal was to cool ambient air from 30 °C to 23 °C through an aluminum duct. Their setup consisted of a fan that blew ambient air through the duct which contained the TECs. The TECs had both their hot and cold sides attached to

20-finned heat sinks (model 9Y692 A00-00), but while the cold heat sinks were used to cool the air in the duct, the hot heat sinks remained outside the duct, cooled by two external fans. The calculated heat load was 222 W and the volumetric flow rate of the intake air was 0.02706 m^3/s. The TECs had optimal voltages of 12 V, optimal currents of 4 A, and power rating ranges from 37.7-48.0 W. Their results revealed that air could be cooled from 32.5 °C to 22.1 °C in ten minutes at these optimal conditions if their fan was blowing air at a velocity of 2.5 m/s [7].

Another project team found that the ratio of geometric factors in the TEC assembly could have a significant impact on its effectiveness. These factors are referred to as the G-factor (ratio of a thermoelectric leg's cross-sectional area to its length) and B-factor (ratio of the thermoelectric leg length and module area to the number of leg pairs and cross-sectional leg area). After theoretical and experimental approaches, the team concluded that the module optimization process is much simpler if the B-factor is prioritized [8]. This research provided a great deal of insight for the design of our TEC assembly and accelerated our TEC selection and current and voltage optimization.

TECs are relatively small modules, but still produce large amounts of heat. Because of this, it is important to consider the Thompson effect and how it applies to TECs. The Thompson Effect is when heat is carried from a heated portion of a circuit to other parts of the same circuit It has a significant impact on TECs due to their large heat flux and internal wiring. A positive Thompson coefficient can result in lower minimum cooling temperatures and can improve the cooling capacity of TECs [9]. However, as the ratio of cross-sectional area to thickness increases, the Thompson effect begins to have a smaller effect of the maximum temperature difference of the TEC. From these results, we concluded that the design of the module itself should be taken into consideration when designing the cooling capacity of the TEC assembly.

1.3 Project Objectives and Goals

The team's overarching goal is to create an improved clothes dryer design through an attachment that incorporates Peltier coolers to dehumidify intake air and then reheat that air before it enters the dryer. This product is expected to work particularly well in geographically humid areas.

The design should accomplish two major goals: increase the energy efficiency of the entire dryer process and reduce the time required to dry clothes. These improvements should be enough to justify the projected retail price of the attachment product. For example, if in five or six years of use the product decreases the energy cost of running the dryer by at least the initial cost of the product, then it can be considered economically viable. The cost analysis of this product is detailed in Chapter 5.

By the end of fall quarter, a rigorous sampling of existing clothes dryers had been conducted to gain a baseline of dryer performance. The team also had gained an understanding of Peltier cooler technology and its applications. Through research and calculations related to the cooling load required to dehumidify the incoming air, an initial design was drafted and prototype parts ordered. A full list of purchased parts is included in Appendix G.

In the winter quarter, the team's main focus centered on three overarching goals: finite element analysis, design drawings, and prototype construction and testing. Within and through these goals, the design parameters were refined. Within COMSOL, inlet and outlet air temperatures of the cold side of the TEC within the isolated design (not attached to a dryer) were measured to test the effect of flow constrictions, heat pipes, additional TECs, and combinations thereof. After FEA testing, the characteristics that yielded the most improvement were ordered and applied to the prototype. Dimensioned drawings were also produced to guide construction of the prototype.

In the spring quarter, the prototype was tested at varying voltage and current ratings to attain the maximum performance with the goal of attaining the largest temperature difference. Using the results from this testing, a finalized design was then constructed. Unfortunately, time and resource constraints prevented testing of this design, but theoretical calculations and projected savings are detailed later in this report.

The two key performance requirements of the proposed design are the temperature differential across the cold side of the Peltier module and the power consumption of the module (for all proposed requirements, see Appendix A). For the design to work properly, it must be able to cool air to below the dew point temperature. In the target humid areas where we can expect air at 27 °C (80 °F) and 80% relative humidity, cooling the air by at least 4 °C would be sufficient to remove moisture from it, thus reducing the humidity of the incoming air. At the same time, this design aims to improve the energy efficiency of dryers. Therefore, the power saved by reducing the dryer time should be greater than the power consumed by the proposed attachment. The ideal power rating will vary based on individual dryer wattage but it is estimated that a power rating between 50-100 W will be sufficient.

The proposed attachment should also have a start-up time much less than the dryer cycle time. In other words, the attachment should be cooling the incoming air for as much of the cycle as possible. Therefore, a start up time of 1-2 minutes is preferred. In addition, the static pressure produced by the added duct, heat sinks, and pre-existing exhaust duct out of the dryer must not exceed the combined static pressure rating of the dryer fan and supplementary booster fan between the dryer and attachment.

There also exist some physical restrictions of the design. For example, it is expected that users may desire to stack other items on top of the attachment (e.g. up to 100 lbs of storage) or slide it around slightly to fit with their existing setup. The size of the unit should also not exceed one foot wide and three feet long (typical clothes dryer dimension) to ensure it can be easily accommodated.

With regards to safety, the temperature of the casing of the unit should not exceed the range 1-43 °C to prevent burns or damage to nearby items. In addition, a quick shut off mechanism should be easily accessible to the user should an emergency situation require its immediate shutdown. Finally, to prevent damage to the unit, it is recommended that it is placed no less than one inch from the dryer.

In the following chapters, the desired performance characteristics will be further defined. In addition, the subsystems and system wide parameters will be discussed in depth, followed by simulation test results and physical prototype results. At every step of the way, the changes in approach and design based on the results and challenges will be expounded upon. This will culminate in our progress to date and our plans moving forward.

Chapter 2: Attachment Performance Requirements

The objective of this chapter is to survey customer needs in the dryer market. In addition, a system sketch is provided detailing the general design of the proposed attachment. The team's functional analysis is detailed, including calculations of the required temperature drop to reach dew point and the pressure loss through the system. Finally, the chapter describes and analyzes the COMSOL simulation results testing various features that can increase heat transfer in the system.

2.1 Customer Needs

The goal of the dryer attachment can be described as "increasing the efficiency of a dryer." To find out if a need for such an attachment existed, interviews were conducted with potential users. The following questions were used to conduct these interviews to find out more about potential customers' clothes dryer setup, performance, local weather, and more. The answers would help to quantify the goals that attachment should be designed to achieve. The results of these interviews are shown below.

Table 2.1: Interview results from three potential product users.

Question	**Interviewee #1:** Honolulu, Hawaii	**Interviewee #2:** Pleasanton, California	**Interviewee #3:** Eugene, Oregon
What are typical temperature/humidity levels in your area?	75-85 °F, 70-80%	60 °F, 65%	50-60 °F, 75%
How long does it typically take for a small, medium, and large load of clothes to dry (<25%, 50%, >75% capacity)?	40, 55, 75 min	35, 45, 60 min	35, 45, 70 min

Do you have a gas or electric clothes dryer?	Gas	Gas	Gas
How much would you pay (flat-rate) to cut this time by 25%?	$150	Depends on electric bill and how much it would save in the long run.	$100
How much space in your "laundry area" could you afford to sacrifice for a dryer attachment?	~1 ft	~2 ft	~1 ft
Does your laundry space have ventilation, and if so, what kind of ventilation (window, vent etc.)?	Exhaust vent to outside	Pretty well ventilated, no window but exhaust fans.	Exhaust vent to outside
What features would you like to see in our product?	Easy to install/use, durable	Ease of access, saves energy/money	Quick ROI

The following questions were used to conduct two interviews with sales representatives from top dryer retailers currently on the market. The results of these interviews are shown below.

Table 2.2: Interview results from three popular clothes dryer retailers.

Question	Interviewee #1: Lowe's Home Improvement	Interviewee #2: The Home Depot	Interviewee #3: Best Buy
What is the difference between gas and electric dryers?	Although both electric and gas dryers use electricity to operate, electric dryers are powered entirely by electricity. The main difference between the two has to do with how they heat air to dry your laundry. Gas dryers use	The main difference between electric and gas dryers is how they're powered. While both types of dryers need electricity to run, gas dryers also require a gas hookup. Gas Dryers: Electricity powers the	The difference is in the hookup. Houses/apartments have hookups for one or the other

	natural gas or propane to generate heat while electric dryers use metal heating coils powered by electricity.	drum, fan, lights and controls, but natural gas or propane generates heat.	
What is the difference between vented and ventless dryers?	Ventless dryers are easier to install, require lower maintenance, and more efficient than vented dryers. However, non-vented dryers also tend to have a significantly higher upfront cost, and though they are gentler on clothes, they tend to take longer than a vented dryer to get everything dry.	Ventless dryers require less maintenance and are more efficient but more expensive than vented alternatives.	The main difference is ventless dryers hold a much lower capacity of clothes.
What are the most popular dryer models you sell?	1) Whirlpool, Model #WED4815EW ($600, Vented) 2) Samsung, Model #DVE45T6000W ($800, Vented) 3) GE, Model #GFD55ESSNWW ($900, Vented)	1) LG, Model #DLEX3700W ($1000, Vented) 2) Maytag, Model #MEDC465HW ($630, Vented)	LG has been Consumer Reports #1 brand the last 3 years. They are anywhere from $500-$800.
Do you sell dryers with integrated dehumidifiers?	No	No	No
Are there any attachments I could buy for my current dryer that would increase its efficiency?	No	No	No
What are the cheapest vented and ventless dryers you sell?	Vented ~ $500 Ventless ~ $1000	Maytag, Amana, Hotpoint are the cheapest brands we sell. Vented ~ $450 Ventless ~ $1000	Vented ~ $480 Ventless ~ $990

Based on the results of the customer interviews, the primary needs that must be satisfied are ease of use, size, and cost efficiency. When speaking with our customers, the main concern was that our product might be difficult to set up and operate. Taking this feedback into consideration, we designed our system to be operated as simply as possible; although not included in our final scope, the retail attachment will consist of a single on/off switch, with an automatic timer for shut off. In terms of size, our customers expressed concerns that their washrooms were already quite cramped and that they could not offer much space behind their dryers. Taking this into consideration, the housing chamber that keeps the coolers, and other electrical systems/wiring is kept to less than a foot wide and no longer than the length of a typical dryer. Finally, the most important feature our customers wanted to see was cost efficiency. Although we mentioned that a return on investment was bound to occur with prolonged use, our customers were concerned that this return would take too long to be noticed. To alleviate this, cost savings graphs and analyses are provided in Chapter 5 detailing the conditions under which it is most effective to run this attachment as well as the estimated savings.

The interviews with the three popular dryer retailers gave us an insight into the industry from a retail perspective. We asked questions that we already knew the answer to such as the difference between gas and electric dryers and the difference between vented and ventless dryers. This allowed us to see how these distinctions are made with customers and sales representatives. The results showed that for a standard customer, the differences between these dryer types are very theoretical with technical details set aside. The other questions we asked served to demonstrate a market need for our product. Questions such as, “Do you sell dryers with integrated dehumidifiers?” and “Are there any attachments I could buy for my current vented dryer that would make it more energy-efficient?" proved that there is a void in the market for devices that can increase the efficiency of people's current dryers at home, especially in particularly humid regions. Finally, we asked about the retailers' most popularly sold dryer models, all of which were very expensive, ranging from $500-$1000. Additionally, we asked about the cheapest models available which still were quite expensive, ranging from $450-$500 for standard vented dryers and upwards of $1000 for ventless dryers. The overall conclusion we drew was that since current dryers on the market are very expensive, they make buying a new one to increase energy efficiency unfeasible.

The following table provides an aggregated list of needs gathered from interviews with potential users as well as the team's personal preferences. The hierarchy runs from top to bottom. The specific needs are addressed more specifically in the following section.

Table 2.3: Hierarchical customer needs table

Categories	Needs
Cost	• System eventually pays for itself • Cheap enough to make buying a new dryer unnecessary
Usage	• System is easy to install and operate • System is not too heavy • System is not too bulky
Functionality	• System is durable/long-lasting • System is easy to clean/does not make a mess

After conducting interviews with potential customers and retailers and reviewing data from the PDS report, our team determined that the sole primary need for our product is that the system pays for itself, ideally within 5 years. While it is necessary for our system to increase dryer efficiency by removing moisture from the intake air, if this increase in efficiency is not substantial enough, our product will not be able to compete with dryers with built-in moisture-removal mechanisms. The secondary needs include "being cheap enough to make buying a new dryer unnecessary" and "the system is easy to install and operate." The former is important because the starting price of our product can be seen as the down payment on an investment: if the initial price is too high, nobody will want to buy the product regardless of its return on investment. Thus, we determined that our product should be mass-producible: designed simply and cost-efficiently with no unnecessary parts. The latter is important because we want our customers to feel comfortable using our product. If a product is effective *and* easy to use, overall customer satisfaction will be increased and which may lead to further advertising by word of mouth. Tertiary needs for our product include light weight, compact size, durability, and ease of cleaning. While these needs are important, they are not strong determinants of the success of our product. Finally, quaternary needs include, but are not limited to, pleasing aesthetics and a catchy product name. While these factors are not important for the scope of our senior design project, they may increase in importance if our product is actually marketed to consumers. However, our group still deemed the primary, secondary, and tertiary needs to be more important than any of the quaternary ones; the quaternary needs mainly tailor to our personal preferences and desires.

2.2 System Sketch

It has so far been established that the design will utilize TECs to cool and then heat dryer intake air. Before describing the physics behind the design, Figure 2.1 shows a sketch of the Drier Dryer with its four main components. These include the housing, heat sinks, TEC, and water collection area. Each component will be discussed in depth later, but for now the process works such that air enters the bottom left end, passes over the cool heat sink, makes a turn over the hot heat sink, and leaves out the top end into the dryer.

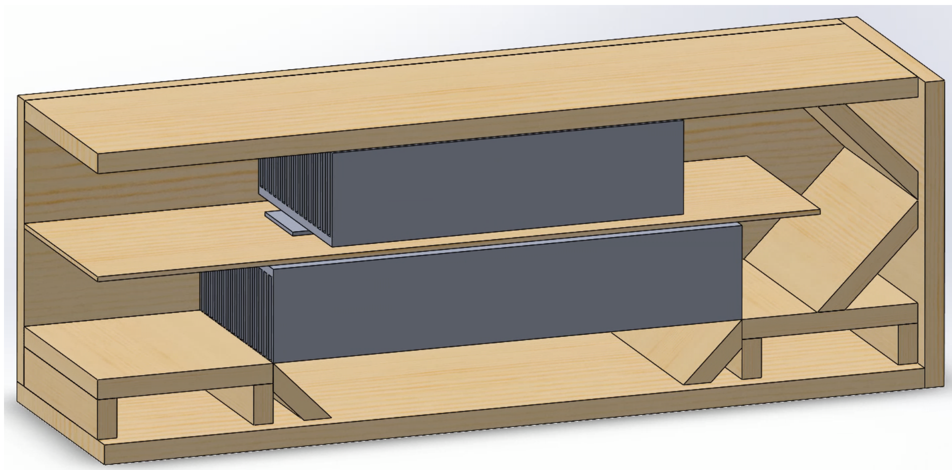

Figure 2.1: The Drier Dryer physical design. The foremost side wall is hidden to reveal the interior of the design. The housing consists of particle boards. In gray are the heat sinks and heat pipes with the TEC sandwiched in between them.

This product will be used by those who wish to increase the efficiency of their dryer without the investment of buying a completely new unit. It will be nearly universally applicable to vented dryers, meaning customers are not restricted by brand or model. For installation, the user must locate the dryer air inlet sections. If the dryer has only one or two circular inlets, the attachment may be connected using the appropriately sized flexible duct. Any additional air inlets may be blocked to maximize air intake from the attachment instead of the ambient air. If the dryer has varied inlet areas or is not tightly enclosed as to let air escape, a line of 4” duct may be run from the dryer intake directly to the heating element inside of the dryer. This process will require partial disassembly of the dryer. This specific attachment method will be discussed more in Chapter 4.

One goal of our product was to increase the efficiency of the dryer to a point where the product pays for itself in energy savings over its lifespan. Although detailed analysis will be provided in Chapter 5, mass-producing this product could lower the return-on-investment period to as low as six years, well within the lifespan of a typical dryer. It is important to note that our product is specifically designed to be of maximum benefit for those operating their dryer in a hot and humid environment. This humidity may be caused by the geographical area or due to a poorly ventilated laundry room. In either of these situations, the higher the humidity and temperature, the greater positive impact our attachment will bring to our customers.

2.3 Functional Analysis

The primary function of the dryer attachment is to cool incoming air to below its dew point temperature to extract moisture from it before it is brought into the dryer. This will be achieved by several subfunctions using the duct, TEC module, and heat sinks.

A combination of supplementary fans and the clothes dryer's built-in centrifugal fan are used to drive air through the attached duct. The air will pass across the heat sink connected to the cold side of the TEC. As the air goes across the cold heat sink, its temperature will decrease. Along this heat sink, the air will reach the dew point temperature for the ambient temperature and relative humidity of the surrounding air. At this point, moisture will begin to condense out of the air and onto the surface of the heat sink (for discussion on specific water removal methods, see Chapter 4). Once the air leaves the heat sink, it will be considered "dry air," as it will be less humid.

This cold dry air will be turned 180° around through two 90° elbows and run across the hot side of the TEC in the same way as it did the cold side. After passing across the hot side, the air will be considered "hot and dry." This final hot and dry air will be passed into the dryer's air inlet where it will be further heated and used to dry clothes.

To decide whether a supplemental fan was necessary, the static pressure of the system needed to be found. Therefore, pressure loss calculations were performed to find if the static pressure was greater than the pressure head produced by the built-in fan. Dryer manufacturers do not readily provide the static pressure ratings of their fans, but they do provide a maximum length of attachable duct. Amongst several dryers, this length is found to be at least 10 m (35 ft). Using Equation 2.1, this length is converted into pressure head by using an average duct diameter of 0.1 m and air velocity of 6 m/s.

$$h_f = \frac{L}{D}\frac{V^2}{2g}f \qquad [2.1]$$

where L is equal to the length of the duct, D is the diameter of the duct, V is the air velocity, g is the gravitational constant, 9.81 m/s^2, and f is the friction factor.

Figure 2.2 displays test results that show that the velocity of air exiting the dryer matches the purported speed of 6 m/s. In addition, these values are used to calculate the Reynolds number of the flow, 42,150. The friction factor for flexible duct is found to be 0.06 using Moody's chart and a roughness factor of 0.03. The maximum allowable head without adding an additional fan is therefore found to be 11 m.

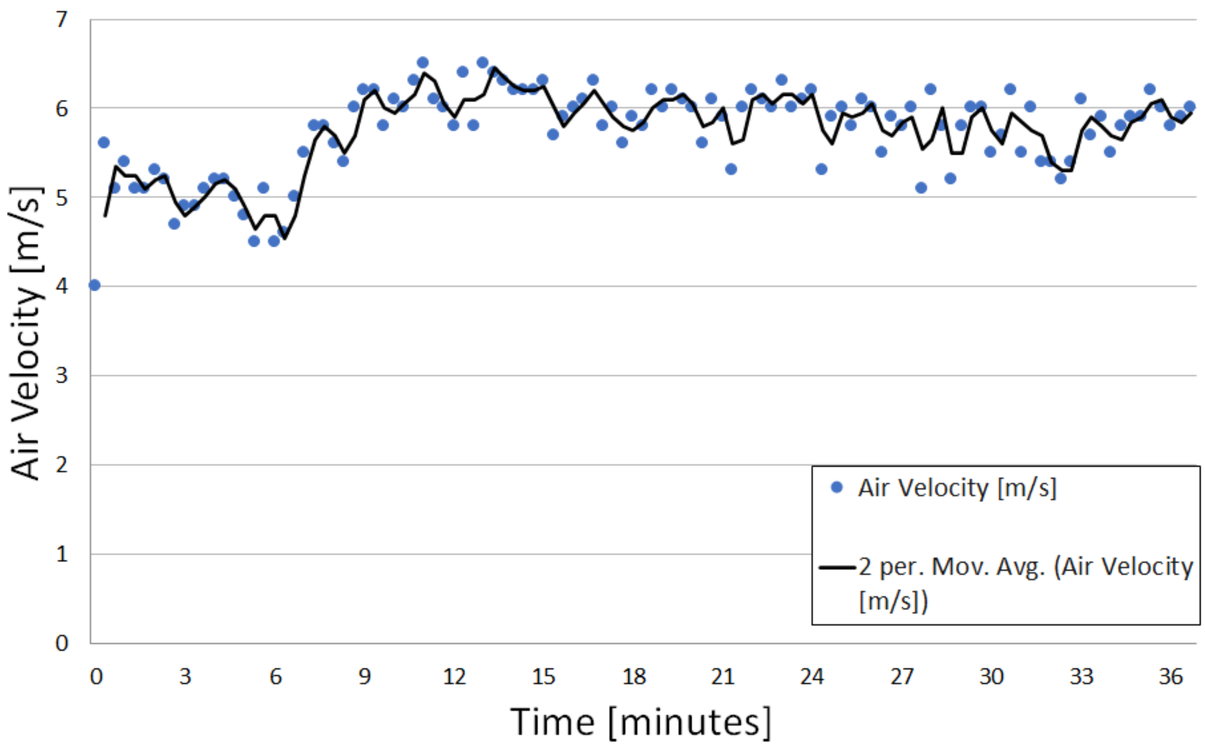

Figure 2.2: Air velocity vs. time for a 40 minute dryer cycle. The average velocity is found to be around 6 m/s for approximately 75% of the dryer cycle.

The proposed attachment is predicted to contain no more than 3 m of duct (about 10 ft). The major loss of 3 m of flexible duct is found to be 3.3 m using the same average values for the variables. In addition, minor losses from a predicted maximum of six elbows are considered — four upstream of the dryer and two downstream. The minor loss coefficient is found to be 0.30 for 4-in-diameter duct and a flanged connection (flanged is assumed because the flexible duct will be bent into 90° elbows without the use of fittings). The pressure loss from these elbows is found to be 2.2 m. This leaves 5.5 m of usable head remaining.

The biggest pressure drop is expected to be due to the heat sink obstruction. This is found using equation 2.3 and converted into head loss [10].

$$\Delta P = (k_c + 4f\frac{L}{D} + k_e)\rho\frac{V^2}{2} \qquad [2.2]$$

This equation is the general equation for a heat sink obstruction in an airstream. Here, k_e has a value of 0.3683 and k_c has a value of 0.2545 for the chosen heat sink. These values represent the pressure loss coefficients due to sudden contraction and expansion due to flow entering and leaving the heat sink flow channels between the fins. ρ is the density of air at standard atmospheric pressure, 1.225 kg/m^3. ΔP is the pressure drop across the heat sink, in Pa. Using the equation yields a pressure drop of 28.36 Pa and 2.22 m of head per heat sink (see Table 2.4). This head, combined with the head of the baffle design, creates an even greater pressure drop and led our team to conclude that supplemental booster fans are required to push air through the attachment and into the dryer.

Table 2.4: Summary of parameters used in equation 2.2 for the selected heat sink cross-sectional dimensions.

Parameter	Magnitude (for the Selected Heat Sink)
k_e	0.3683
k_c	0.2545
Pressure Drop	28.36 Pa

The required cooling load is calculated using the specific heat of air, average mass flow rate of air through a clothes dryer, and the average expected temperature difference to get the air to its dew point. The product is targeted to areas with average humidity of at least 60%. Average temperature and humidity from Florida and Hawaii summers and winters are plotted on a psychrometric chart to find the corresponding dew point temperature (see Figure 2.3). In addition, when the relative humidity is above 50%, equation 2.3 can be used to find the approximate dew point temperature in °C.

$$T_{dewpoint} = T_{amb} - (100 - \mathbf{\Phi})/5 \qquad [2.3]$$

where $T_{dewpoint}$ is the approximate dew point temperature, T_{amb} is the ambient temperature, and Φ is the relative humidity of the ambient air expressed as a percent. This relation was used to plot the required temperature versus relative humidity in Figure 2.4.

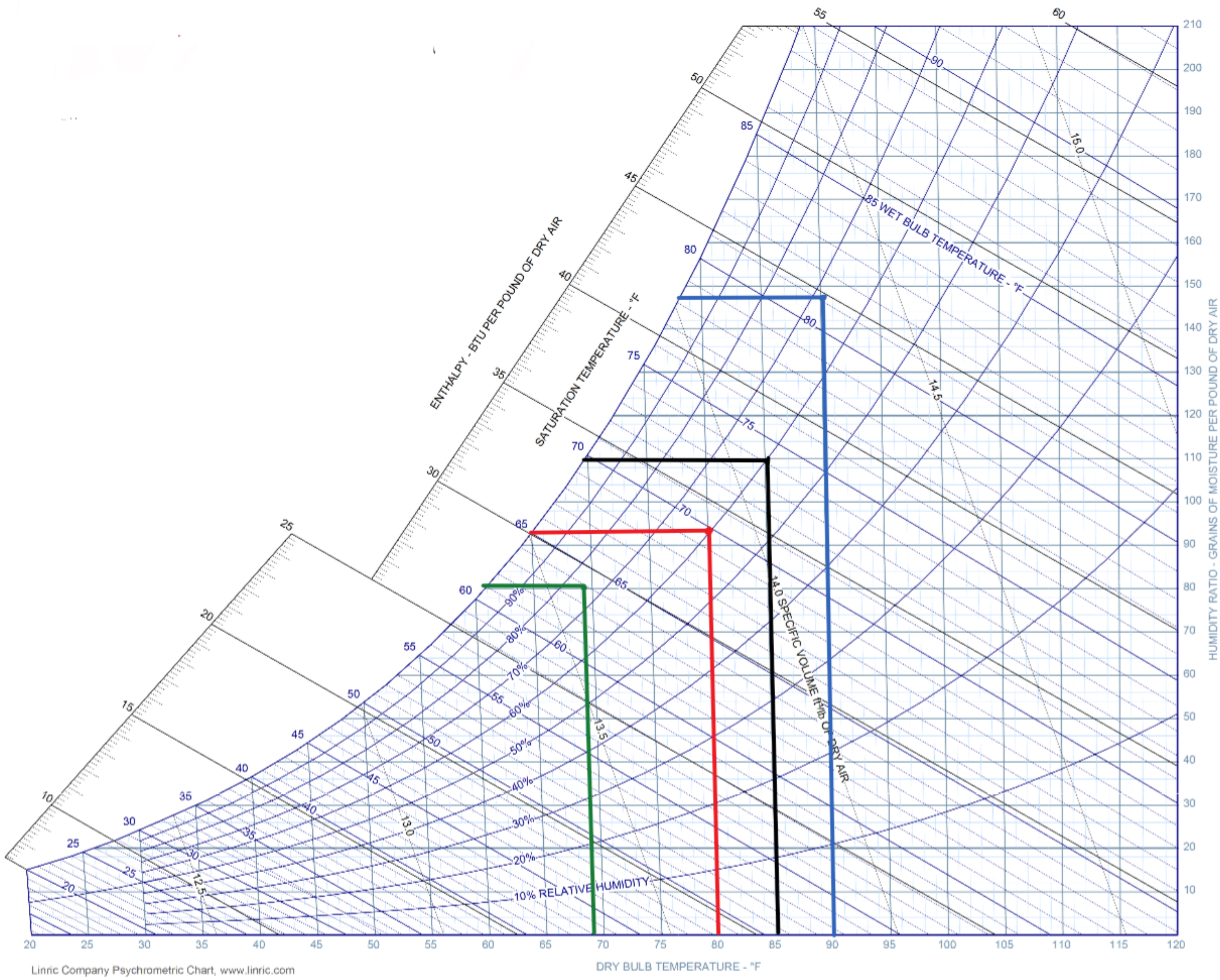

Figure 2.3: Psychrometric chart showing the dew point temperature for four climates: Florida winter (green), Florida summer (blue), Hawaii summer (black), and Hawaii winter (red). (Psychrometric chart used without permission from owner) [11].

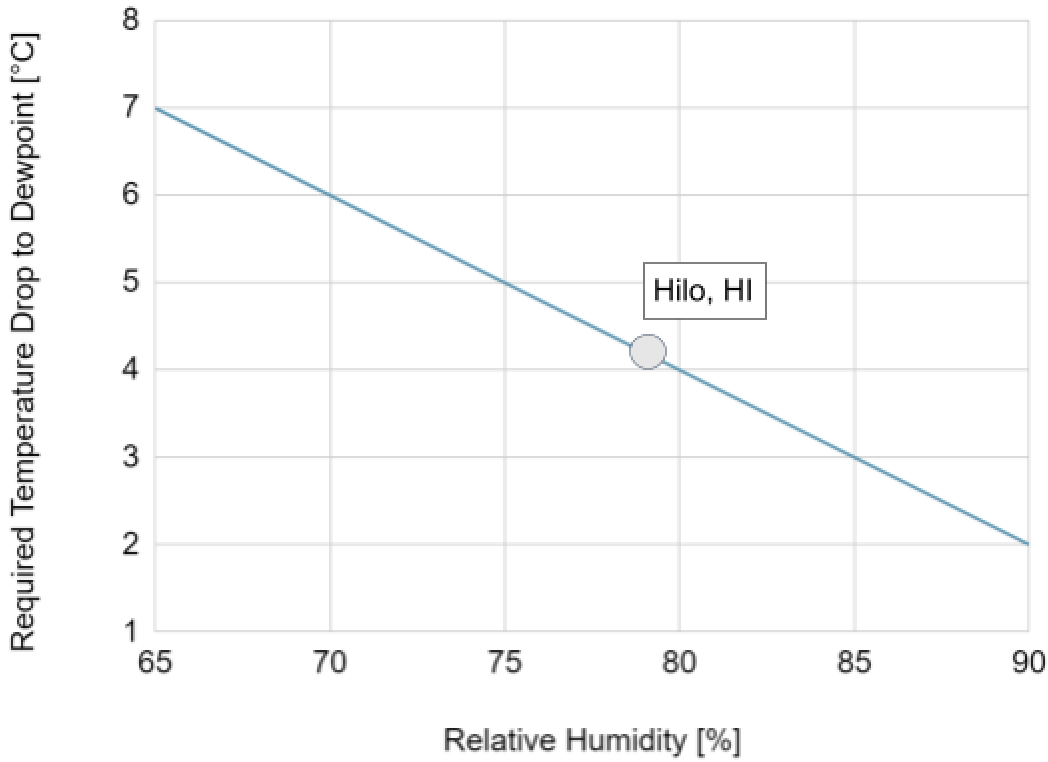

Figure 2.4: Required Temperature Drop based on ambient relative humidity. For an average summer day in Hilo, HI a 4 °C temperature drop is necessary to reach dew point.

Although our design condition in Hawaii or Florida would only require a maximum temperature drop of around 6 °C, a 9 °C temperature drop was used to calculate a conservative cooling load required to attain this temperature drop (Equation 2.4).

$$q = \dot{m} C_P \Delta T \tag{2.4}$$

where q is the cooling load in watts, $\dot{m}$ is the mass flow rate of air in kg/s (calculated using the area of the duct, velocity of air, and the standard density of air), and ΔT is the air temperature drop in °C. Using the aforementioned estimated values, a cooling load of nearly 500 watts was found.

The TEC is known to maintain a constant temperature on both the cold and hot side. This information is used along with the relationship between temperature difference, cooling load, and thermal resistance to calculate the allowable thermal resistance of the attached heat sinks. The steady-state temperature of the cold side of the TEC was found to be around 13 °C based on initial testing of a module. The allowable thermal resistance is found to be around 0.02 °C/W. Assuming standard fin heights, a width of 10 cm, and aluminum material, the length of the heat sink is estimated to be around 33 cm long. Figure 2.5 shows the relationship between fin height and required heat sink length.

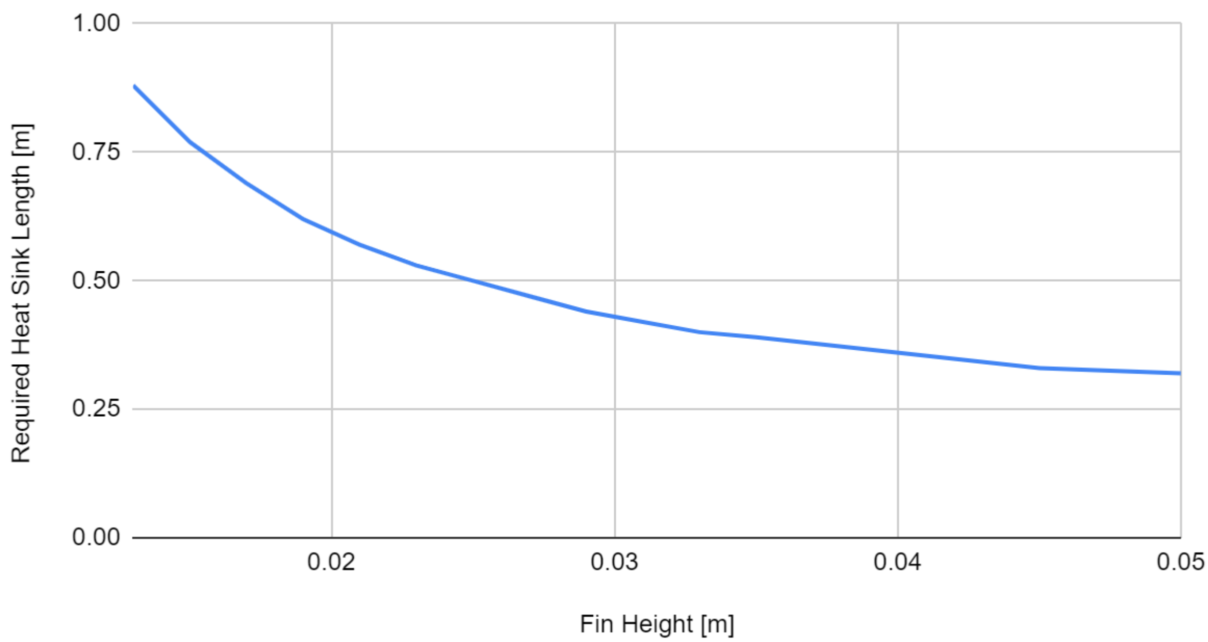

Figure 2.5: Relationship between fin height and heat sink length. As the height is increased the required heat sink length is decreased to an asymptote at around 0.35 m.

Based on this analysis, we decided to purchase heat sinks from Mouser that were about five inches wide and a foot long.

2.4 Benchmarking Results

Currently a number of dryer exhaust attachments already exist. These attachments are often used to direct the exhaust out of the room with the dryer. However, there are also attachments that both filter any remaining lint and pump the hot air into the room. Products like these are described as energy-saving because they use the hot exhaust to heat the room, thus supplementing conventional heating methods.

While attachments for dryer exhaust air exist, none have been found for dryer air intake. In other words, incoming dryer air cannot be altered by existing products. However, there are a few products that aim to increase the energy and time efficiency of dryers. The first are ventless dryers (see Figure 2.6). These dryers recycle exhaust air by cooling and dehumidifying the air before it passes back through the dryer. The lack of exhaust means that these dryers may be placed nearly anywhere indoors. At the same time, they require monthly maintenance and cleaning by the owner. While they generally cost less to run per year in terms of electricity, their drying times are also longer than that of vented dryers. In addition, they typically cost around 50% more to purchase than vented dryers [12]. The market reveals that ventless dryers are still not economically feasible for most people. According to Energy Star, as of 2011, 80% of households own a clothes dryer, but only 2% of these households own a ventless dryer [13]. In other words, 98% of all personal dryers are vented dryers. Many of the same manufacturers that produce vented dryers also produce ventless models.

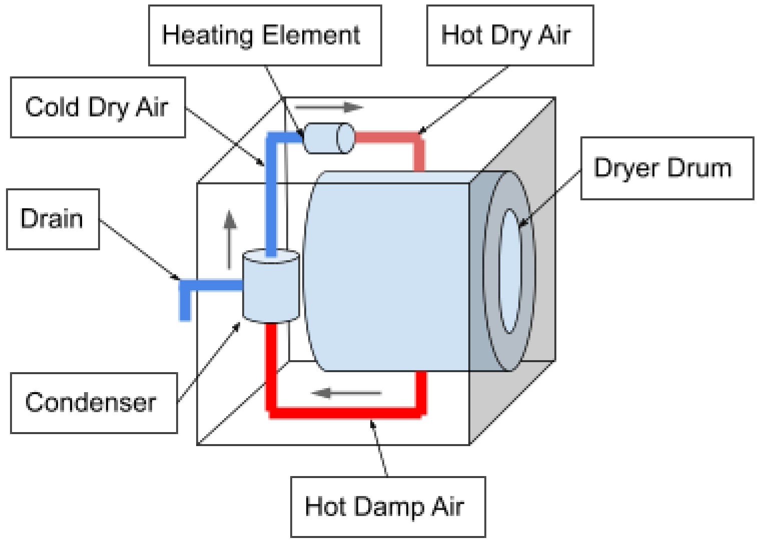

Figure 2.6: A flow diagram of air for a ventless dryer. Air is recycled and water is continuously condensed out of the circulating air.

One key goal of the proposed attachment is that it would decrease the dryer cycle time. Various existing brands of “dryer balls” also claim to decrease dryer time by up to 25% (see Figure 2.7). However, experiments with these balls have revealed that they often severely underperform despite their claims to reduce cycle time. These balls are often made of either condensed wool, plastic, or rubber. Wool balls are used to help absorb moisture from fabrics to decrease drying time. Over time, these balls shed their wool which may block air flow. In addition, they must be regularly replaced every 8-12 months. The alternative plastic and rubber balls do not shed or absorb moisture but help prevent clothes from bunching up, in theory increasing the quality of airflow over clothes. Neither of these solutions actively remove moisture from the air passing over the clothes. Therefore, the proposed attachment could only supplement and augment the effects of these solutions.

Figure 2.7: Typical wool dryer balls used to decrease dryer cycle time and keep clothes fresh. (Used without owner's permission) [14]

Table 2.5: Specifications of ventless dryers and dryer balls.

Technology	**Ventless Dryers**	**Dryer Balls**
Manufacturers	● General Electric ● LG ● Bosch ● Samsung	● Smart Sheep ● Woolzies ● Kikkerland ● Dryer Max
Approximate Sales Volume	2% market share	Unknown
Cost	50% greater than vented dryer counterparts	~$3.50/ball (2-6 balls used at once)
Energy Impact	~50% more efficient	N/A
Cycle Time	~25% longer than vented dryers	10-25% reduction (claimed)
Life Span	12-16 years (equivalent to vented dryers)	● Wool: 8-12 months ● Plastic/Rubber: Indefinite

None of the aforementioned products (or other existing products on the market) affect the temperature or humidity of the incoming dryer air. While ventless dryers exist, the upfront cost is often too expensive for people to buy into. In addition, many people are satisfied enough with their current dryer to warrant not wanting to purchase a new dryer for a small boost in energy efficiency. On the other hand, dryer balls offer a cheaper alternative that claims to reduce dryer time. However, there is great scepticism surrounding these claims, with several studies showing that the balls can have negligible impact on cycle time. Moreover, the balls must be occasionally replaced and if made of wool, they may clog the dryer, inhibiting air flow.

Since 98% of existing dryers are vented dryers, the proposed attachment could be widely adopted. It will be nearly universally applicable and the user will not have to worry about lint buildup since the exhaust air will not contaminate the incoming air. At the same time, the relative humidity of the incoming air is the number one determinant of dryer cycle time and efficiency. The proposed attachment will uniquely tackle this factor while maintaining an appealing and compact form factor. Most dryers are installed with wall clearance in mind, meaning that the attachment would not require a repositioning of the clothes dryer in most cases. In summary, the primary opportunity for improvement lies in increasing the energy efficiency to compete with ventless dryers at a fraction of the cost while also decreasing dryer cycle time.

2.5 Systems-Level Design Layout

Unlike existing technology which aims to increase dryer efficiency, our product treats incoming air. After several design iterations, this is achieved through three subsystems: the heating module, water collection system, and dryer attachment system. The specifics of these subsystems will be discussed in Chapter 3, but their basic orientation and purpose are shown in Figure 2.8.

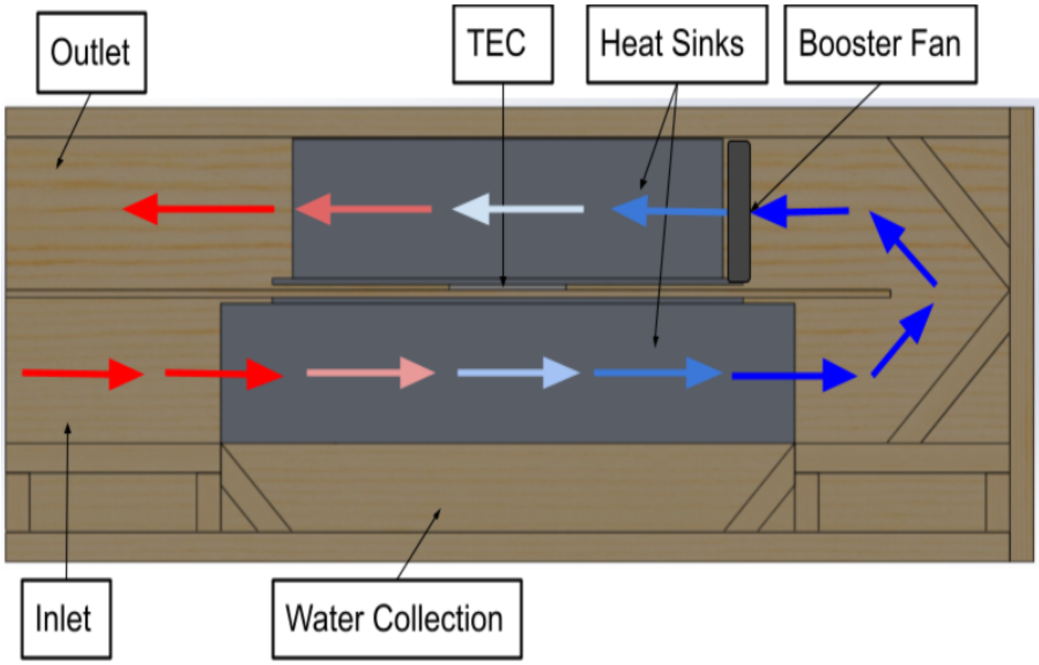

Figure 2.8: Air flow direction and temperature diagram for the Drier Dryer. The air passes over the cold side heat sink where it is converted into "cool dry air". The air is then directed around two 90° elbows and passed through a booster fan and the hot side heat sink where the air is then expelled as "hot dry air."

Each subsystem has an individual role in the entirety of our design problem. When combined, the process works in four steps in order of the arrows in Figure 2.8. First, air is brought in through the inlet and cooled below its dew point temperature as it passes over the cold heat sink. Second, moisture that has been condensed on the heat sink is absorbed by the wicking material (not pictured in the figure) and collected in the tray below the cold heat sink. After passing the cold side, the air is directed around a near 90° flange design. While this is not ideal for air flow, the 90° turn forces the air to slow down; since the air passes as slowly as possible over the cold heat sink, heat transfer is maximized. Air is then reheated across the hot heat sink on the upper channel of the design. Finally, the air is expelled from the rectangular outlet transitioning to a 4" round duct which connects the design to the dryer's inlet.

2.6 Key System Options

One major system issue occurs when the heat generated by the Peltier cooler is not dissipated well enough, causing the hot side of the module to heat up rapidly. This creates a large temperature difference between the module's cold and hot sides. This increased temperature on the hot side causes the cold side of the module and the cold heat sink to heat up rapidly as well. To solve this problem, the heat sink on the module's hot side needs to have air flowing through it at all times so that its temperature is well-regulated. Additionally, the heat sink's fins need to be oriented so that the accumulated heat can transfer into the incoming air. In other words, the heat sink fins need to be parallel to the air flow.

Another factor that can affect the performance of the system is the thermodynamic properties of the heat sinks. In order to maintain cold and hot temperatures for the cold and hot heat sinks, respectively, their thermal resistances must be as low as possible. This creates another issue because heat sinks with lower thermal resistance are relatively large, forcing the system design to compensate for a very large heat sink. On the other hand, it is possible for the system to include a smaller heat sink, but it would likely have a larger thermal resistance and consequently reduce the efficiency of the system. This option and others will be addressed in the next chapter using finite element analysis simulations.

2.7 Team and Project Management

COVID-19

The main challenges posed to our project team came through the COVID-19 virus. Due to restrictions on gathering, we were not able to meet in-person until late winter quarter. Instead we met mostly online via Zoom. During this time, our team was able to meet multiple times a week (with our advisor as well as just our team) in order to ensure that work was distributed evenly and was being completed in a timely manner. Being close to campus meant that even when we could not meet physically, we were also able to drop off testing instruments and sample Peltier coolers to equip most of us with hands-on testing experience.

Another challenge our team faced was our inability to access the necessary tools and machines to begin constructing a prototype of our preliminary design early-on. Our solution to this issue was to perform numerous tests to collect data on dryer intake air flow rate and temperature, drying times under varying conditions, and steady state temperature and settling time for a Peltier cooler. We also ran simulations and theoretical calculations in programs such as COMSOL Multiphysics and MATLAB to estimate the performance of our system once it was constructed. Having used this data, we were able to save time and funding since we did not have to buy as many different Peltier coolers, heat sinks, or heat pipes to test before reaching our final design.

Budget

In formulating the budget for our project so early-on in the production process, we were faced with several issues. One issue we ran into was gauging a material cost for different subsystems of the design. While we had created a preliminary system sketch and laid out our subsystems, we still had not yet decided on what material we would use for different systems. This meant that we were unsure of how expensive the material would be and if we would need to test various materials. Additionally, the purchased Peltier modules and heat sinks needed to be tested to find the optimal combination to reach peak efficiency for our system. In other words, we performed multiple tests at varying voltages and design combinations to experimentally determine the best setup for our design.

Another issue that our team faced when preparing the budget was regarding the testing equipment. While we are able to determine the types of tests we were to conduct and the accompanying equipment needed, we could not foresee what testing equipment we would need to conduct further experiments. Therefore, the budget remained flexible from conceptual design through construction.

Timeline

The team's timeline can be most conveniently broken into the three quarters of the school year. The focus of fall quarter was to provide a theoretical proof of concept through thermal analysis, market research, understanding clothes dryer technology, and interviews. Among the initial primary concerns was to examine what existed on the market for increasing dryer efficiency. This was accomplished through interviews with local dryer suppliers as well as internet research. To better understand how clothes dryers operate, team members conducted standardized tests to get a range of performance data. To gage the level of interest in such an attachment, user interviews were conducted. Their responses relating to a reasonable price point and space restrictions guided our design in following quarters. Fall quarter also included research on TEC technology, including research produced by Santa Clara University students and staff.

The winter quarter consisted of three goals, finite element analysis, the creation of drawings, and prototype construction. COMSOL Multiphysics was used to test design alterations like flanges, heat pipes, and multiple TECs to maximize the temperature differential across the TEC module. The results informed how we created our 3D model and drawings in SolidWorks.

We were simultaneously able to obtain and test a clothes dryer and construct a working prototype.

In spring quarter, a final design was put together based on the updated drawings. In addition, updated FEA informed design changes including the baffle. Although the design was unable to be tested, simulations and projected savings calculations strongly suggested that the system would be able to fulfill a majority of its design goals.

Our general approach to designing our system was relatively simple. Early-on in our brainstorming process, we determined that a Peltier cooler would be the ideal cooling/heating mechanism since we could utilize both its hot and cold sides, its small size, and its relatively low cost. We knew that hot, dry air was ideal for drying clothes, so we decided to have the air cooled first to remove as much moisture as possible before having it reheated to decrease its overall relative humidity. Next we tried to figure out how to get the air to pass over both sides of the cooler in this order. We decided that snaking a flexible, insulative duct in a U-shape would allow the air to smoothly pass by both sides of the cooler while undergoing minimal static pressure losses. In order to aid heat transfer between the cold/hot sides of the cooler and the dryer intake air, heat sinks for both sides were also included in our preliminary design. Overall, our design process took the form of "recognize a problem," "address the problem," and "determine how the solution will affect the system and if it will create more problems." In doing so, we continued to perform tests, iterate calculations, and refine our design to determine its final specifications.

Safety

The two main safety concerns our project posed were the use of tools for fabrication and the exposure to extreme temperatures. The former was addressed by having all team members undergo proper machine shop safety training prior to its use. All proper PPE such as safety glasses, gloves, and appropriate clothing (jeans/slacks, covered shoes etc.) was used. The extreme temperature concern was alleviated by avoiding testing our Peltier cooler near flammable objects. The cooler was not left on for longer than ten minutes without attached heat sinks and regular temperature readings, or longer than an hour with heat sinks attached. Our team was also familiar with fire extinguishers and we were ready to use one should the need have arisen.

Work Breakdown Structure

Each of our team members was given a title which describes their area of expertise and their field of interest within the project. Thomas is the chief simulation officer, Josh is the chief financial officer, Daniel is the chief design officer, and Justin is the chief testing officer. Although we have these titles, all responsibilities under these classifications did not solely fall upon the respective officers. Our top priority was that all team members felt they were contributing an equal amount of work and that everyone put forth quality work. In order to achieve this, we understood that sometimes we may need to delegate work to our associates that fell under our own job classification. This allowed us to collaborate between areas of the design process while producing quality work at an efficient rate.

Chapter 3: Temperature and Flow Simulation

The design of the module and its corresponding heat sinks is crucial to our system and its functionality, which is why multiple design options were evaluated in order to minimize our cost while maximizing functionality. The complexity of the system posed a limit to the number of hand calculations possible. Therefore, to predict the behavior of certain design elements, COMSOL Multiphysics was used. A possible system design change included the use of multiple Peltier coolers and heat sinks, but this option would require more energy to operate. This would ultimately lead to an increase in cost for both production materials and power consumption. Changes could also be made to the design of the system ducts, such as the width and height to accommodate different types of air flow and heat sink installation. This option would require more fabrication and possibly increase the cost depending on the shape of the duct used, but could also potentially reduce power consumption.

3.1 System Modelling

To simplify the system, we focused our analysis on the airflow through our system's housing, specifically around the cold-side heat sink near the system's air intake. This area is of critical importance because this is where moisture will be extracted. Using the model of our system, shown in Figure 3.1, we were able to narrow down which design changes were most effective in cooling air. In this case, performance was measured by the temperature difference of the air at the inlet versus the outlet. Success is defined by larger temperature differences.

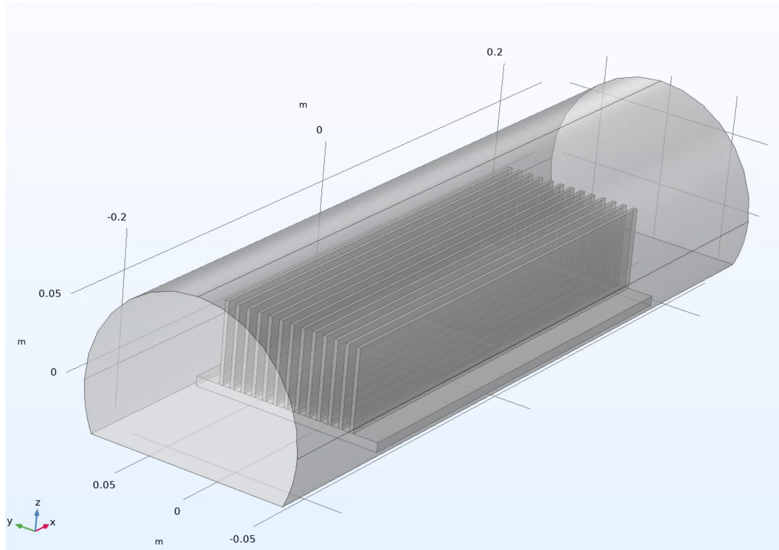

Figure 3.1: Basic model of the cold-side heat sink within the system's duct. This basic model was used and modified to run multiple simulations with varying conditions within COMSOL.

One main design addition considered incorporating heat pipes into our design to allow for even dispersion of heat transfering from the TEC to the heat sink. At the same time, the use of multiple TECs was considered.

The finite element analysis ultimately allowed us to simulate our system's response to ambient conditions without having to invest time and money in ordering parts, constructing extraneous prototypes, and conducting physical tests.

To achieve the goals above, a FEA program with a combination of thermal and flow analysis is required. COMSOL Multiphysics 5.5 was chosen for its versatility and because it is available through the engineering computing center (ECC). This software is able to run several physics models in one simulation. In addition, it has many predefined material options with the option to manually input material properties when necessary. Finally, the software has a section dedicated to user-defined variables that can be changed at any time. This allowed us to quickly change parameters and view their impact on performance. The materials for the heat sink, duct, heat pipes, TEC, and fluid include aluminum alloy 6063-T83, copper (with a modified thermal conductivity), aluminum oxide, and standard air, respectively. The temperature and velocity of both the air and heat sink were tracked using a nonisothermal flow from the multiphysics selection.

To compare the performance of the various tests, several variables will be kept constant throughout the test. These parameters include: 6” duct, inlet pressure of 0 Pa (gage pressure), outlet linear speed of 3 m/s, ambient temperature of 293.15 K, constant cold-side TEC temperature of 265 K, and the exterior walls will be given a surface radiation boundary condition to better simulate heat loss to the surroundings. All results will be compared to a control setup, with laminar flow, no constriction, and no heat pipes as seen in Figure 3.1.

3.2 COMSOL Simulation Results

The first problems we wanted to solve were determining whether the airflow through our system’s duct was laminar or turbulent and the ramifications of the type of airflow. There was a concern that turbulent flow might prevent steady heat transfer from the warm intake air into the cold heat sink. In COMSOL, two simulations, one with each airflow classification, were run where ambient air was passed over a heat sink mounted on a single TEC. Pictured below are the temperature profiles of the two simulations. It is important to note that all temperature values in this section are presented in kelvin unless otherwise specified.

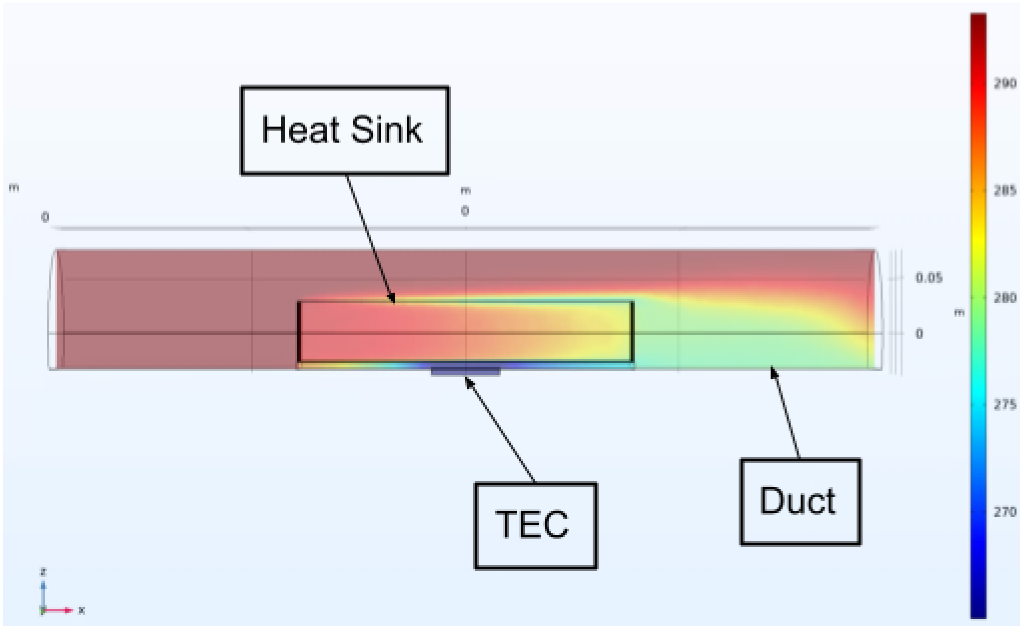

Figure 3.2: Temperature profile for laminar flow simulation in COMSOL.

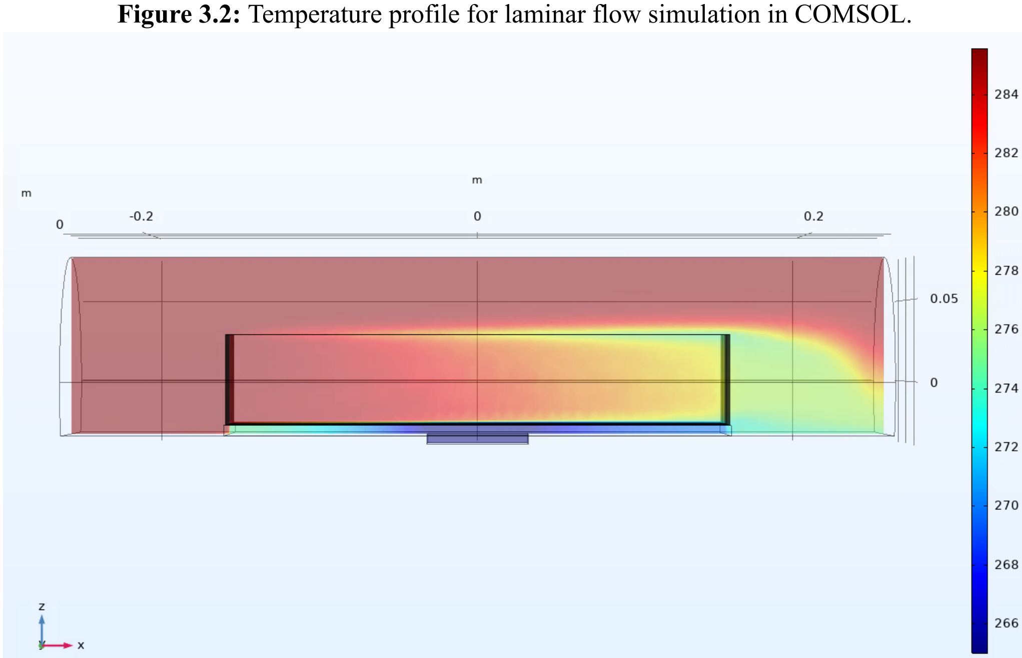

Figure 3.3: Temperature profile for turbulent flow simulation in COMSOL.

The results from this first simulation proved that the difference in airflow type posed to heat transfer in our system is negligible. The temperature profile of the air directly behind the heat sink was similar in both simulations with barely distinguishable temperature differences. Thus, it was determined that manipulating the airflow type in our system was unnecessary. In future simulations, laminar flow was used in order to cut simulation time, even though hand calculations of the Reynolds number show the flow to be turbulent.

The laminar and turbulent flow simulations also presented another problem. In both simulations, a significant amount of intake air was passing directly over the cold-side heat sink without transferring any heat at all. This was shown in Figures 3.2 and 3.3 by the large red-colored patch of air passing over the heat sink without any change in temperature. To prevent this from happening, we inserted flow restrictions at both ends of the heat sink to channel all the intake air through the fins of the cold-side heat sink. The following figures show the velocity profiles of intake air passing through the duct first without and second with the new flanges.

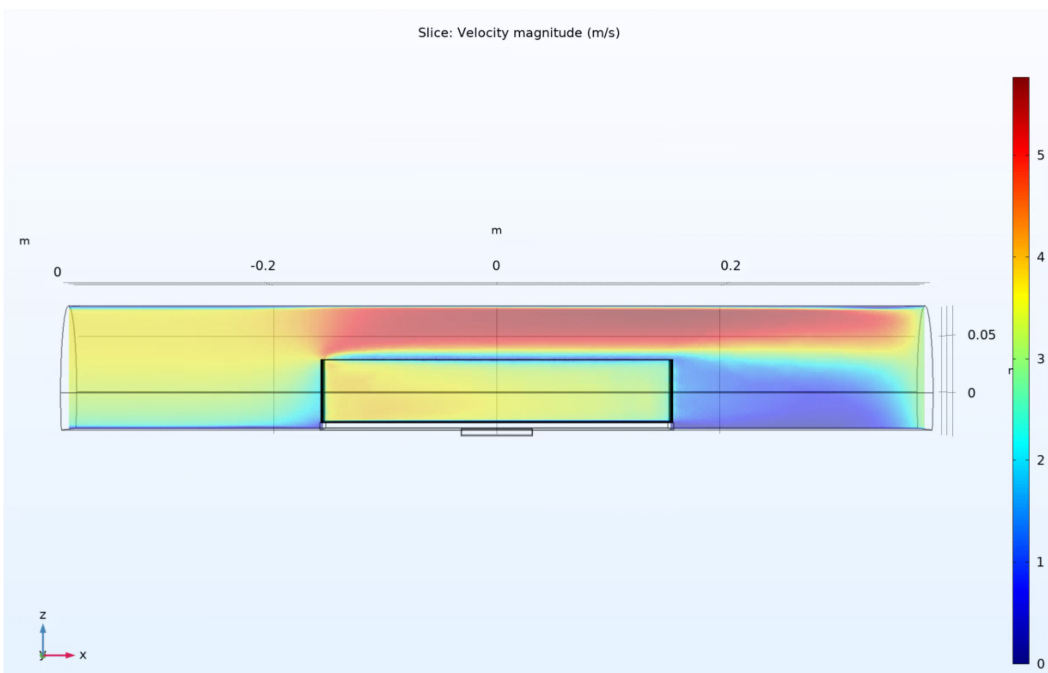

Figure 3.4: Velocity profile for airflow through duct without flanges.

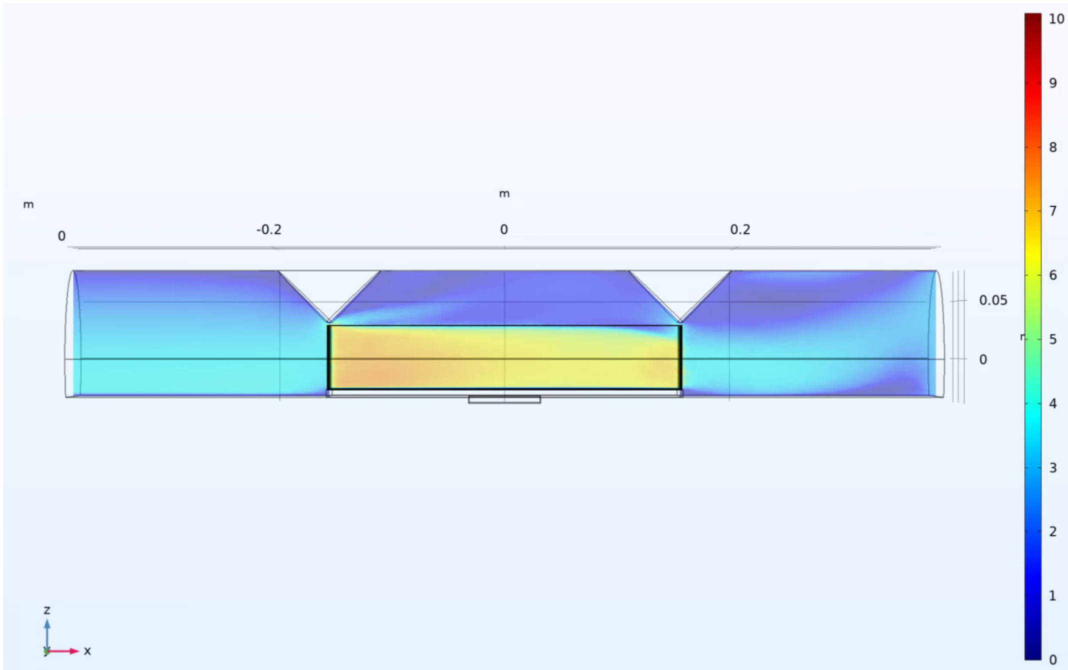

Figure 3.5: Velocity profile for airflow through duct with flanges.

In Figure 3.4, fast-moving air (shown in red) can be seen passing directly over the heat sink. This proves that a design without flanges will fail to efficiently cool all of the intake air that passes through the duct. However, Figure 3.5 shows that all of the intake air is channeled through the cold-side heat sink. The flanges not only prevent intake air from passing over the heat sink, but they also allow it to circulate in a small chamber between the flanges and above the heat sink. This will encourage further cooling and moisture removal from the intake air. The results of this simulation prompted more flange-inclusive simulations to be run, specifically to determine the effect of the flanges on the temperature profile of the air.

Since the inclusion of flanges proved to be beneficial by channeling airflow through the fins of the cold-side heat sink, a simulation was run to test their effect on intake air temperature. Pictured below are temperature profiles of the airflow taken from two different viewing planes:

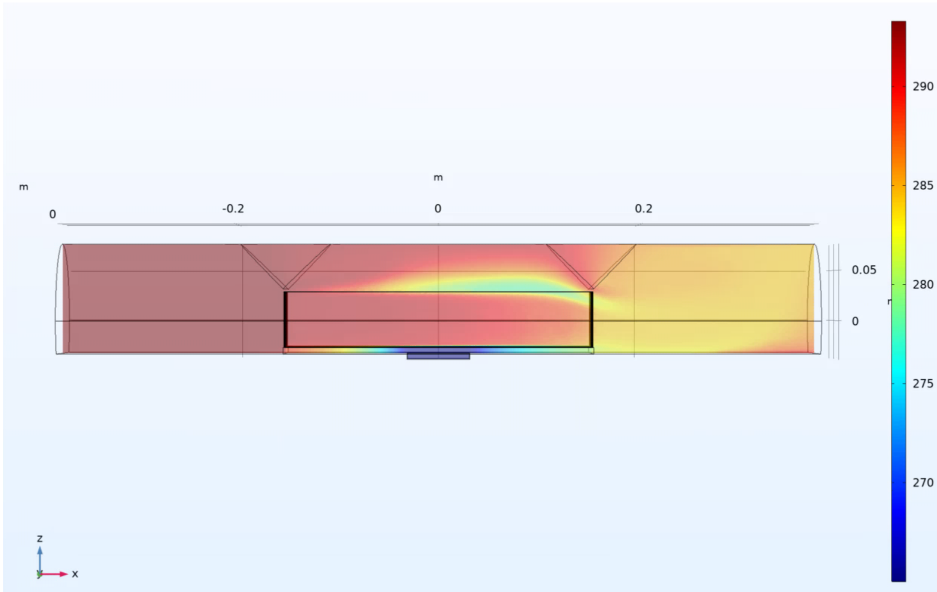

Figure 3.6: Temperature profile for airflow through duct with flanges, viewed in the X-Z plane.

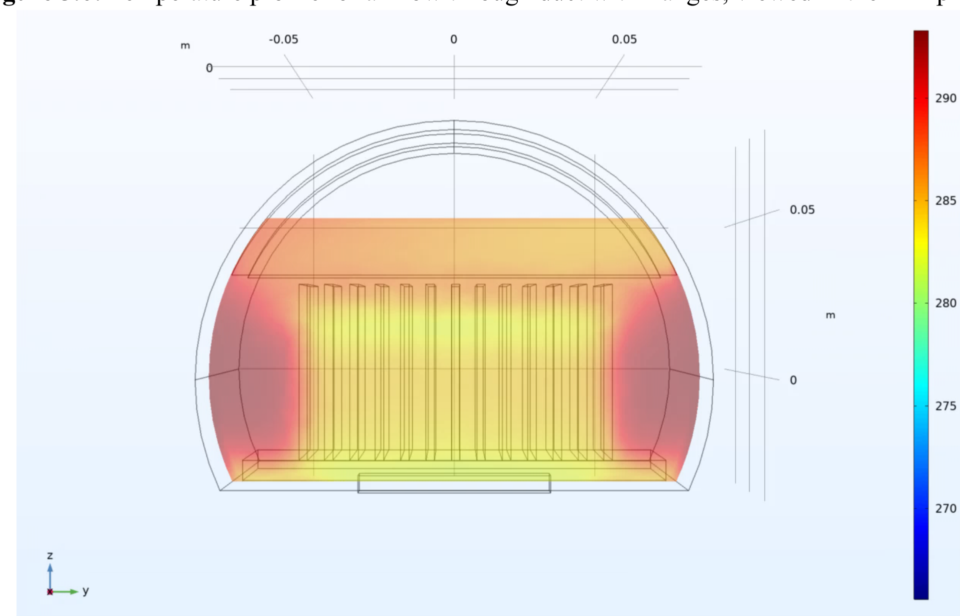

Figure 3.7: Temperature profile for airflow through duct with flanges, viewed in the Y-Z plane.

The results of this simulation confirmed that the inclusion of flanges is beneficial to the uniform cooling of intake air. In Figure 3.6, the chamber created by the flanges mentioned above allows air to circulate and reach temperatures as low as ~277 K. Both figures also show that the air that passes through the heat sink reaches a uniform temperature of ~285 K.

The following simulations were carried out for the purpose of comparing the thermal efficiency of the use of heat pipes in comparison to other thermal-resistance-reducing agents. To briefly clarify the function of heat pipes, as seen in Figure 3.8, they are most commonly made of aluminum or copper and offer a high thermal conductivity. The heat pipes will rest between the TEC and the heat sink and serve to enhance the transfer of heat between the two surfaces.

We compared the effectiveness of the heat pipes to using two TECs. However, using two TECs meant our power draw would increase. The results of the comparison showed that with the same inlet temperature of 293.15 K, the model with heat pipes lowered the temperature of the air by 8.79 K, compared to 7.65 K for the two TECs. Relating this to our control model these temperature changes show a 28.1% efficiency increase with the two TECs and a 47.2% efficiency increase with the use of the heat pipes. It was concluded that using heat pipes over multiple TECs was favored as the heat pipes are more efficient and do not require additional power draw.

Following our previous two simulations, we added the flange restrictions to the duct in addition to the heat pipes as seen in Figure 3.7. With these two modifications over the control model, we achieved an 88% efficiency increase, or a change in temperature across the heat sink of 11.21 K.

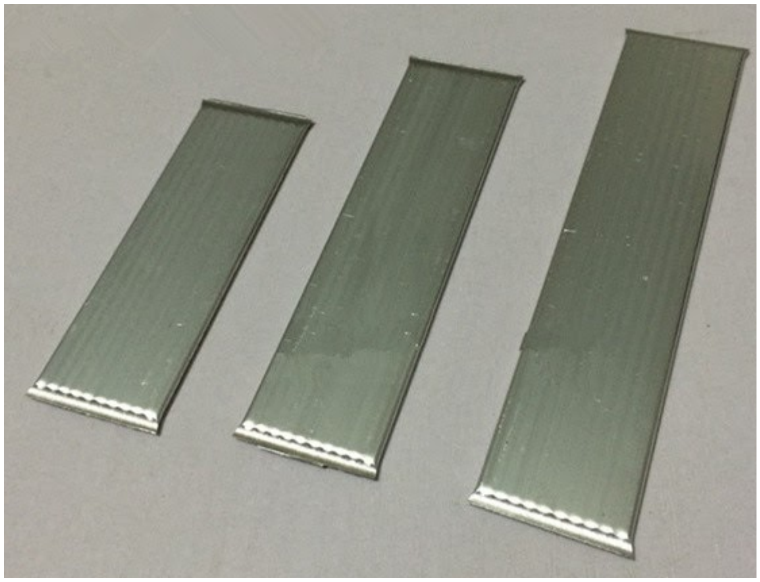

Figure 3.8: Flat aluminum heat pipes

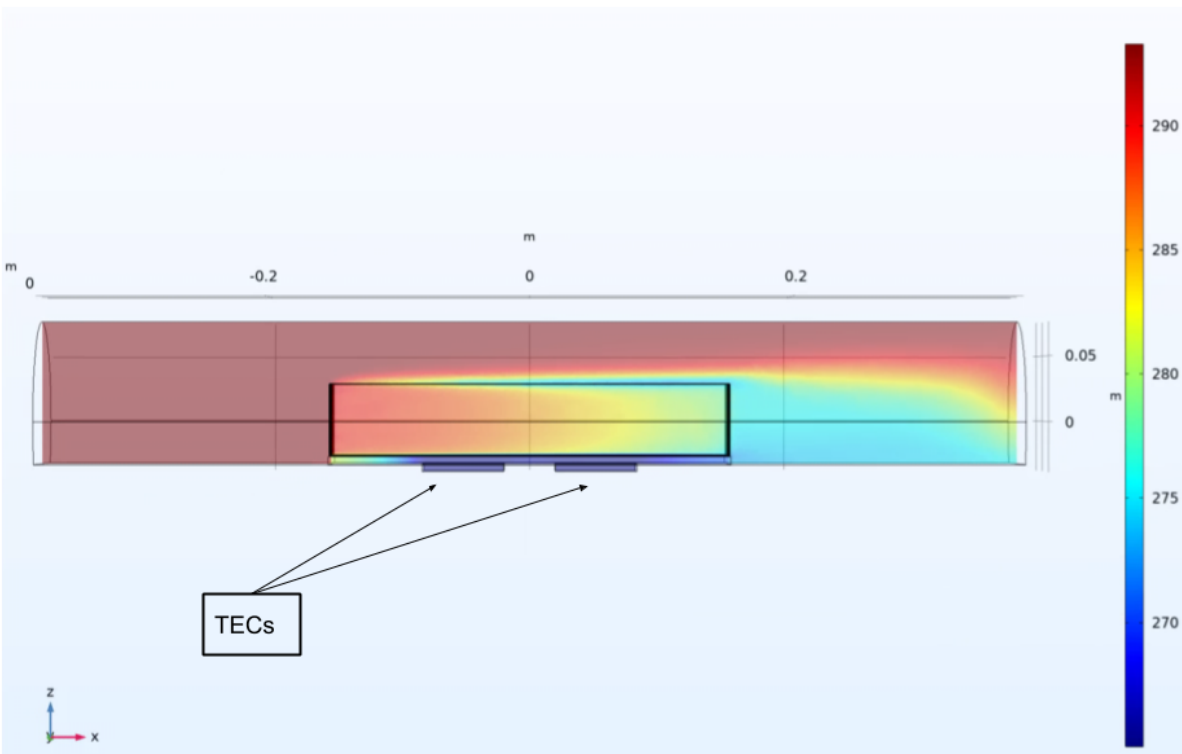

Figure 3.9: Temperature profile for airflow through duct with two TECs, viewed in the Y-Z plane.

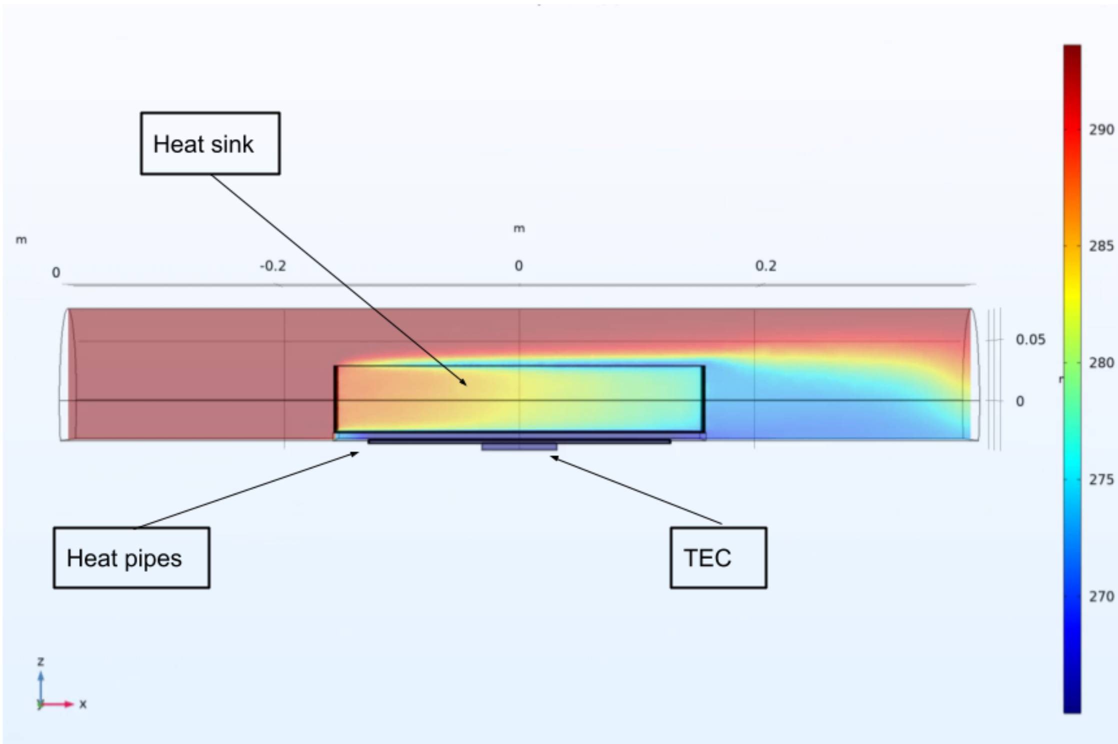

Figure 3.10: Temperature profile for airflow through duct with heat pipes, viewed in the Y-Z plane.

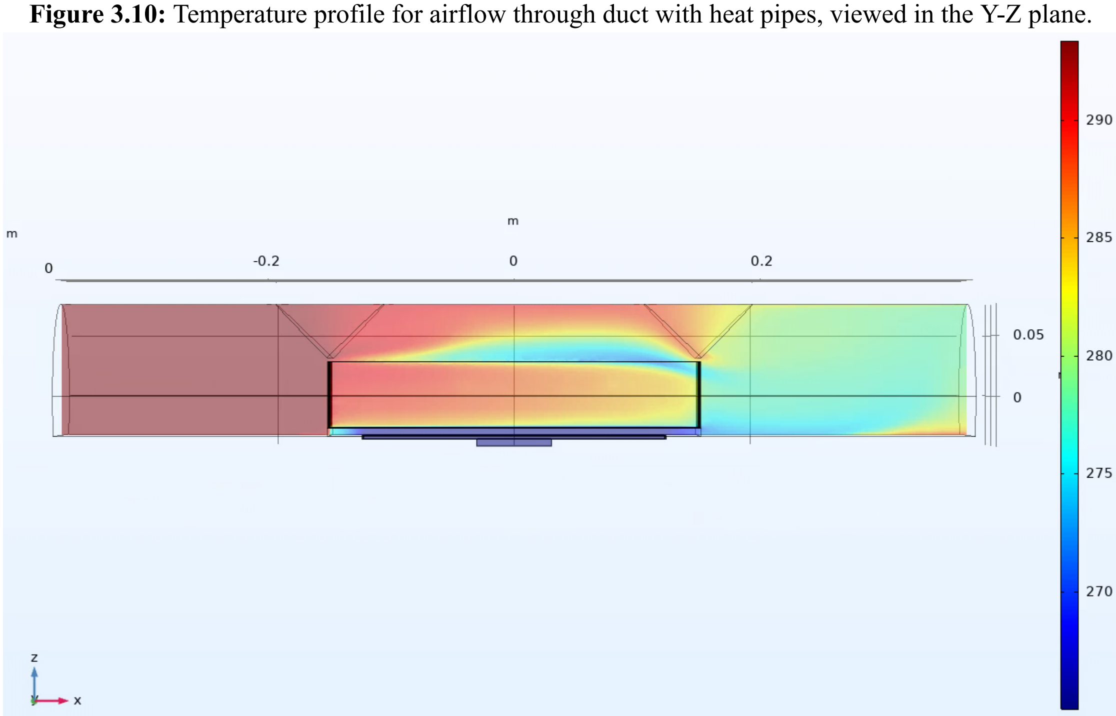

Figure 3.11: Temperature profile for airflow through duct with flanges and heat pipes, viewed in the Y-Z plane.

Physical prototyping of a full-length constriction revealed that the temperature of the air is highly affected by the amount of time the air remains in contact with the heat sink. Therefore, a baffle design was considered (see Figure 3.12). A series of baffles created two results. First, they increased the time the air was in contact with the cold heat sink. This brought the air's temperature closer to the temperature of the heat sink by the time the air exited the heat sink's fins. Second, the baffle created an order of magnitude increase in the pressure drop across the airstream. The latter result solidified our need to install at least one booster fan along the airstream. To maximize heat transfer over the hot-side heat sink, it was ultimately decided to place these fans directly before the air passed over this heat sink. Overall, adding the baffle design, implementing heat pipes, and the aforementioned flanges yielded the largest temperature difference of all the previous tests, being 21.5 K.

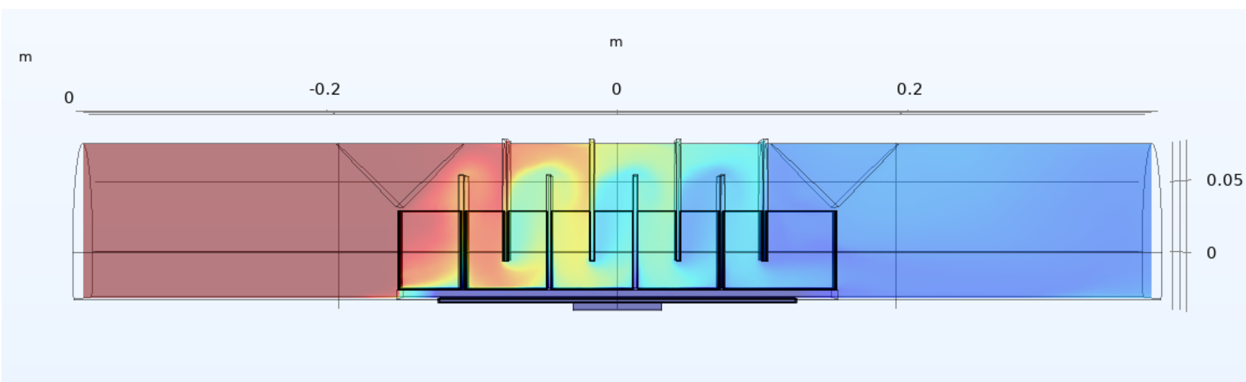

Figure 3.12: Temperature profile for airflow through duct with flanges, heat pipes, and a baffle viewed in the Y-Z plane.

3.3 Simulation Summary and Recommendations

Table 3.1 and Figure 3.13 contain a summary of the results from the primary COMSOL tests, where heat ratio is defined as the percentage increase in heat transferred compared to the control test. Adding the baffle yielded a heat ratio of nearly 250%, making it a clear choice to increase heat transfer. Our hand calculations predicted that at least 480 W of cooling load would have to be delivered from the TEC to the system (see Section 2.3). Although the chosen heat sink has a higher resistance than is required, we were able to reduce the temperature of the TEC and use heat pipes in conjunction with the flow constriction and baffles to reach the required cooling load. For example, with the heat pipes, constrictions, and baffles, around 1190 W of cooling load is generated, which exceeds the requirements set by the hand calculations by nearly triple.

Table 3.1: Summary of COMSOL testing results where the results for the varying features are compared to the control setup.

Feature	deltaT [°C]	q [W]	Heat Ratio [%]
Control	5.97	340.19	0.0
Constriction	6.69	381.21	12.1
Heat Pipes	8.79	500.88	47.2
2 TECs	7.65	435.92	28.1
Flange Constriction & Heat Pipes	11.21	638.77	87.8
Flange Constrictions, Heat Pipes, Baffle	20.78	1184.10	248.1

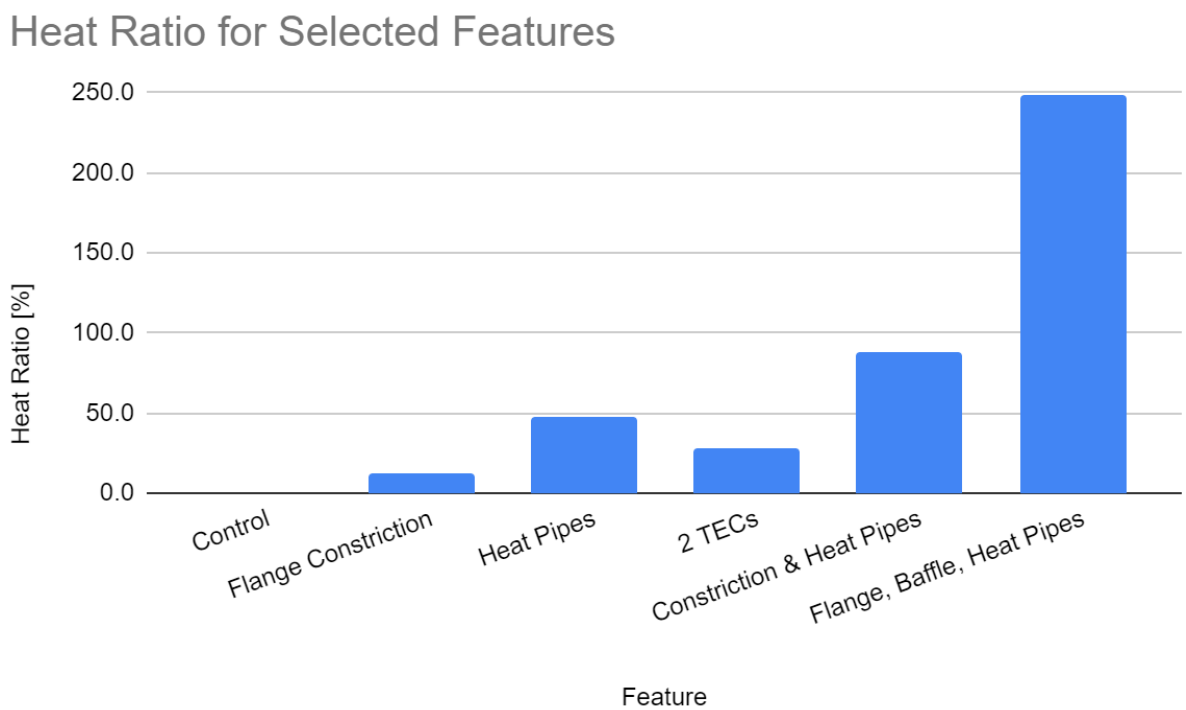

Figure 3.13: Graphical representation of the efficiency increase of the various features.

In summary, based on our FEA results, the use of flanges, heat pipes, and baffles would result in the greatest increase in performance for our design. With the use of flanges, more air will be forced through the heat sink. By adding heat pipes to our design, the TEC can disperse hot/cold energy more evenly across the heat sinks so that the incoming air has more time to absorb this energy at more locations across the heat sinks. The baffle greatly increases contact time. However, it also greatly increases the static pressure. Therefore, it requires the addition of fans inside the housing. Finally, from the FEA results, we found that the use of two TECs is not recommended as it requires twice as much power consumption and yields little gain in performance.

Chapter 4: Subsystems

4.1 Heating Module

The main goals of the Peltier cooler(s) (thermoelectric modules, TECs) and heat sinks subsystem are to use the cold side of the TEC to bring the incoming air below its dew point temperature to enable moisture extraction and to reheat the dehumidified air flowing across the hot side of the TEC and heat sink. Three different geometric layouts of the heat sinks and TECs were considered. The optimal one is that which maximizes moisture removal while minimizing manufacturing cost and power consumption.

The first design option, as depicted in Figures 4.1 and 4.2, has TECs in series with one another inside a duct with a constant cross-sectional area. Initial design calculations reveal that the heat sink for a single TEC system may need to be as long as 90 cm. Alternatively, this design will allow for shorter heat sinks that can fit into a small area. However, using two TECs will inevitably result in increased power consumption.

One benefit of using two TECs in series is that the duct would retain a constant cross-sectional area, making it relatively simple to fabricate. Across all designs, the fins of the heat sinks on top of the modules would be kept parallel to the air flow to minimize the pressure loss across them. This design is repeated on both the hot and cold side of the modules. Such symmetry is required due to the operation of TECs with a hot and cold side exactly opposite of each other.

As seen in the figures below, the cold operating area is on top, above the hot operating area. As a result of the moisture being removed from the air on top in this design, effective sealing would need to be done around the base of the heat sink to ensure the water does not flood into the compartment where the TECs and their wiring are located. Additionally, a wicking material will need to line the base of the heat sink fins and lead out of a small exit hole to the side of the duct where the water can be collected. This process can be seen in the simplified model in Figure 4.3.

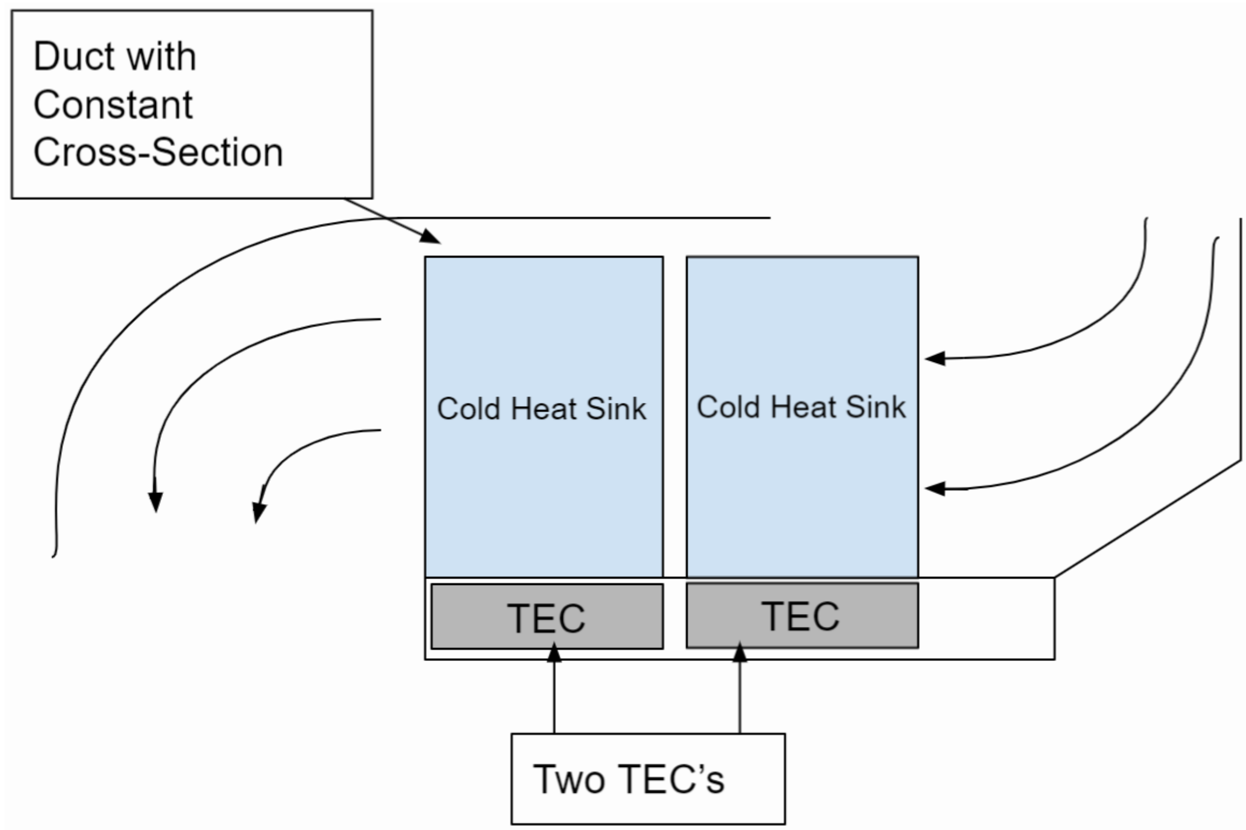

Figure 4.1: Design Option 1, cold side of TEC's and heat sinks.

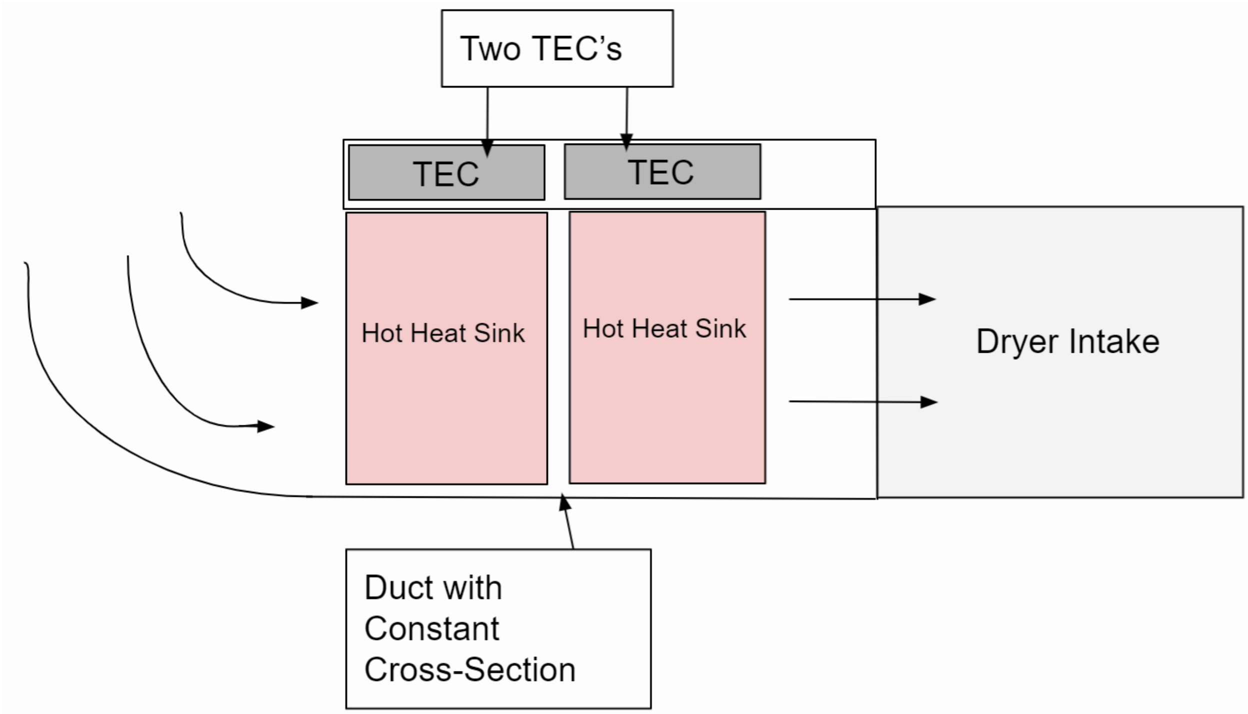

Figure 4.2: Design Option 1, hot side of TEC's and heat sinks.

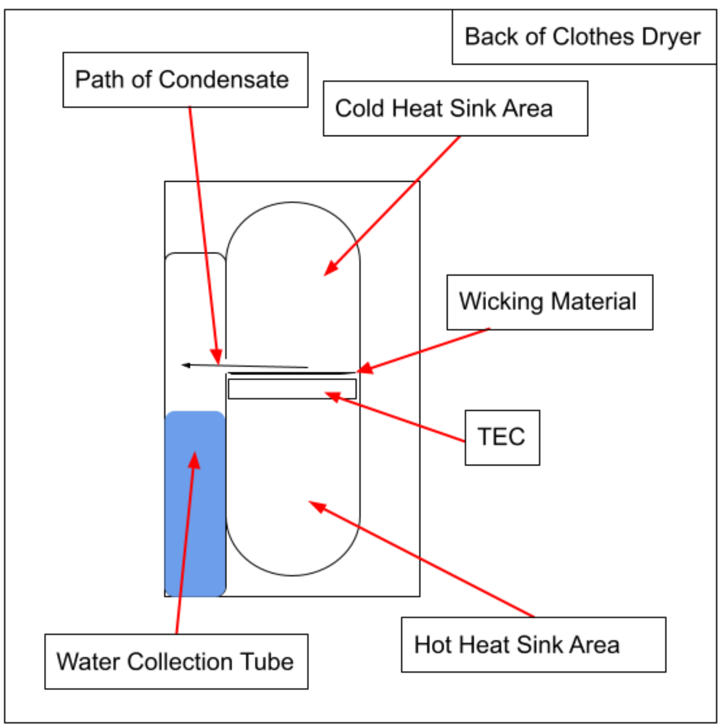

Figure 4.3: Example of the combination of subsystem options for the purpose of demonstrating the water collection method used in Design Option 1.

The second design option, as depicted in Figure 4.4 and Figure 4.5, features two main differences from the former design. First, the regions in which air comes into contact with the hot-side and cold-side heat sinks open up to a duct with a wider cross-section before narrowing down when transitioning between said regions. After brainstorming potential problems with our system, one of the concerns that arose was that the air might be travelling too quickly for it to have its moisture properly removed by the cold-side heat sinks. In other words, the hot side would not be able to sufficiently reheat the air as well. Creating a wider cross-sectional area where air comes into contact with the heat sinks causes the air to slow down by constant volume flow rate, thus providing the cold-side heat sinks with more contact time to remove moisture from it. In order to fit all the heat sinks in this wider cross-section, they must be aligned perpendicular to the flow of air, as pictured below. This design would use a similar water collection method as depicted in Figure 4.3.

Although this design solves the problem of the air having too little contact time with the heat sinks, it would likely be difficult to fabricate. It is unlikely that a flexible duct with this shape is sold online, so it would most likely have to be custom fabricated by our team. Another potential issue with this design is that introducing the changing cross-sections may cause disturbances within the airflow that will consequently lead to a drop in efficiency.

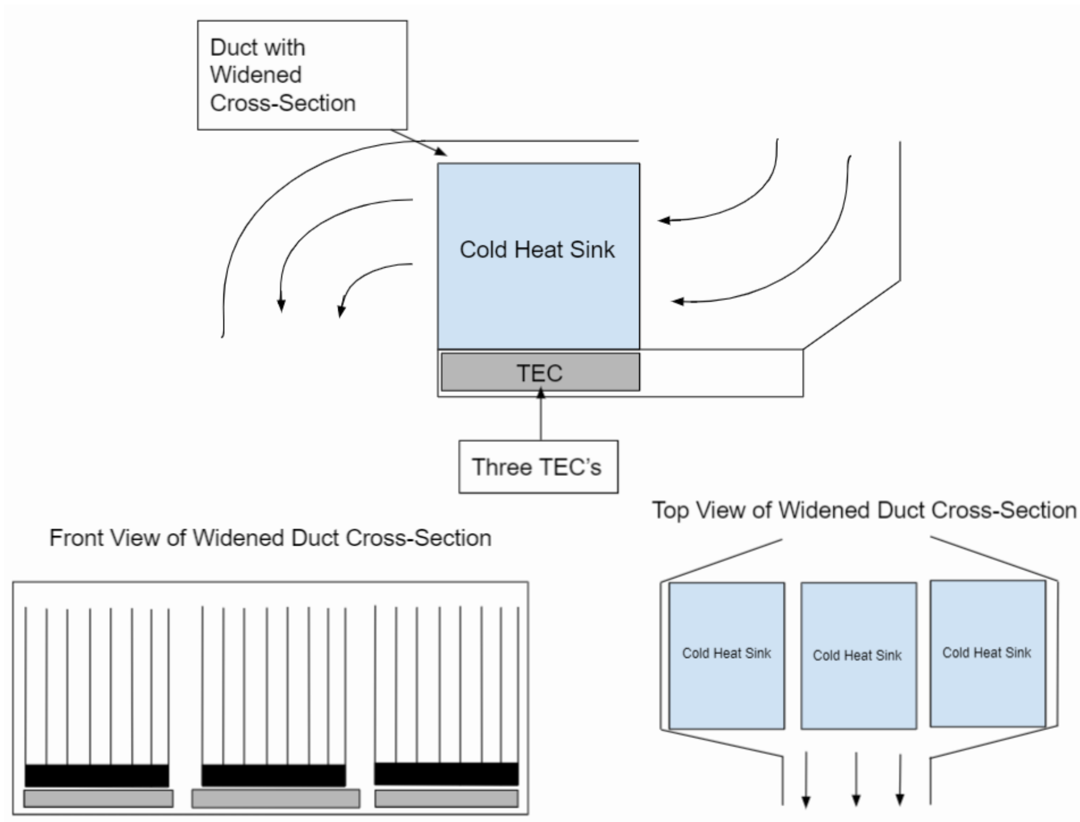

Figure 4.4: Design Option 2, cold side of TECs and heat sinks with widened duct cross-section.

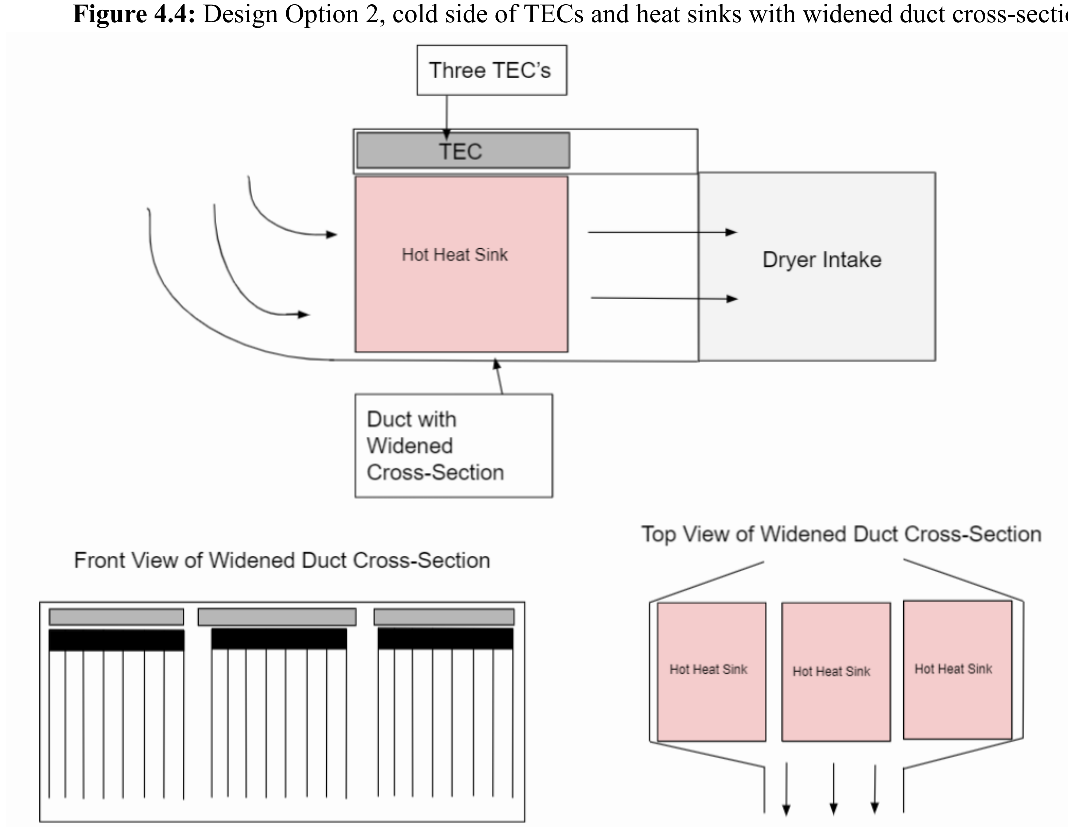

Figure 4.5: Design Option 2, hot side of TECs and heat sinks with widened duct cross-section.

The third design option, as depicted in Figure 4.6, features a taller cross-section at the cold-side heat sink region and a shorter cross-section at the hot-sink heat sink region. Since the main goal of the system is to remove moisture from the dryer intake air, the taller cross-section enables the use of a larger heat sink which will increase the rate of heat transfer between the cold fins and the air. Similar to the last design, the increase in cross-sectional area in this region will also lead to a decrease in flow speed, granting the fins more contact time to remove moisture. This design is applicable to both previous design options as well.

This design shares a similar problem to the last design: it assists the problem of air having too little contact time with the heat sinks but will likely be impossible to purchase premade. The need to fabricate the specific ductwork geometry makes this idea less appealing, but it is certainly within the realm of plausibility. Further testing and analysis will need to be conducted with a prototype model to determine the loss versus gain value of these geometrics.

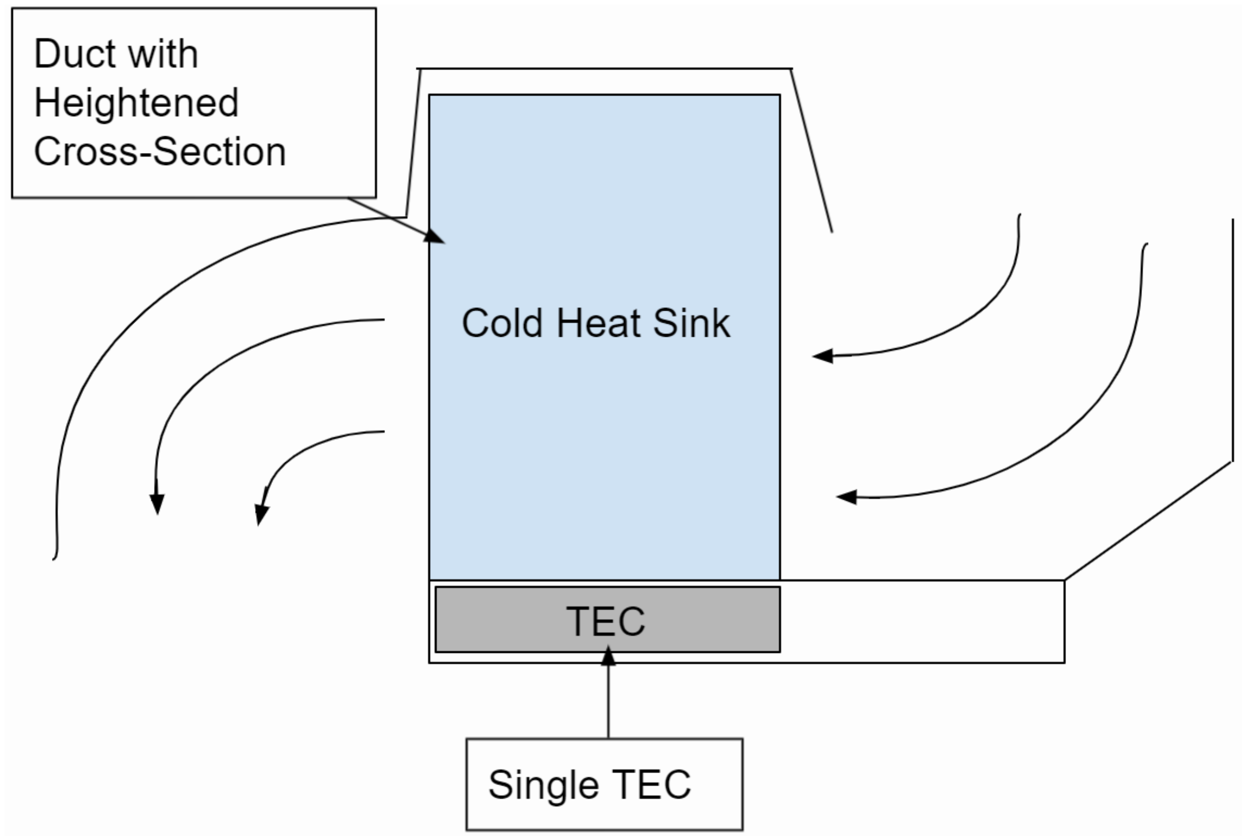

Figure 4.6: Design Option 3, cold side of TECs and heat sinks with heightened duct cross-section.

The final design option, as depicted in Figure 4.7, utilizes a duct with a constant cross-sectional area, where air can flow through a heat sink. The heat sink would be oriented parallel to the air flow as in previous designs. This design is the most recent sketch we have created. It was inspired by the building of the prototype where we came to the conclusion, while discussing the water collection method, that it may be easier and safer to invert our system and have the cold heat sink on the bottom. This allows for the moisture being removed from the ambient air to collect on the heat sink fins and be fed by gravity down into the base of the duct. A wicking material will then guide the moisture to a collection tray located at the bottom of the system housing. The purpose of this design option is to minimize the risk that moisture will leak either into the compartment where the TEC and its wiring lies, or down the ductwork to where the hot heat sink is in previous design options.

Another change to this design option from previous ones is the air intake ductwork. As seen in Figure 4.7, as the ambient air is taken into the system from the intake, it travels down and into the side of the system below the wiring area. This winding of the ductwork allows for a minimalistic overall footprint of our system as the design should not be too bulky.

This design option would be one of the easiest to manufacture and assemble because no changes to the cross sectional area of the duct would need to be made. However, this design uses only one thermoelectric module, which may require a very long or tall heat sink in order to cool the air to dew point. Additionally, if testing proves necessary or beneficial, this design option can be combined with previous ones to incorporate changes in the ductwork geometry.

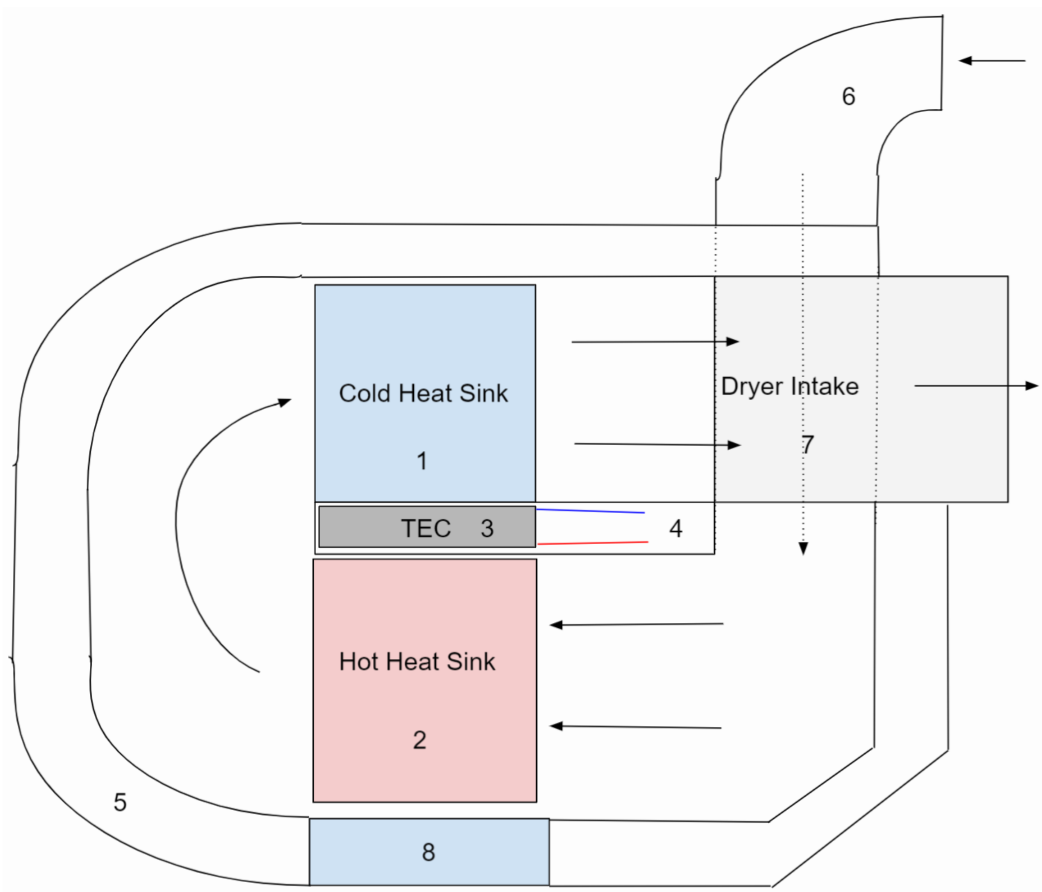

Figure 4.7: Design Option 4, inverted design with TEC hot side on top and TEC cold side on bottom. Numeric labels are as follows: (1) Heat sink attached to hot side of Peltier cooler (2) Heat sink attached to cold side of Peltier cooler (3) Peltier cooler (4) Wiring to power supply on backside of module in reference to figure side view (5) Insulative material inside outer housing (6) Ambient air intake (7) Dryer intake (8) Water collection tray with wicking material.

Our COMSOL test simulations in Chapter 2 and initial peltier cooler testing outlined in Chapter 5 determined that the cooling load needed for our design purpose could be created with larger heat sinks and TEC's. Heat pipes, thermal paste, and heat sink baffles were also implemented in order to promote smoother heat transfer between the TEC and heat pipes while improving airflow through the system. An exploded view of the design is shown in Figure 4.8.

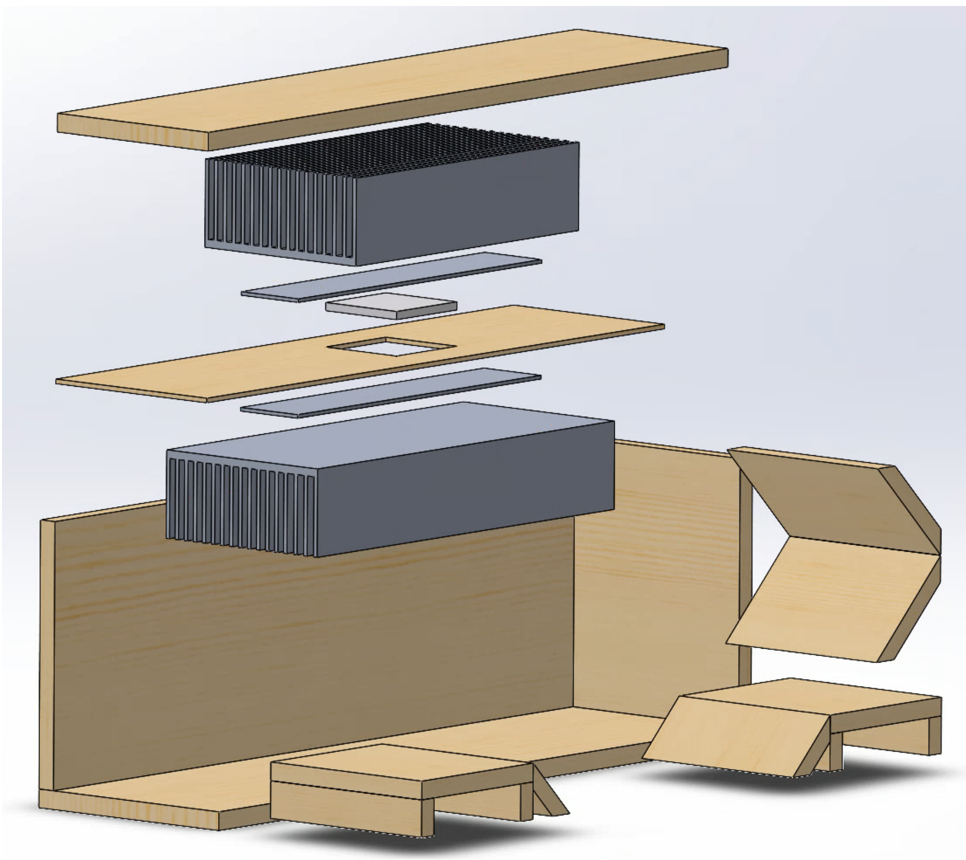

Figure 4.8: Exploded view of heating module and water collection system.

4.2 <u>Water Collection System</u>

The water collection subsystem serves the purpose of collecting moisture that has been removed from air passing through the system. As can be seen in Figure 2.8, the water collection system resides below the cold heat sink in the lower channel of the design. The subsystem is made up of two components. The first is the collection tray which is embedded in the bottom portion of the wooden housing box. The second component is a wicking material acting as a liner around the collection tray and along the tops of the heat sink fins (due to the upside-down orientation of the heat sink in the lower channel) which allows moisture collecting on the fins to drop down with the pull of gravity and absorb in the wicking material. The moisture is then drawn down through the wicking material into the collection tray reservoir. Due to the collection tray being made from wood in this design, there is a waterproof liner on the inside wall of the tray. This prevents water from seeping into the wood and causing mold.

The design process of creating the water collection system went through various iterations. In the early stages of our design, we did not plan for including a method of collecting excess moisture. Our assumption was that we could rely on evaporation during non-operating hours to clear the system of moisture that had been removed from the air. In fact, we had the cold heat sink in the upper channel of our system in the first sketches of our design as can be seen in Figure 4.9 and Figure 4.10.

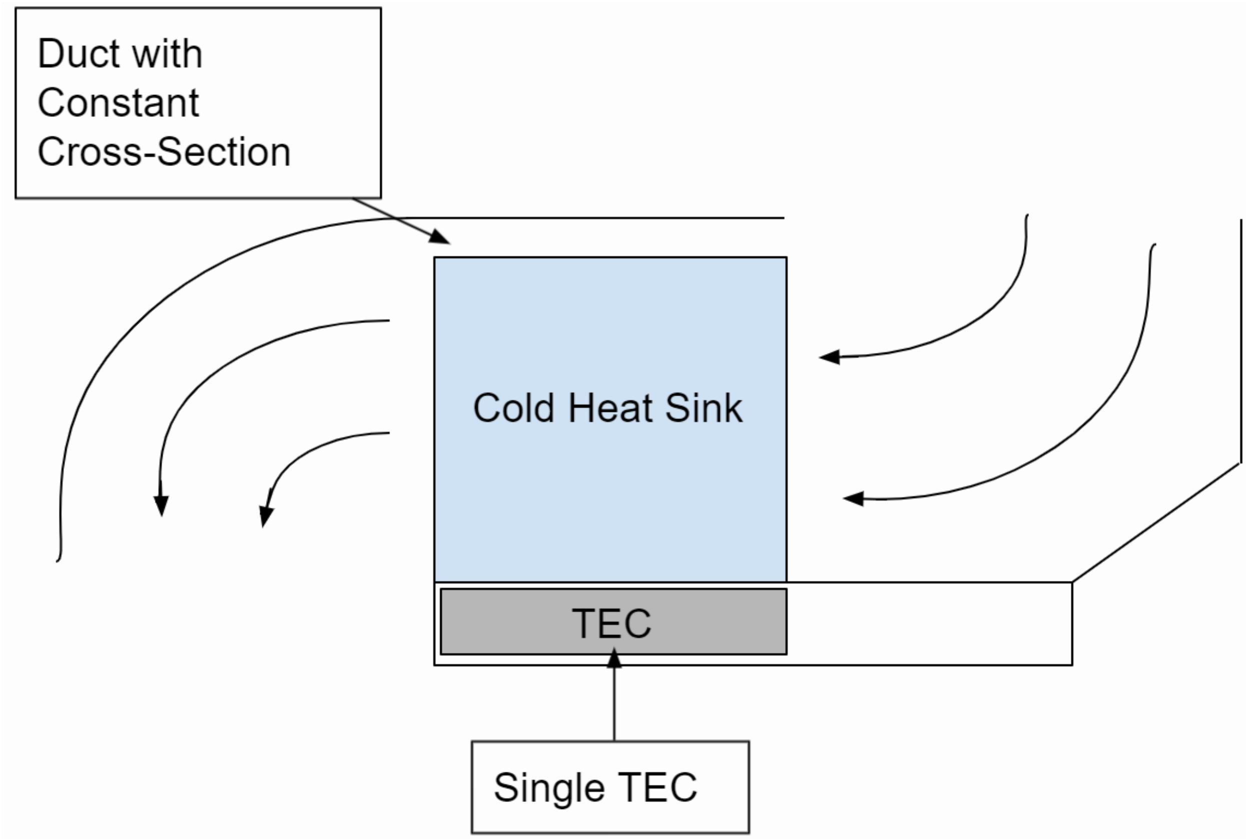

Figure 4.9: First iteration of heating module design (cold side).

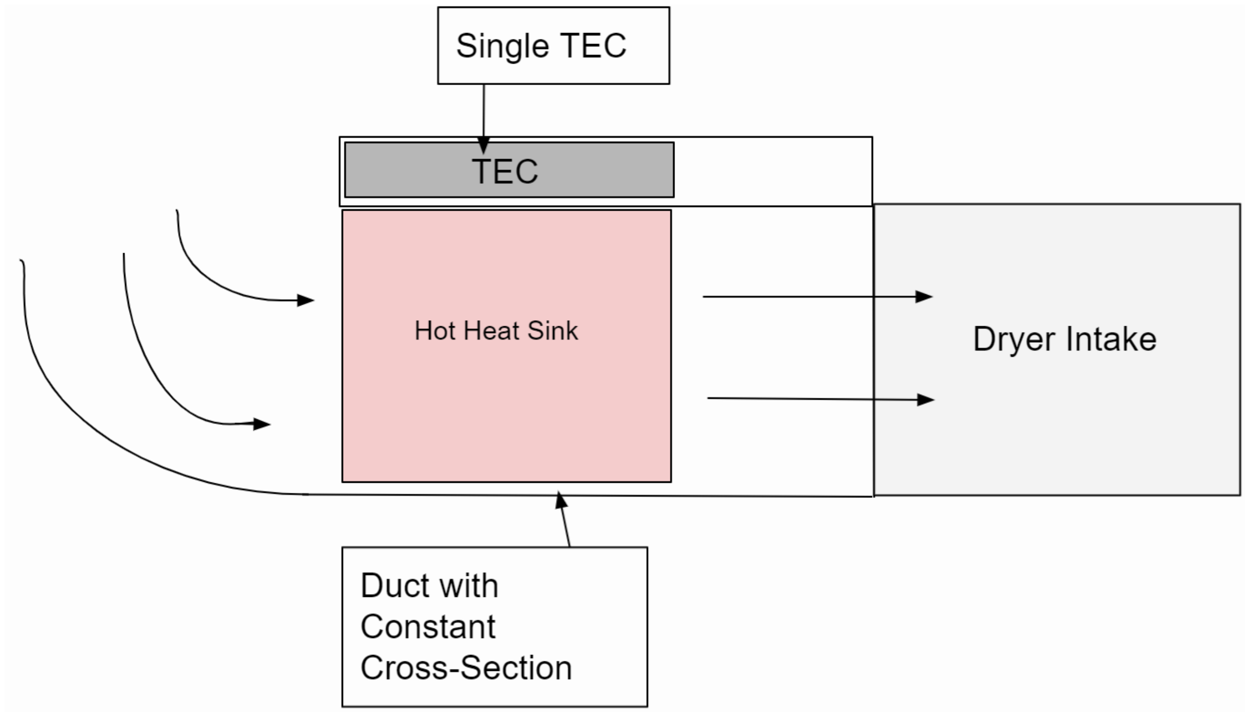

Figure 4.10: First iteration of heating module design (hot side).

After further research we found that there was potential, especially in particularly humid areas, for our system to remove enough moisture from the system that it could cause issues within the system. We also determined that in order to incorporate a method for collecting excess moisture from the system we would need to flip the orientation of our heating module, meaning that the cold and hot designated heat sinks switch places in the design. Otherwise, because the cold heat sink is the one forming condensate, if it is placed in the upper channel the excess moisture would collect on the base of the heat sink which lies directly above the TEC causing a clear hazard to this expensive piece of electrical equipment which our system relies on. Additionally, changing the orientation of the heat sink to place the cold heat sink on the bottom would allow for the moisture that collects on the fins to naturally drip off due to gravitational forces.

The next step in the design process was to draw up our vision of what a water collection system could look like in this new design configuration. In our first dimensioned drawing of the design, shown in Figure 4.11, we utilized a thin divider to separate the fins of the cold heat sink from the water collection tray. This divider has an arrangement of holes in an equidistant 2x8 fashion. A layer of wicking material lies between the divider and the heat sink fins. This wicking material also feeds in through the holes of the divider and into the collection tray. Hence, the condensate forms on the fins of the cold heat sink, drips down after accumulating, and comes into contact with the wicking material which draws the moisture in through the holes and directs it into the tray.

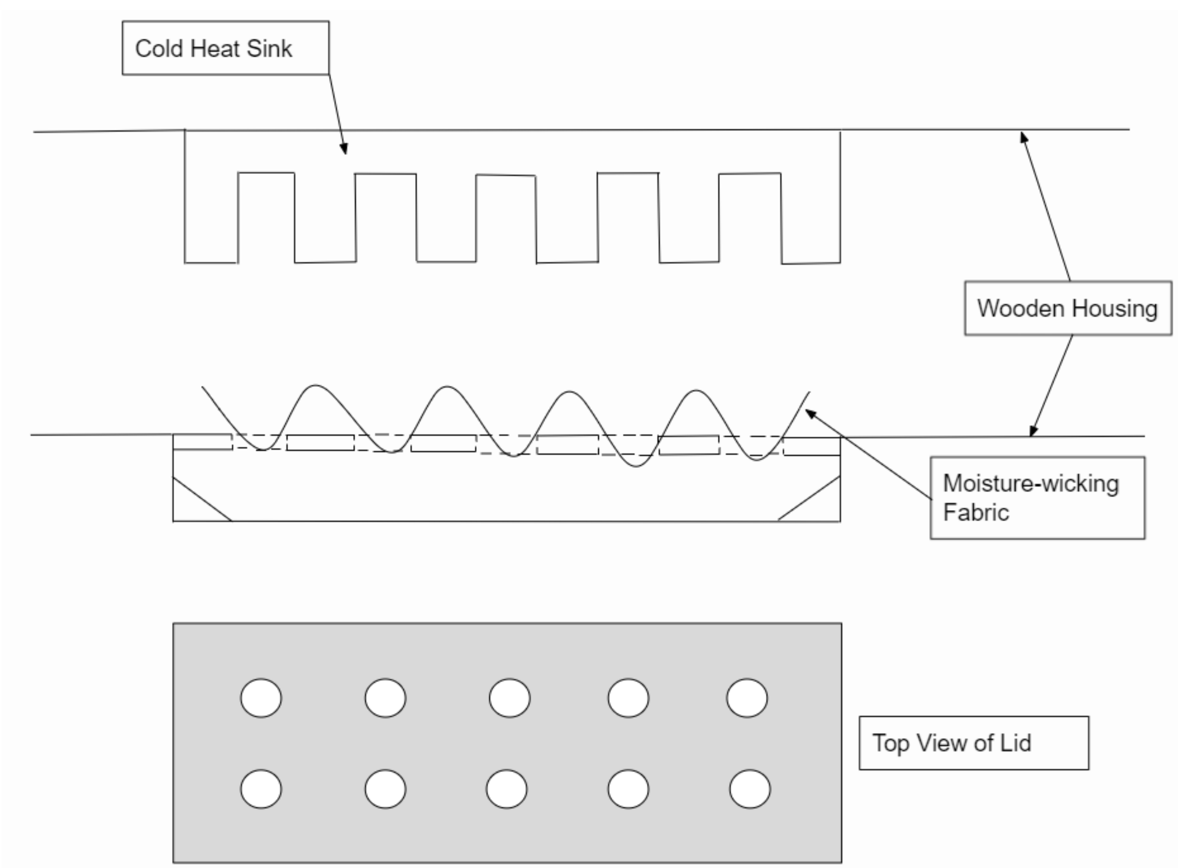

Figure 4.11: First Concept drawing of water collection system design.

The first prototype we constructed of the water collection system was directed towards testing the performance of the heating module more so than it was for mocking up a full and complete design. Additionally, the pieces of the prototype were not secured in order for them to be removable for ease of access to the system during testing. This made a water collection system not necessary in this first prototype. As we moved into our second prototype and a more complete design, we constructed the water collection system which can be seen in Figure 4.9. This served as our first prototype of the water collection subsystem. In this design we left out the divider as we planned to use from Figure 4.11 due to conflicting space with the baffle design we incorporated after already producing the first dimensioned drawing of the water collection system. Besides this divider not being included, the premise of the subsystem remains the same and can be seen pictured in our second prototype in Figure 4.12.

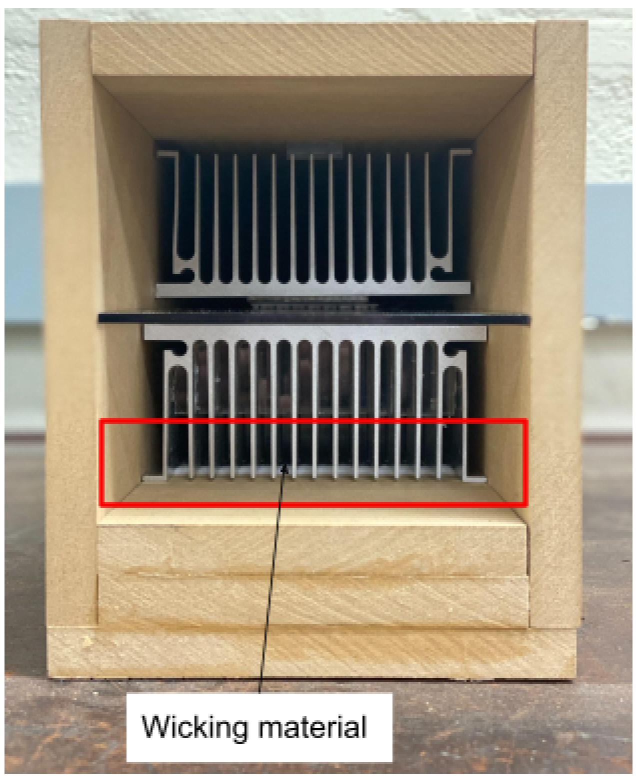

Figure 4.12: Front view of wicking material leading to water collection tray lining the fins of the cold heat sink.

As a result of limitations on time and resources due to the COVID-19 pandemic, our team was unable to conduct thorough testing on the second prototype and thus did not achieve verification of our design of the water collection subsystem. We plan in the future on continuing testing on the second prototype to allow us insight into the potential faults and successes of our current design for the water collection method. Accordingly, we will make adjustments if needed to this subsystem to allow for optimal removal of excess moisture from the system.

4.3 Dryer Attachment System

The dryer attachment system is the link between our product and the clothes dryer. The main component of this subsystem is our custom 3D-printed outlet attachment (see Figure 4.14). This part attaches to the outlet of our system, which is simply the exit point of the air traveling through the upper channel of the system. Due to the rectangular nature of the channels in our design, and the circular inlet to the dryer, we needed to create a part that would transition the rectangular channel to a circular 4” duct. To accomplish this task we used Solidworks CAD software to create this transitional part with the appropriate dimensions for our system. The result can be seen in Figure 4.15, Figure 4.16, and Figure 4.17. We made the circular section of 4” diameter match up with the 4” duct we would use to feed into the dryer inlet. The two flanges pictured at the bottom of Figure 4.15 wrap around the outside of the wooden housing of the main system and are adhered and screwed in to ensure no air escapes to the ambient environment during this transition point.

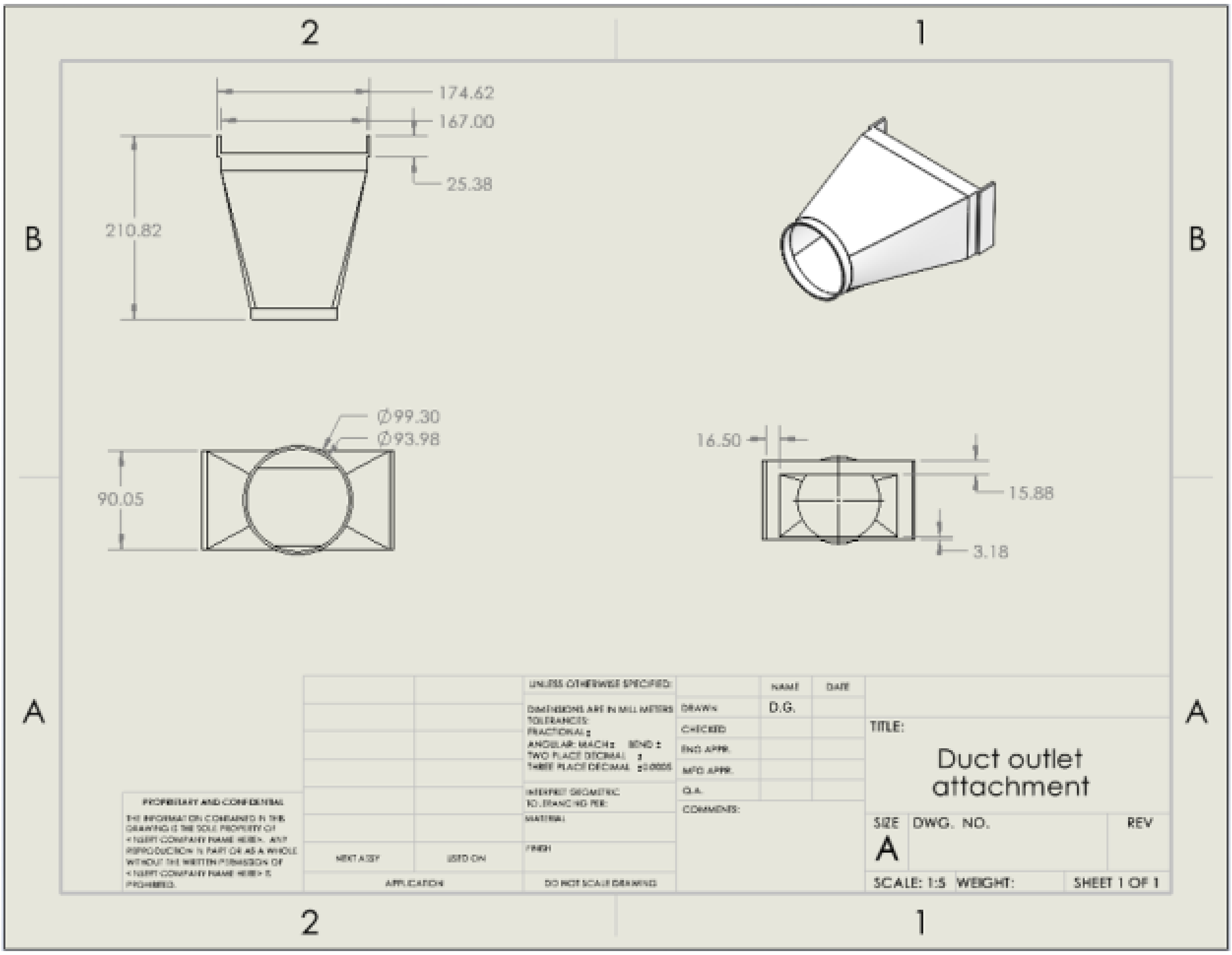

Figure 4.13: Dimensioned CAD drawing of dryer attachment system.

(a)

(b)

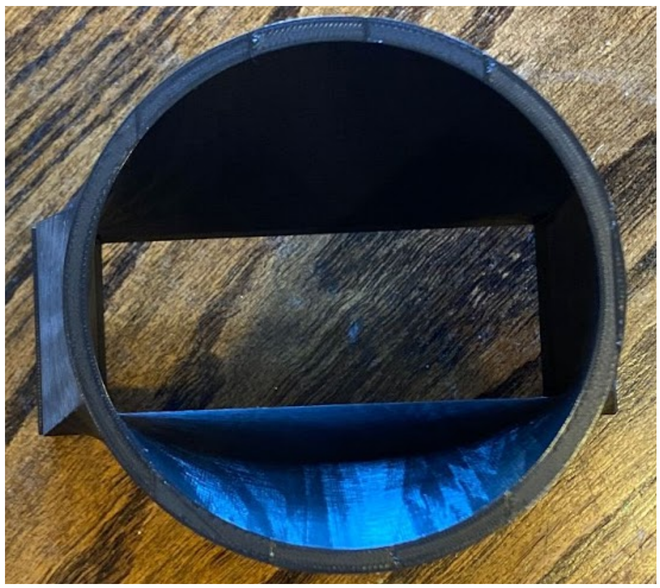

(c)

Figure 4.14: Dryer attachment system (a) side view, (b) top view, (c) bottom view.

Our team's design for the dryer attachment subsystem started out based on research we had done in the Fall quarter on vented clothes dryers. This research showed us that many dryers take in air from a set of vented slots located on the back panel of the dryer. Figure 5.15 shows these vents from an internal view of the dryer. Our team had plans to access a clothes dryer in the Santa Clara University machine shop for research and testing, but due to the restrictions of COVID-19 at this time we were confined to a virtual meeting format. This meant our research on methods of attaching our system to the dryer had to be done through the internet and use of our personal clothes dryers. In fear of our personal hygiene, we chose not to take apart our personal clothes dryers and from our online research we believed that in order to control airflow into the dryer we would need to completely enclose the vents I mentioned above. Thus, we created our first design iteration for the dryer attachment method as shown in Figure 4.18 and Figure 4.19. Figure 3.18 shows the entire design with a modified outlet to feed directly into a 6” duct. We planned to have this duct feed into the wooden housing unit from Figure 4.19. This housing unit would be sealed around the vents to control airflow into the dryer. However, once we were able to meet in person and gain access to the Santa Clara University provided clothes dryer, we took it apart and found lots of valuable information we had missed by just viewing our personal dryers from the outside. We found that the dryer had a slot we could use to feed a 4” duct directly into the dryer (see Figure H.1 and H.5) which we previously assumed to be an exhaust duct routing slot. Through this dryer inlet slot we could route the 4” duct directly to the air heater (see Figure 5.15). This new information we had gained from taking apart the clothes dryer is what led our team to redesign the dryer attachment system to what it is in Figure 4.14.

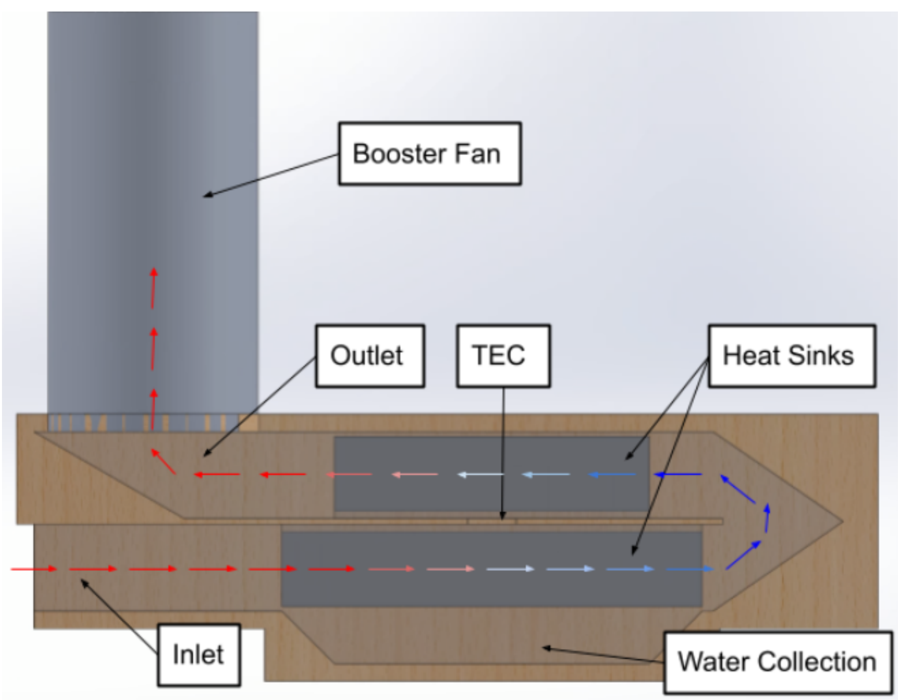

Figure 4.15: First design iteration of dryer attachment system (attachment method).

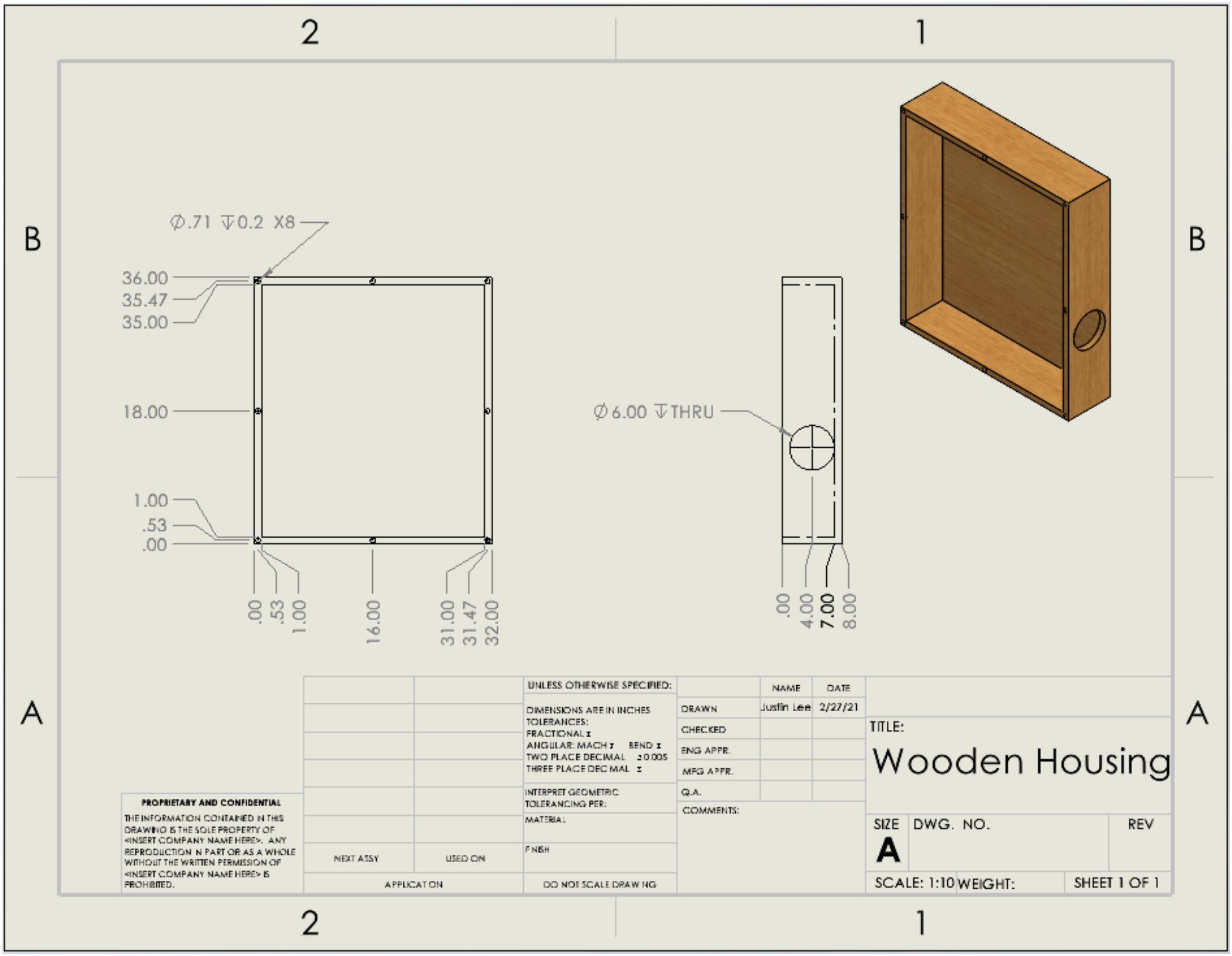

Figure 4.16: First design iteration of dryer attachment system (wooden housing).

Chapter 5: Testing and Prototype Construction

This chapter summarizes the test results performed on the Peltier coolers and prototypes and a brief analysis of the dryer obtained from the SCU Frugal House. The initial Peltier cooler tests were performed with the objective of finding the most optimal power level and voltage to run the coolers at in order to obtain the coldest TEC temperatures while maintaining an economical level of power consumption. Obtaining the most optimal voltage values also accelerated the prototype testing process by providing a reference voltage for the first few prototype tests.

5.1 Initial Peltier Cooler Testing

To test the capabilities of the heating module, preliminary tests were performed before any prototype construction. These tests measured factors such as lowest TEC temperature, lowest cold heat sink temperature, and the time and power needed to achieve these temperatures. These tests were run by a single team member at their house using a single TEC, small computer fan, DC power supply and probe thermometer. Figure 5.1 shows an early setup used to find the cold temperature range of a TEC. At the time, the TEC was wired in parallel with the fan because only one power supply was available. Measurements were made with the probe thermometer by holding the thermometer tip against the cold side of the TEC for extended periods of time. These tests were run for about three minutes because the lowest TEC temperature would usually occur after one minute and then it would slowly begin to rise. With this arrangement, the lowest temperature reached was 8.3 °C at 4.75 V after 50 seconds. This testing setup was used until new heating subsection components were obtained.

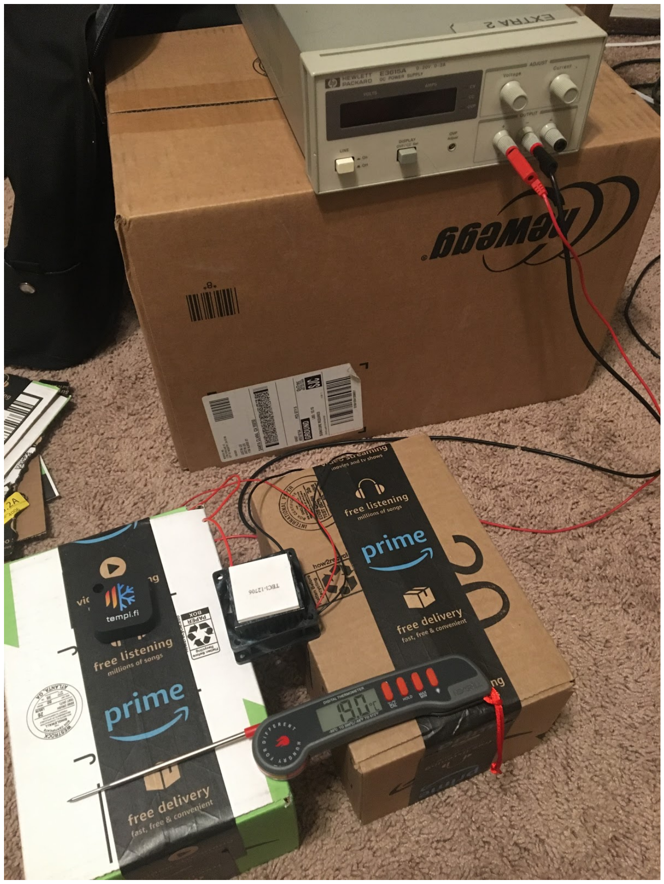

Figure 5.1: First TEC Testing Setup.

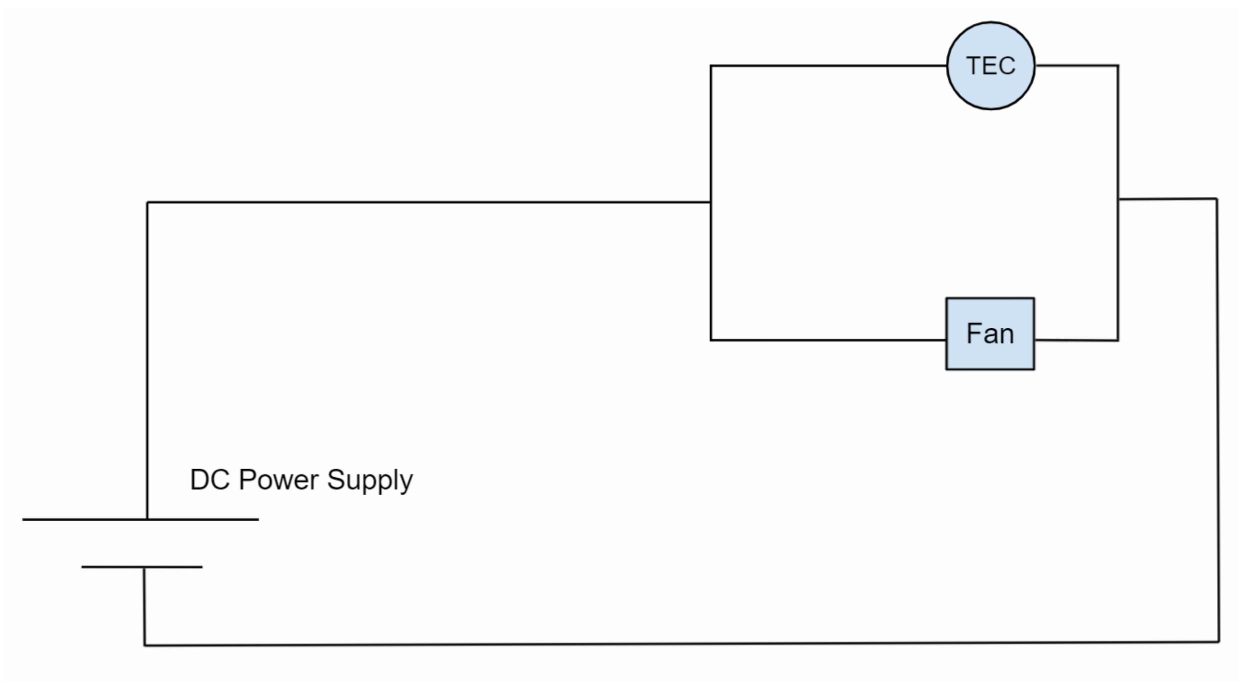

Figure 5.2: Circuit Diagram for first TEC Testing Setup

After ordering larger heat sinks and new TECs to test, the testing setup was adjusted in order to accommodate for the change in heat sink size. Figure 5.2 shows the setup for these tests. The largest change to the setup components are the use of new TECs and heat sinks, which were able to reach much lower temperatures than the original TEC in the first testing setup. Another important addition was the use of a fan blowing upwards against the hot heat sink. This allowed for more heat dissipation which kept the hot side of the cooler from overheating. The last change is the use of a separate power supply that can power the TEC separately so that the power applied to the fan and TEC could be controlled and measured more easily.

A total of three new coolers were purchased and tested which will be referred to as Coolers A, B, and C. Coolers A and B are both larger in size and can produce larger cooling loads than Cooler C and the original cooler. The lowest temperature that Cooler A was able to reach was -22 °C at 10 V after two minutes. At near freezing temperatures, condensation began to form on the surface of the TEC and as the temperature lowered, small shards of ice began to form as well. However, Cooler B did not produce temperature differences that were as consistent and high as Cooler A. The lowest temperature that Cooler B was able to reach was 6.4 °C at 6.6 V after one minute. Additionally, Cooler C was able to produce consistent results, but the temperatures achieved were not as low as Cooler A. The lowest temperature that Cooler C was able to reach was -3 °C at 9 V after one minute. After achieving these results, more focus was placed on finding the lowest possible temperature that a cold heat sink could achieve. Since the other coolers were not performing as well, Cooler A was tested more often during the initial Peltier cooler tests and heat sink tests.

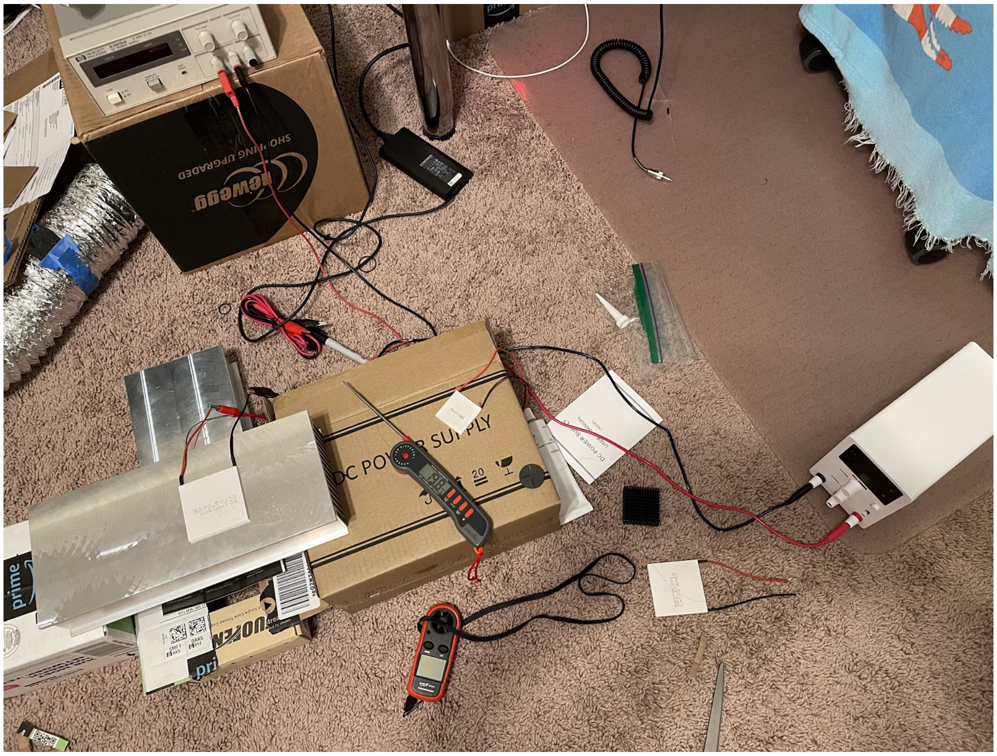

Figure 5.3: Second TEC and heat sink testing setup.

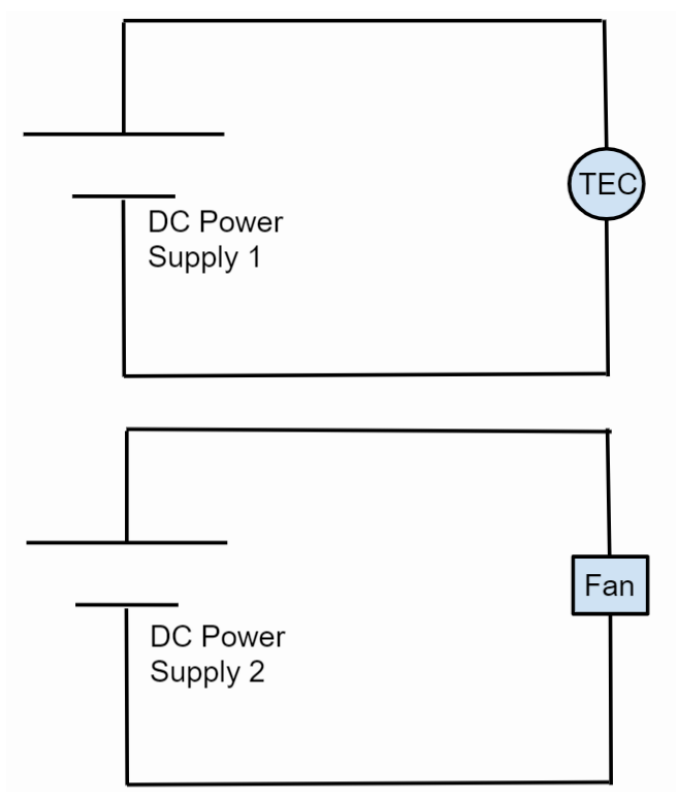

Figure 5.4: Circuit Diagram for Second TEC and heat sink Testing Setup

To test and measure the temperature of the cold heat sink, the TEC was placed in-between the hot and cold heat sinks with the cold heat sink facing upwards. In order for the TEC to cool down the entire heat sink, the TEC would need to be powered for a significant amount of time. These tests were run for approximately thirty minutes to allow enough time for the cold heat sink to cool down. The thermometer tip was propped against the cold heat sink fin tips so that the temperature measurement would be representative of the entire heat sink. These tests were able to measure the lowest temperature achieved on the cold heat sink fins, but the temperature difference between initial and final temperature was used as a more accurate indicator of the cooler's effectiveness. During the first prototype construction in winter quarter, Coolers A and B were both malfunctioning and Cooler A was replaced with the same model. However, this new cooler was performing slightly worse than the original, with lowest temperatures that were several degrees warmer than expected. Luckily, the new cooler was still able to achieve higher temperature changes in the cold heat sinks at any given power level than Cooler C. These results are shown below in Figure 5.3 where the temperature difference achieved by each cooler is compared to the power level supplied to achieve these cooling loads.

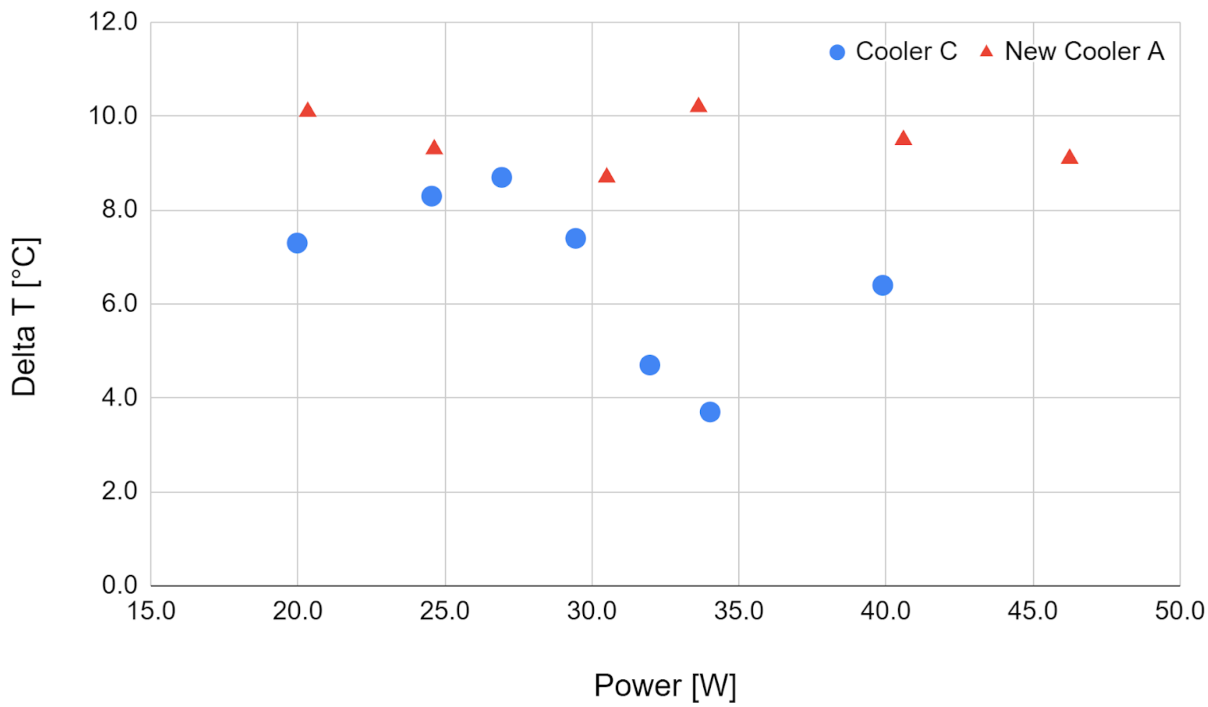

Figure 5.5: Performance characteristics of replacement Cooler A vs. Cooler C.

5.2 Prototype Construction

During the construction of our first prototype we were severely restricted due to COVID-19. Unable to work in-person as a group and with no individual access to the Santa Clara University machine shop, this left us with limited resources to fulfill our construction plans. Despite these challenges, we were able to produce an initial prototype while collaborating remotely.

Construction was conducted by an individual team member in a personal garage, with the only tools available being a miter saw, circular saw, a drill, and a hot glue gun. For this reason, combined with not being to work as a team yet, we simplified the first prototype design to leave out the water collection system as we were not concerned with managing water collection as much as we were with testing the design to see if it would remove moisture from the air in the first place. It is also worth noting that the components inside of the outer wooden housing box are all removable to allow us access to place sensors for testing in places that would otherwise be closed off and inaccessible. However, the heating module functions normally without the water collection system in the design.

As shown in Figure 5.4, the lower channel airflow through the cold heat sink and the upper channel airflow through the hot heat sink are divided. Figure 5.5 shows this division from clearly where the thermoelectric cooler lies between the heat sinks and surrounded by an insulative layer. The flange design at the back of the prototype directs the airflow through a 90° turn from the lower channel to the upper one.

Overall, the prototype served its purpose of allowing us to begin testing for experimental results to compare to our theoretical calculations. It also allowed us to identify problems with the design and construction process.

Figure 5.6: Front view of first prototype design with top panel removed.

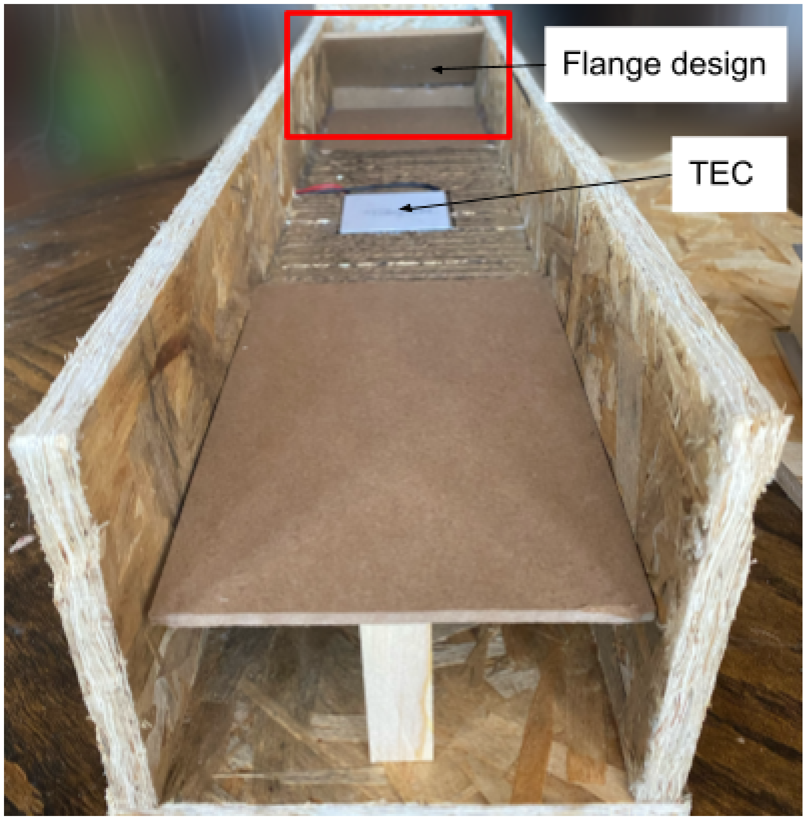

Figure 5.7: Overlooking view of first prototype design with upper hot heat sink removed.

After testing with our initial prototype, it was clear we needed to make some changes to increase the efficiency of our design, as our experimental results were not matching up with the results we got from COMSOL simulations. To address this issue we utilized the results of the COMSOL simulations on different features to incorporate new ideas into a second prototype.

These feature additions included adding baffles to our cold heat sink in addition to the heat pipes and flange restrictions carried over from the previous prototype. As seen in Table 3.1, this is the ideal combination for maximizing the heat ratio of our system.

Figure 5.6 shows a close up of the baffles slotted into the heat sink. The baffle design consists of rows of laser cut ⅛" acrylic pieces placed longitudinally offset along the length of the heat sink. This creates obstructions to the path of the air, forcing it to slow down and take a longer route while passing through the heat sink fins.

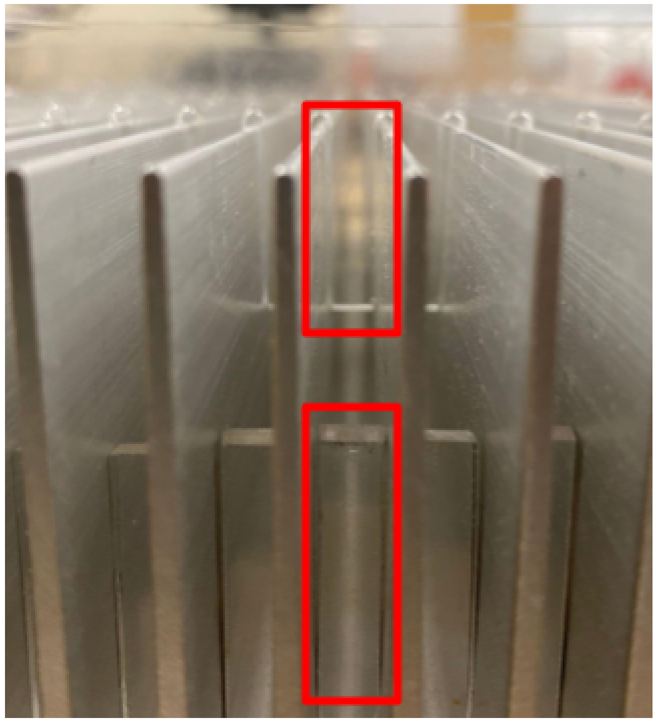

Figure 5.8: Close-up view of baffles slotted in the cold heat sink. One upper row and one lower row baffle are boxed in red for clarification on the distribution of baffles.

Another issue we addressed in the construction of our second prototype was the precision of cuts on our wooden housing. By manufacturing a more precise design, we were able to virtually eliminate any cracks between mated wood pieces that had allowed air to escape out of the first prototype. We also added wood glue in addition to screws mating the wooden pieces together to further seal the inside of the system from escaping air. The construction process went seamlessly in comparison to construction of the first prototype. This round of construction we were able to collaborate in person with access to the Santa Clara University machine shop throughout Spring quarter. We spent much more time prior to construction to plan out every detail including dimensions and tools, as we had learned from the first prototype construction that this would save us time in the long run. The machine shop provided us access to all the tools we needed to ensure a precise, well-made prototype that would vastly improve efficiency over our first model. Overall, this second prototype served as a vast improvement over the previous model. We plan on continuing to improve our product in future design iterations as well as performing further testing on this prototype.

Figure 5.9: Front view of second prototype.

Figure 5.10: Top view of second prototype with upper hot heat sink and top panel removed.

Figure 5.11: Close up view of division between upper and lower channel with view of wicking material under the fins of the cold heat sink.

5.3 Test Results

For the first prototype testing, an Arduino board paired with two DHT22 temperature and humidity sensors was used to measure the air conditions before and after passing through the cold heat sink. The use of an Arduino board allowed us to instantly record the temperature and humidity data to a spreadsheet which made the data analysis process much faster. In our prototype, the sensors were placed at the entrance and exit of the cold heat sink, indicated by the green boxes in Figure 5.10.

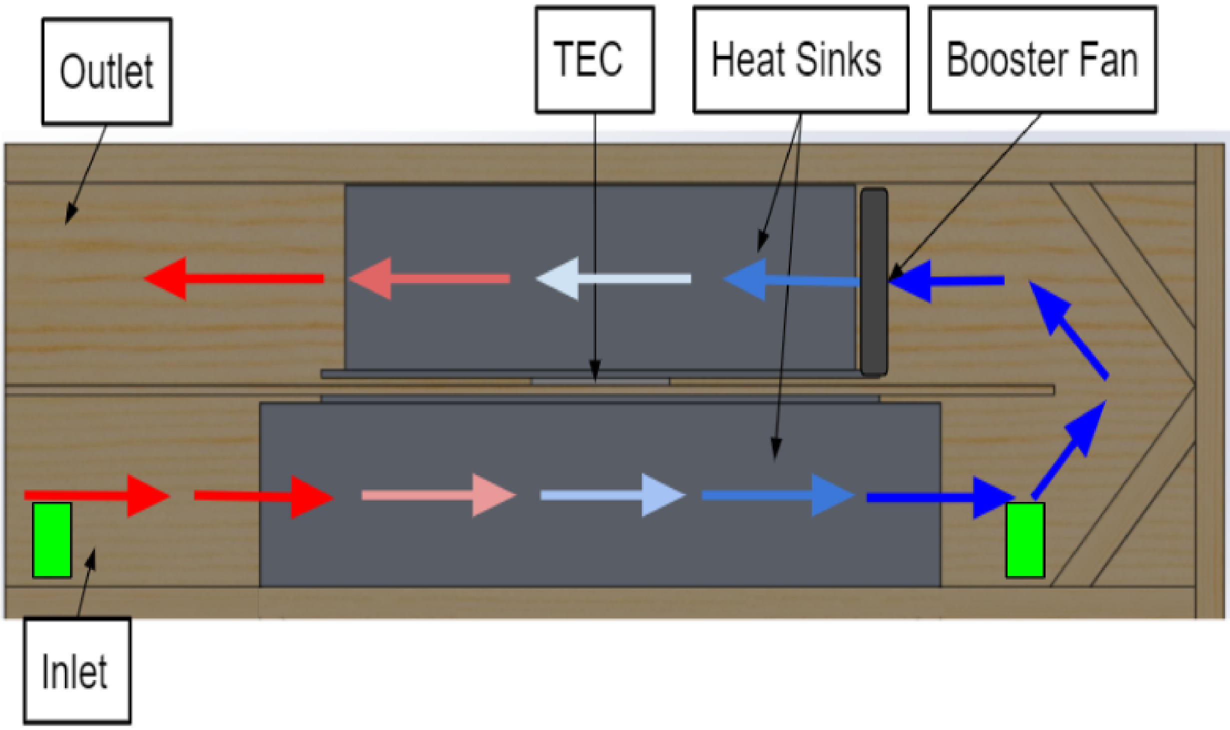

Figure 5.12: Diagram of first prototype testing setup with sensor locations.

A test was conducted on our first prototype with the TEC voltage set at 10 V. The sensors were able to read a temperature drop of 2. °C after the air had passed through the cold heat sink. The sensor readings are shown in Figure 5.11. Although the air was able to be cooled, there was no moisture collected on the cold heat sinks fins.

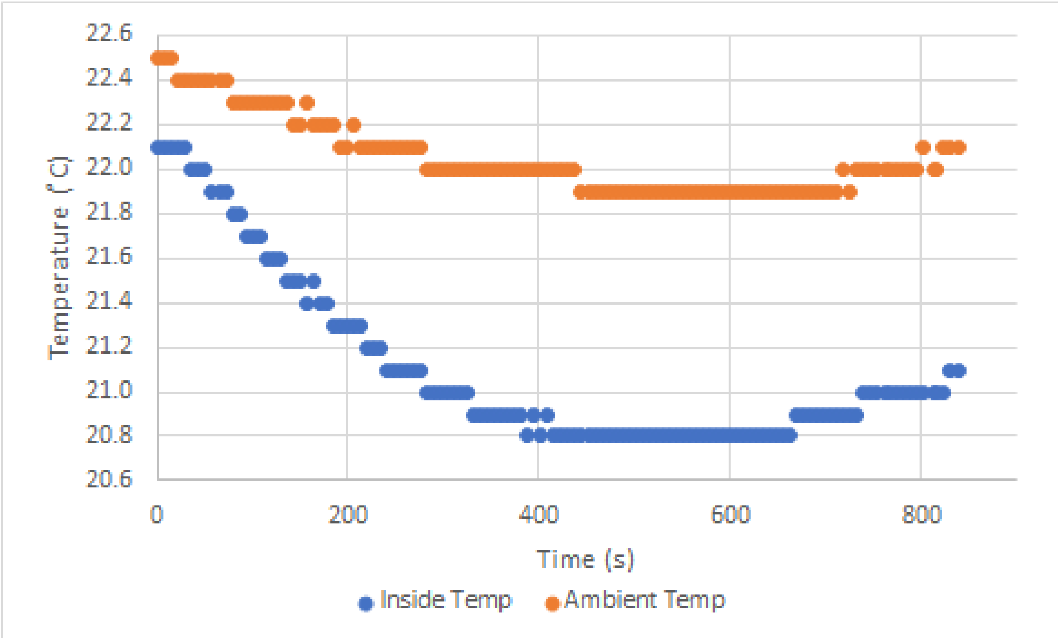

Figure 5.13: DHT22 sensor readings for first prototype test.

The low change in temperature could be attributed to a variety of factors such as the temperature that the cold heat sink was able to reach and the smoothness of airflow throughout the system. To measure the temperature of the cold heat sink, more tests were performed using a test setup similar to the initial heat sink and cooler tests. Figure 5.12 shows how these tests were set up in the SCU machine shop. These tests were able to isolate cooling factors such as thermal paste, heat sink orientation, and applied voltage. The thermal paste and heat sink orientation were perhaps the most noticeable differences between this testing setup and the pre-prototype setups. With this setup, the cold heat sink was only able to achieve temperature differences of about 7 °C, while the previous setups were able to lower the heat sinks by almost 9 °C. The second prototype will use the same heating module setup as the first prototype in order to determine the effect that the water collection system and improved housing material have on the test results.

Figure 5.14: Testing setup after first prototype test.

<u>**5.4** Dryer Analysis</u>

In Spring Quarter, we were given access to the clothes dryer from the SCU Frugal House. We were able to disassemble its parts in the machine shop and analyze its air flow path. Figures H.1 through H.7 in Appendix H show different views and sketches of the disassembled dryer and its components.

The dryer air takes the following path as illustrated by Figure 5.15:

1. Air enters the dryer through holes in the side of the dryer (1) The air is collected throughout the entire shell of the dryer.

2. The air gets sent through the heating element (2) which is then sent into the back of the drum. [On the way there, there is a small opening near the grill on the back of the dryer which probably acts as either a supplementary air inlet or a pressure relief section. Either way, we can use it as a pressure relief section, so that the pressure inside the dryer from the booster fan is greater than the surrounding air. Therefore, all air going to the clothes would be preprocessed air.]
3. Air passes through the tumbler.
4. Air enters the centrifugal exhaust fan (3), blasting air through the exhaust duct (4) and out the dryer. All air flow is controlled by this one exhaust fan.

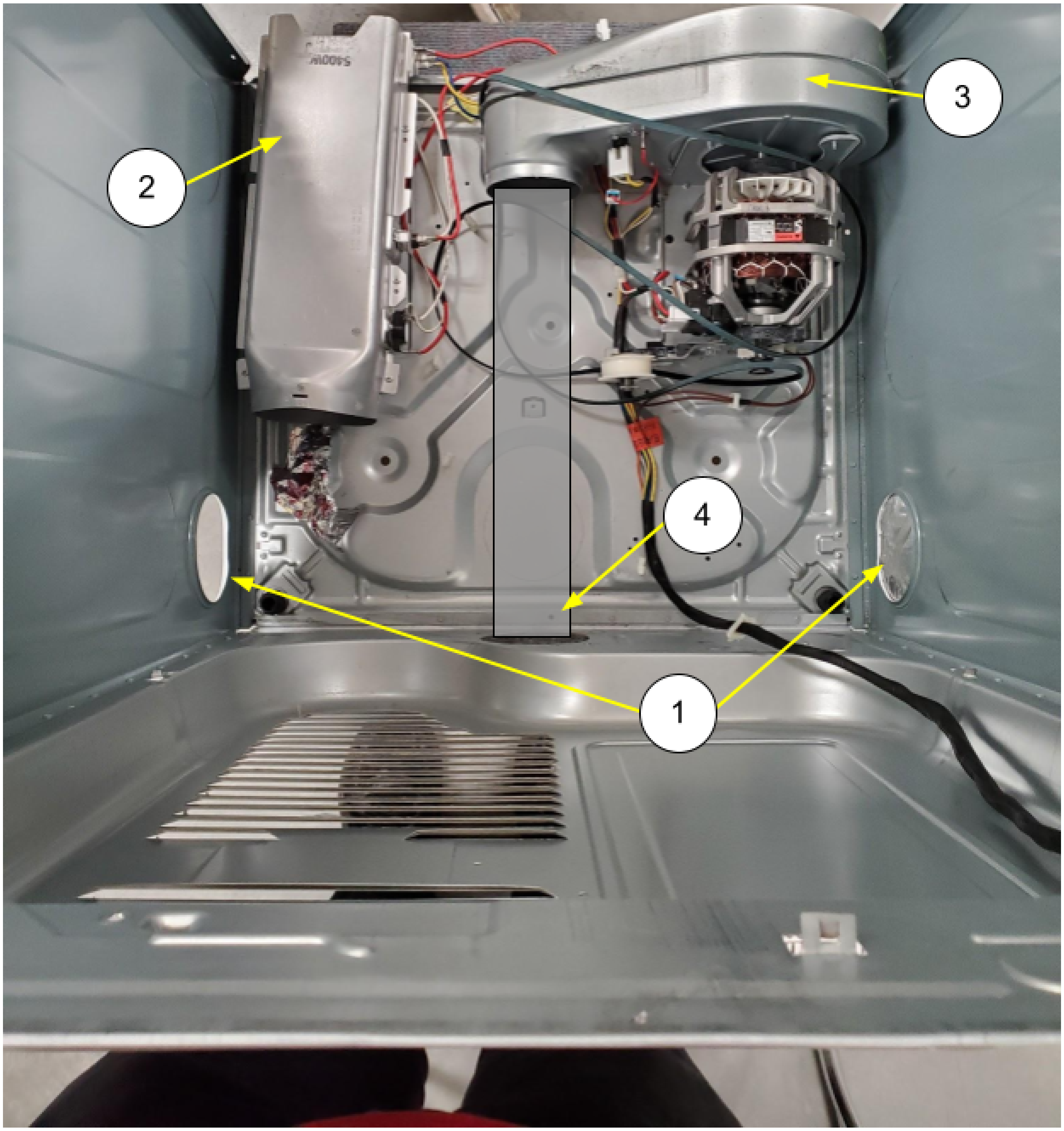

Figure 5.15: Top view of dryer components with indicators for airflow path.

Chapter 6: Cost Analysis

In order to determine how much money and time the Drier Dryer would save, preliminary calculations were performed to determine an approximate increase in efficiency it would provide. The ambient conditions that were used in these calculations represent the range of temperatures and relative humidities that the system should be run in for the user to save both time and money. Specifically, the analyzed temperature range was 22-34 °C and the relative humidity range was 70-100%. Using combinations of temperature and relative humidity values in these ranges, an estimated cost-savings (cents/cycle) and increase in efficiency could be determined for a specific combination. This section details the methods used to determine said savings and the overall impact they will have on the user in the long run.

6.1 Background Assumptions

The first assumption made in these efficiency calculations was that the Drier Dryer could first cool the air to a certain temperature and then reheat it to its original temperature. This assumption was made since the intake air should have the same contact time with the cold heat sink as the hot heat sink. Also, the energy used to power the TEC generates an equivalent positive temperature difference on the hot side as a negative temperature difference on the cold side (in comparison to the ambient air). With this assumption and the information gathered from the COMSOL simulations, it was estimated that the system could reduce intake air temperature by around 22 °C. However, since this was the ideal case, cases where the system could only reduce intake air temperature by 11 °C and 5 °C were also analyzed. Specifically, these cases entail that the Drier Dryer could cool the intake air by the given temperature value and reheat it by the same amount, returning it to its original temperature. While this may seem aimless, it is important to note that cooling air past its dew point temperature allows condensation to form, removing humidity from the air. When this dehumidified air is reheated, the final relative humidity value would be lower than that of that of the original air.

6.2 Savings Calculations

In order to calculate the efficiency provided by the Drier Dryer, the actual vapor pressure of both the treated and the ambient air must be determined. The assumption made earlier that the system could reheat the cooled air to its original temperature is effective in simplifying these calculations. The equations used to calculate the vapor pressures of ambient and treated air are functions of both air temperature and relative humidity and are detailed below:

$$P_{act,\ ambient} = \left(\frac{RH_{ambient}}{100}\right) * 0.6108 \exp\left(\frac{17.27T_{ambient}}{T_{ambient} + 237.3}\right) \quad [kPa]$$

[6.1]

$$P_{act,\ treated} = \left(\frac{RH_{treated}}{100}\right) * 0.6108 \exp\left(\frac{17.27T_{ambient}}{T_{ambient} + 237.3}\right) \quad [kPa]$$

[6.2]

In these equations, ambient temperature is given in °C and RH is given in a percent value ranging from 0-100%. Any combination of ambient conditions could be entered into the first equation, but in order to determine the relative humidity of the treated air, a dew point calculator was used. For example, using the case in which the system could reduce air by 22 °C, the relative humidity of the treated air could be determined with the current temperature of the air and its dew point temperature (which in this case would be 22 °C below the current temperature). If the current temperature was 34 °C, and therefore the dewpoint temperature was 12 °C, the current relative humidity of the air would be ~25%. For the three cases of the Drier Dryer being able to cool air by 5 °C, 11 °C, and 22 °C, the relative humidities of the treated air under any of the temperature conditions were approximately 74%, 50%, and 25% respectively.

Next, the saturation vapor pressure of the dryer-heated air must be determined. It was determined that on average, clothes dryers heat intake air to temperatures of ~55 °C [15]. Using this value, and ignoring the relative humidity term from Equation 6.1, the saturated vapor pressure of the dryer-heated air was determined to be a constant 15.746 kPa. Next, the difference between the dryer-treated-air saturated vapor pressure and either the ambient- or treated-air actual vapor pressure were determined. The pressure difference between the dryer-heated air and the intake air is important to find since it has a direct relationship to the rate at which moisture can be removed from wet clothes within the dryer. In other words, increasing this pressure difference results in an increase in the dryer's moisture removal rate and vice versa. A simple way of viewing the Drier Dryer is that it is a system which increases pressure difference, and consequently dryer moisture removal rate, by dehumidifying dryer intake air.

The increase in efficiency that the Drier Dryer provides was calculated using the following equation:

$$\%\ Increase\ in\ Efficiency = \frac{dP_{dryer-system} - dP_{dryer-ambient}}{dP_{dryer-ambient}}$$

[6.3]

In this equation, $dP_{dryer-system}$ represents the pressure difference between the dryer-heated air and the system-treated intake air and $dP_{dryer-ambient}$ represents the pressure difference between the dryer-heated air and the untreated ambient intake air. The resulting increase in efficiency is given in percent and can be multiplied by dryer cycle time to determine how much time is saved from the dryer cycle. In order to simplify calculations, a one-hour cycle time was used as the time it takes for a dryer *without* the Drier Dryer to dry a load of laundry. For example, if a 20% increase in efficiency was found, that would equate to a 12-minute time-savings and a 48-minute dryer cycle time for the purposes of cost-savings calculations.

Time-savings is one benefit of using the Drier Dryer, but cost-savings is its main selling point. A one-hour dryer cycle typically uses 4 kWh of energy. Using the electricity rate in Hawaii, which is 32.76¢ per kWh, the cost of running a dryer for one hour in Hawaii is roughly $1.31 [16]. The total estimated energy consumption of the Drier Dryer is about 0.052 kWh, resulting in a cost of 1.71¢ per one-hour dryer cycle. To calculate the net cost savings per cycle that the system provides, this 1.71¢ must be subtracted from the product of the increase in efficiency and the dryer cycle cost ($1.31).

The following graphs show the net cost-savings in cents (z-axis) when the system is used in different combinations of temperature (x-axis) and relative humidity (y-axis). The graphs assume that intake air can be cooled by 5 °C, 11 °C, and 22 °C respectively. The code used to produce them can be found in Appendix D.

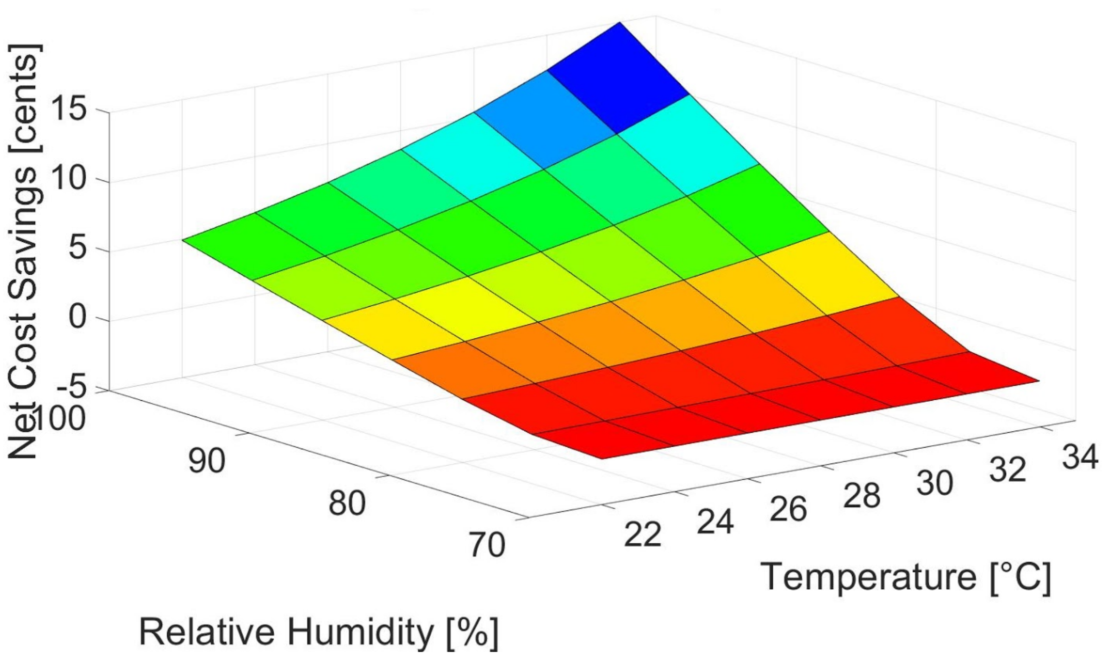

(a)

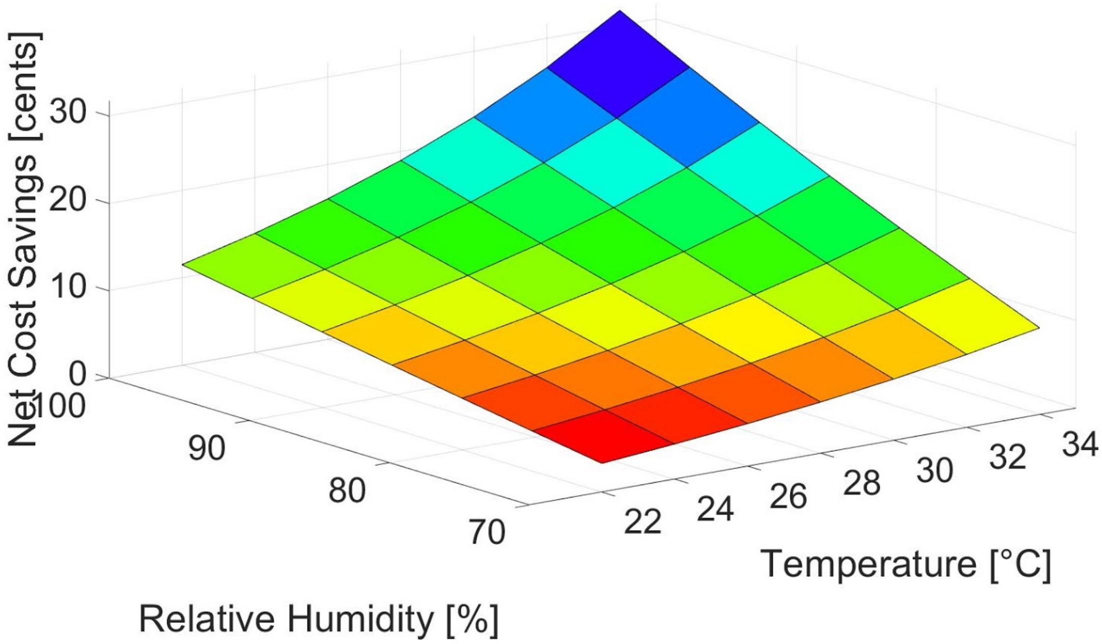

(b)

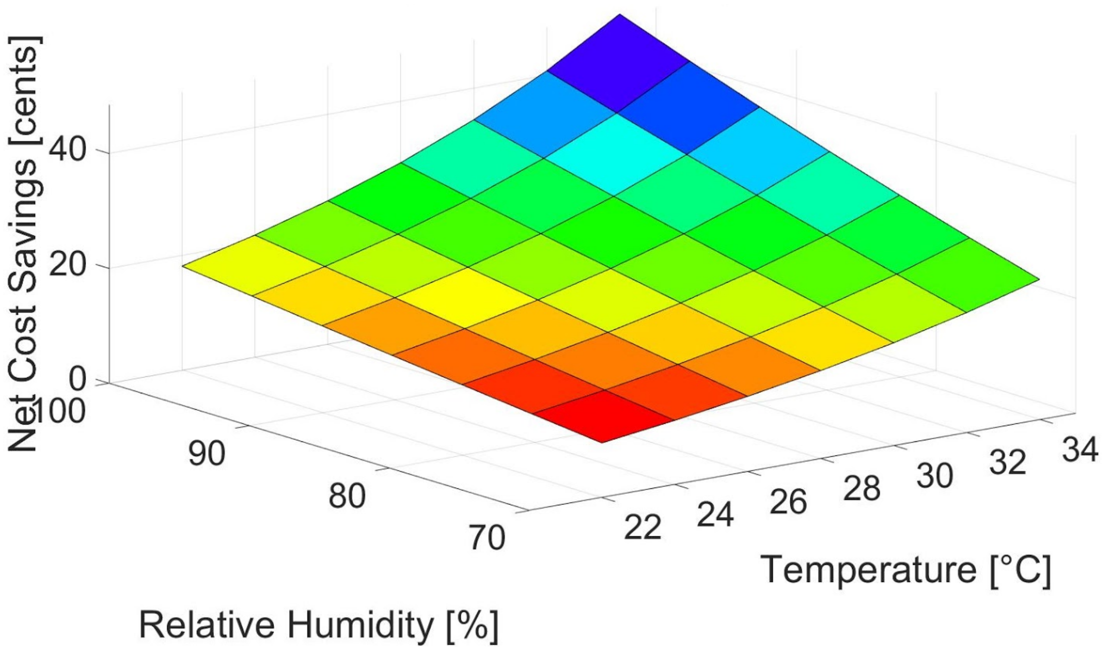

(c)

Figure 6.1: Net cost savings graph assuming the Dryer Drier can cool dryer intake air by (a) 5 °C, (b) 11 °C, (c) 22 °C.

As shown in the graphs, the system is the most effective when conditions are their hottest and most humid. The net cost savings per cycle at the 34 °C and 100% relative humidity point on each of the graphs are 15¢, 33¢, and 48¢ respectively. Consequently, the system does not perform as well when temperature and relative humidity are lower. The net cost savings for the 11 °C and 22 °C decrease graphs at the 22 °C and 70% relative humidity point are only 3¢ and 9¢ respectively. In the case of the 5 °C decrease graph, running the Dryer Drier in these conditions will actually incur a net loss due to the system not being able to cool air to its dew point temperature. This is because the system removes no moisture from the intake air and ends up costing its user 1.71¢ per hour due to its power consumption.

Ultimately, it is important to determine whether the system can save its user a significant amount of money to make its purchase worthwhile. Using the net cost savings graph for the 11 °C temperature decrease and assuming ambient conditions similar to Hawaii (27 °C and 80% relative humidity), the system would save about 9¢ per one-hour dryer cycle. More importantly, this would save users $27 annually. Depending on the method of production, the return-on-investment period of the Drier Dryer varies.

6.3 Production Costs and Return-on-Investment

As of right now, each prototype requires the use of at least one Peltier cooler, two heat sinks, two heat pipes, wicking material, wooden housing material, and the use of thermal paste and screws. The most expensive materials are the heat pipes, heat sink, and TEC, but if these components were to be purchased in large quantities for mass production, their cost can be reduced significantly. The largest price reduction comes from the heat sinks. Since they can be manufactured from raw material, the price of two heat sinks can be reduced from $169.68 to about $10 for the cost of raw material and manufacturing. The purchase list in Appendix G shows the cost of all prototype materials without any price reductions. The initial price of a prototype costs about $400, but with the discounts applied through bulk purchases, the cost is reduced to about $165. The bill of materials for the prototype is shown below in Table 6.1, which compares the original prototype cost to the bulk cost. The cost of larger quantity items such as screws and wood glue were estimated in order to keep the BOM more organized and provide a more accurate prototype cost. If the first prototype was fully purchased, consumers would be able to have a return-on-investment after almost 15 years, but with the bulk cost reductions, this return-on-investment period lowers to about 6 years.

Table 6.1: Original and Bulk Prototype Bill of Materials

Prototype Materials			
Category	**Description**	**Original Cost**	**Bulk Cost**
Housing	Wood	$ 9.20	$ 9.20
	Water Collection Tray	$ 1.89	$ 1.89
	Misc. (screws, glue, thermal paste)	$ 10.00	$ 10.00
Heating Module	Moisture Fabric and Insulation	$ 10.00	$ 10.00
	TEC	$ 85.11	$ 57.15
	Heat Sinks (2)	$ 169.68	$ 10.00
	Heat Pipes (2)	$ 107.35	$ 67.22
	TOTAL	$ 393.23	$ 165.46

Chapter 7: Patent Search and Disclosure

When compared to other dryer-based patents, the Drier Dryer uses similar concepts and design approaches. However it is unique because of its specific use of a Peltier cooler with a wooden housing unit. This chapter will describe similar existing patents which may have the same purpose or components as the Drier Dryer, but do not utilize the economic benefit of a wooden frame with the Peltier cooling effect. By using wood as its core construction material and maximizing the use of a single Peltier cooler, the Drier Dryer is able to achieve low manufacturing costs while maintaining the same level of dehumidification as other patents.

7.1 Background

For our project, our team designed a system which removes humidity from dryer intake air in order to increase the efficiency of a clothes dryer. The system utilizes a peltier cooler to cool and heat two heat sinks which airflow is channeled through. When the air passes through the cold-side heat sink, it will be cooled to its dew point temperature. This will cause condensation to form due to the air being dehumidified. The hot-side heat sink simply serves to heat the treated air back up before it enters the dryer drum. This allows the dryer to expend less energy to heat the air to its target temperature, which often depends on user-defined dryer settings and preferences. While the general concept of a dehumidifier for clothes drying has been designed before, our system is unique in that it is a dryer attachment that uses a wooden housing in conjunction with the peltier cooler for this specific purpose. Patenting this specific combination of design choices will ensure that even if competitors try to design a similar dryer attachment, they will not be able to cut production costs with the use of both wood and a peltier cooler.

Our system is called the "Drier Dryer" and is designed to help families living in hot, humid climates save time and money. When the system is able to remove moisture from the dryer intake air, the time the dryer takes to completely dry the wet clothes inside it decreases. This time savings also translates into cost savings since a shorter cycle time equates to a lesser annual power consumption. Using cheap components such as wooden housing, a peltier cooler, and fabricated flow baffles, our system is able to provide a significant dehumidification at a fraction of the cost of existing dehumidifiers. In addition, the Drier Dryer uses minimal power to run and only costs about 1¢ to operate for an hour.

While dehumidifiers exist that aid in clothes drying, none of them are specifically designed to attach to an existing clothes dryer. Competing products are equally, if not more, expensive than the Dryer Drier and simply dehumidify air of a room. This means that clothes must be hung out to air-dry and will still take much longer to dry than if they were dried in a clothes dryer. Dryers with built-in dehumidifiers also exist, but these are much larger and more costly than typical dryers. Thus, the Dryer Drier fills a niche in the clothes-drying market for families who want to dry their clothes quickly *and* inexpensively as opposed to one or the other. It is a relatively cheap product that can attach to any existing clothes dryer. Since it is unique in both design and application, it has no direct competitors.

The Drier Dryer was designed by the Dry Guys: Daniel Anderson, Justin Lee, Thomas Morey, and Joshua Sunada. It was invented in October 2020 and will be publicized in May 2021. The product is expected to be brought to market beginning January 2022. Since it is a clothes dryer attachment, it would likely be sold in hardware stores like Lowe's and Home Depot.

7.2 <u>Summary of Patent Classifications</u>

The Drier Dryer utilizes wooden housing material and a single Peltier cooler in order to reduce the humidity of incoming dryer air and increase dryer efficiency. The economic use of wood and a single Peltier cooler is unique to the Drier Dryer and can also reduce its manufacturing cost compared to similar products which may use more expensive materials or more heating and cooling components.

Figure 2.8 depicts the aesthetic and function of the design. In addition, Figure 7.1 represents the cover sheet of the drawing set, detailing the specific dimensions and makeup of the design (see Appendix C for the complete set of engineering drawings).

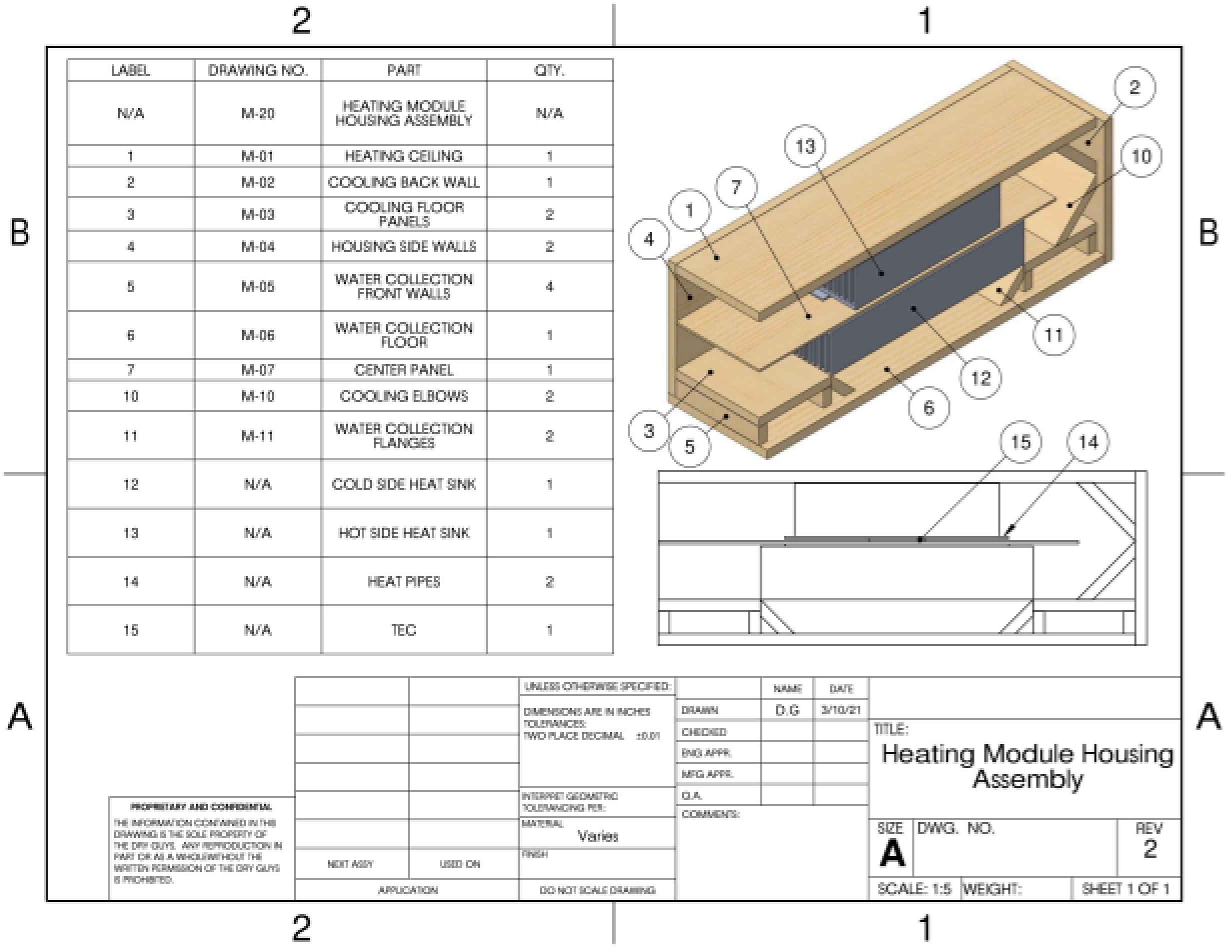

Figure 7.1: Cover sheet for the heating module housing assembly drawings. The parts of the patent elements are labelled and quantified.

<u>7.3 Review of Relevant Patents</u>

1. Name: Clothes dryer with a dehumidifier

   Patent Number: US 20060117593 A1

   June 8, 2006

   The patent for a clothes dryer with a dehumidifier seeks to perform a similar task as our design. It claims to dehumidify the exhaust air of a dryer to prevent the humidity increase of the room containing a dryer without exterior exhaust routing. This also ensures that the incoming air is not as humid as the exhaust air. This patent is especially useful when there are occupants or humidity-sensitive equipment in the dryer room and when it is impractical to run a line of exhaust duct to the outside. Although this design and ours share the similar goal of increasing dryer efficiency, our design is distinguished from this patent design because ours exclusively treats incoming air. In addition, this patent does not utilize peltier coolers, but instead uses a thermodynamic heat exchanger cycle consisting of a compressor and expansion device.

2. Name: Energy efficient clothes dryer

   Application Number: 06/457,528

   January 13, 1983

   Although a fairly old patent, this design forms the basis for ventless dryers as they exist today. Most of the claims are synonymous with a regular clothes dryer design, including the round drum compartment on a fixed axis. However, this design uses a heat pump system including a compressor, condenser, expansion valve, and evaporator comprising a closed refrigerant circuit. All of the air runs in a closed loop, including the condenser, drum interior, evaporator, and compressor. The main claim of the design is that the heat throughout the dryer is recirculated. The design also uses a series of baffles in the evaporator to facilitate heat transfer and condensation of entrained moisture from the air stream. Compared to our design, we do not process the exhaust nor reuse any air. Our design focuses on the humidity level of the incoming air, while the patent design focuses on maintaining temperature levels of the circulating air. While our design also implements a series of baffles, we incorporate the baffle design along the length of a heat sink to facilitate heat transfer by increasing the contact time between the air and cold heat sink.

3. Name: Thermoelectric use of air conditioners for dehumidifier

   Patent Number: KR 100376384 B1

   March 17, 2003

   This design consists of a dehumidifier operated by a thermoelectric module. Similar to our design, air enters on the cool side of the TEC, makes a 180° turn, and passes over the hot side of the same TEC before being expelled out the side via a fan. While our design uses heat sinks on the hot and cold side of the TEC, this design does not specify the exact heat absorbing material on the cold side of the TEC. However, it does claim to condense air on this cold side and discharge it to the outside through a drain port. Our design uses a wicking material to collect water from the cold sink and stores it in a water collection basin where it can evaporate away. The patent dedicates a large amount of its claim descriptions to describe how the design can remove pollutants from the air, therefore producing clean air. In addition, a negative ion generator is added to the housing and is claimed to be good for human health. Our design does not claim to remove pollutants nor provide health benefits, only a boost in vented dryer efficiency.

4. Name: Drum washing machine and clothes dryer using peltier thermoelectric module

   Patent Number: US 7526879 B2

November 4, 2005

This patent discusses an invention that utilizes a recirculated exhaust air and the use of a thermoelectric module, with such nature as a Peltier cooler, to increase the efficiency of a standard drum washing machine. While this patent's objective is aimed at a washing machine rather than a clothes dryer, the concepts used are similar to those displayed in our team's design. The patent's invention uses a thermoelectric module where the exhaust air from the washing machine crosses the head absorption side of the TEC and condenses the air. The air is then reheated using the heat dissipation side of the TEC. This design, however, differs from ours due to their use of multiple TECs stacked to form a multi-layer structure with gaps in between TECs. Each pair of TECs has the heat absorption sides opposing each other. Similarly to our design, the TECs act as a drying apparatus to remove moisture from the air being recirculated into the washing machine.

5. Name: Drying apparatus

   Patent Number: US 20050044744 A1

   August 7, 2003

   This patent provides insight into the state of the field of improvement of clothes dryer efficiency. This drying apparatus is to be used in dryers or washing machines with a drying function performed after a wash is completed. The invention utilizes a heating pump made up of a compressor device and decompressor device, a cooling coil and heating coil. It functions by heating laundry with the heating coil and using the cooling coil to coagulate the moisture removed from the drying laundry. This system is interesting as the concepts are similar to those employed in our own team's design. However, the purpose of this drying apparatus is slightly different and perhaps less specific. The patent notes various issues encountered with their invention. These issues can be useful to our team to analyze for use in predicting where errors may occur in our own design further down the line.

7.4 Patent Conclusion

After careful consideration of similar patented products, we believe that the Drier Dryer can be patented due to its specific use of a peltier cooler in a wooden housing unit. Patent KR 100376384 B1 uses a thermoelectric module and drying chamber similar to our heating module design, but our design also incorporates the use of baffles in one heat sink in order to promote airflow. Patent US 20060117593 A1, Patent 06/457,528, and Patent US 20050044744 A1 are also used for the purpose of increasing dryer efficiency, but use multiple heat exchangers and components rather than a single peltier cooler (see Table 7.1). These patents also treat external and recirculated air while the Drier Dryer exclusively treats incoming air. Patent US7526879B2 also treats recirculated air, but is different from the other patents and the Drier Dryer because it uses multiple peltier coolers and can also be used for a washing machine.

One important difference between the Drier Dryer and similar patents is that the Drier Dryer is the only product to use wood as its main housing material. This allows for a cheaper manufacturing cost while maintaining the degree of insulation needed for smooth airflow and heat transfer. While other patents may use multiple Peltier coolers and thermodynamic components, the Dryer Drier minimizes power consumption by only incorporating the use of one Peltier cooler. This will further reduce the manufacturing and energy cost, which will allow for more cost effective drying cycles while achieving the same amount of dehumidification.

Table 7.1: Summary of existing technology claiming to increase dryer efficiency or dehumidify air with thermoelectric coolers. See Appendix E for the first page of the patents listed.

Patent/Application Number	Title	Date
US 2006/0117593 A1	Clothes dryer with a dehumidifier	June 8, 2006
06/457528	Energy efficient clothes dryer	January 13, 1983
KR 100376384 B1	Thermoelectric use of air conditioners for dehumidifier	March 17, 2003
US 7526879 B2	Drum washing machine and clothes dryer using peltier thermoelectric module	November 4, 2005
US 20050044744 A1	Drying apparatus	August 7, 2003

Chapter 8: Engineering Standards and Constraints

The Santa Clara University Engineering Handbook examines eleven standards in the profession of engineering. In this document, five of these standards will be examined in relation to the team's project. In each category, national standards will also be discussed. These standards address manufacturability, sustainability, usability, health and safety, and the economic implications of our team's clothes dryer attachment.

8.1 Manufacturability

A key concern for any design to be produced on a large scale is that it must be simple to manufacture. This does not necessarily mean that it is easy to fabricate but that the process is as streamlined as possible with minimal opportunities for error. This can be achieved by simplifying the design and reducing the number of parts, standardizing parts and materials, designing specifically for ease of fabrication, avoiding unnecessary surface finish requirements, and considering modular products among others.

In general, as the number of parts is increased, the probability of error increases. Error can include defective parts and even make part failure later in its life cycle more difficult to identify and correct. The dryer attachment design calls for a limited number of standardized and easily-accessible components including the length of 4" duct, a Laird TEC, fans, two Newark heat pipes, and two Mouser heat sinks. However, within these components, steps were taken to reduce the number of parts required. For example, rather than using multiple series of short rigid ductwork connected with numerous fasteners, a single run of flexible duct was used. The same principle can be applied to the heat sinks. The housing was designed in such a way that no modifications to the heat sink geometry were required, cutting down on fabrication time and complexity. Finally, the attachment requires insulative material. To keep these components manufacturer-friendly, all insulation can be repurposed to fit several areas of the system - around the housing and between the heat sinks.

To ease manufacturability, the design should minimize the number of tight tolerances. At the same time, the design should minimize the amount of flexible parts. The dryer attachment bridges these factors. Because a flexible duct is used, tolerances concerning connections between the dryer and attachment are no longer a factor, as the duct can be easily stretched to the required length and compressed to the desired diameter. However, flexible duct introduces assembly difficulties, particularly in making cuts and drilling precise holes. In the attachment design, no such precise cuts are required, as these cuts will take place in the main housing which is made of plywood.

The use of modular components can ease assembly and ease maintenance during a product's lifespan. The dryer attachment can be broken down into four major assembly components: the TEC module and attached heat sinks, duct connection, and housing. The design allows the TEC and heat sinks to be easily laid and slid into place, respectively. The parts will be adhered using thermal paste. The walls of housing will also be sealed with wood glue to contain air. If part replacement is required, it will be possible to remove the side wall of the system. This will make maintenance and replacing singular parts possible. Overall, this assembly process will allow the heat sinks, heat pipes, TECs, and duct components to be manufactured independently of each other, leaving only the housing to be fabricated using the preceding parts.

8.2 Sustainability

As the United Nations defines, “sustainable development is that which meets all the needs of the present without compromising the ability of future generations to meet their own needs.” Using this definition and the standards set forth by Energy Star, the dryer attachment can be considered a positive influence on sustainability in the world of residential clothes maintenance technology in two categories: energy efficiency and material savings.

The main purpose of this product is to reduce the energy consumption of dryers. For consumers, this means a lower utility bill. For the environment, this means less electricity or natural gas consumed. Power savings analysis reveals that at most, 25% less energy is required to run a dryer with the attachment. The average dryer uses 770 kWh. This means that customers can reduce energy consumption of their dryer to 580 kWh simply by using this attachment. Over the lifetime of a dryer, about 16 years, this attachment can save nearly 3100 kWh.

In addition to energy savings, the attachment provides an alternative to buying a new dryer. Buying a new dryer not only requires $400-2,000 but also a wide range of materials, as a clothes dryer is among the largest appliances in households. In contrast to using this material to construct a new dryer, the attachment gives the same or better increased efficiency and reduced cycle time without compromising on the amount of the material required.

8.3 Usability

Although typically applied to infrastructure, we aim to make our product comply with ADA guidelines - to effectively make our product accessible to as wide a range of people as possible. Almost universally, products for the general public should aim to be easy to use. This includes being easy to set up, learn and remember, effective and efficient, relatively free of failures, satisfying to use, and sustainable.

The dryer attachment is currently designed to be installed and “forgotten about” except for the occasional cleaning of the water collection system. Therefore, the main priority of design is that the attachment is easy and simple to install. Installation of this attachment requires no disassembly of the existing dryer. In addition, the unit is not greater than three feet long, meaning that it can fit flushly behind nearly all clothes dryers without the need to readjust nearby appliances or furniture. During the installation process, it is expected that the unit may be dropped or mishandled in other ways. Therefore, the unit is designed to withstand an impact from as high as four feet off the ground.

Our design calls for a cleaning and wick replacement anywhere between 4-8 months depending on the frequency of use. The area behind or next to a dryer is expected to be somewhat awkward to access. However, the replacement procedure does not require the entire unit to be removed. Instead, the use of pull tabs can be used, requiring no heavy lifting or technical knowledge.

8.4 Health and Safety

OSHA standards document regulations related to workplace safety. For our project, this means the fabrication process should be safe. This also applies to users with the attachment because if the attachment is deemed unsafe for users, manufacturer employees may also be at risk, or vice versa. According to OSHA standards, it is our responsibility to develop, implement, and establish operating procedures and effectively communicate the requirements to workers. This section will serve to establish these procedures and act as the first step of safety training.

History is filled with examples of engineering oversights and resulting failures which at times has even led to death. There are many reasons why these failures occur. Some include material failure, poor design, environmental effects, human error, or any combination of these. The main concern surrounding the attachment relates to the proper dissipation of heat.

It is known that without proper ventilation and heat dissipation, a TEC can reach temperatures above 100 °C. This number is well below the melting point of aluminum but contact with this range of temperature may cause serious burns. Thankfully, the attachment will not rest in a regularly accessed area, limiting the risk of burns. However, the user or fabrication team will be required to interact with the unit to turn it on and occasionally inspect the water collection tray. A note to be included with the product in the inspection instructions will warn users to exercise caution by avoiding touching areas near the hot side of the TEC. Any intrusive operations should be conducted at least several minutes after power has been disconnected.

8.5 Economics

ISO 9001 stands as a key standard for us to acknowledge, as it shows that a company or product can be trusted - that a product can deliver its proposed output given an input. This is relevant to us given that we claim this product can increase dryer efficiency.

Analytically and ideally, the attachment is found to make the dryer at most 25% more energy efficient. This corresponds to a 25% reduction in cost to run the dryer. To make this claim, such an increase must be measured and documented. To date, the attachment has been shown to produce a 2 °C temperature difference of air across the heat sink. While this is on the right track, it is not nearly enough to produce the 25% time reduction. At the same time, our team has not been able to test our attachment with a dryer, and not in the ideal weather conditions for the product to perform to this standard. Before putting this product on the market and advertising for it, it will be necessary to perform these tests. Dryers cost around $100 to run annually. If 25% of cycle time is saved, then a user can save $25 a year. Under these conditions, it is expected that this product will be able to pay for itself if run for around the lifespan of a dryer - or 16 years simply through the time saved on cycle time. This will make using this attachment a much more cost effective solution compared to buying a brand new dryer. In fact, interviews with potential customers reveal that they are willing to purchase and use such a device particularly if it decreases their energy bill. Of course, in all tests and with all measurements, a log of calibration for all measurement tools will be kept up to date to meet ISO 9001 requirements.

Chapter 9: Conclusion

9.1 Summary

After considering the high amounts of energy that clothes dryers consume, we designed the Drier Dryer as a way to reduce energy consumption for all households while saving money for users in locations with high energy costs. Despite the challenges presented to our team by COVID-19, we were able to test the capabilities of Peltier coolers and create two prototypes for the Drier Dryer. The first prototype testing resulted in an air temperature difference of only 2 °C, but the second prototype includes improved design changes that promote smoother airflow and water collection. Testing and troubleshooting for the second prototype has not been performed, but is a core element for the future plans of our group.

9.2 Future Plans

As of today, we have been able to construct our second prototype, but testing the system before the Senior Design Conference was unfortunately not possible due to resource and time constraints. Our first order of business in terms of future plans would be to test the system with our temperature sensors to see if it could reduce intake air temperature by 11 °C. After this testing, two basic improvements that could be made to the system include optimizing TEC voltage and heat sink combinations to lower cold heat sink temperature and refining the system's design to improve airflow. Finally, once we design and build our final model, we would like to test it with an actual clothes dryer and compare the increase in efficiency to our projected savings calculations. If we can improve our system to a point where it can help a large enough group of people, we can move forward with submitting a patent for our design and market The Drier Dryer as a consumer product.

Bibliography

[1] Casey, Allison. “16 Ways to Save Money in the Laundry Room.” *U.S Department of Energy*, [Available online at https://www.energy.gov/energysaver/articles/16-ways-save-money-laundry-room]

[2] “Rates and Regulations: Average Price of Electricity.” *Hawaiian Electric*, [Available online at https://www.hawaiianelectric.com/billing-and-payment/rates-and-regulations/average-price-of-electricity]

[3] Fuchs, John. “Drying - The Effect of Temperature on Relative Humidity.” *Cleaning Technologies Group*, 2013, [Available online at https://techblog.ctgclean.com/2013/05/drying-the-effect-of-temperature-on-relative-humidity]

[4] Patil, Rajendra P., et al. “THERMOELECTRIC REFRIGERATION USING Peltier EFFECT.” International Journal of Engineering Sciences & Research Technology, vol. 6, no. 5, May 2017, pp. 614–616.

[5] Technologies, Laird. “Thermoelectric Handbook.” Thermal Technical Library, 2018, [Available online at www.lairdthermal.com/thermal-technical-library/handbooks/thermoelectric-handbook]

[6] Crotti, Nancy. “Thermoelectric Cooler Solutions for Medical Applications.” *Medical Design and Outsourcing*, 22 Nov. 2019, [Available online at www.medicaldesignandoutsourcing.com/thermoelectric-cooler-solutions-for-medical-applications/]

[7] Totala, N. B., et al. “Study and Fabrication of Thermoelectric Air Cooling and Heating System.” International Journal of Engineering Inventions, vol. 4, no. 2, Aug. 2014, pp. 22–30.

[8] Pietrzyk, K., Ohara, B., Watson, T., Gee, M. Avalos, D., Lee, H. “Thermoelectric module design strategy for solid-state refrigeration.” Energy, vol. 114, Nov. 2016, pp. 823-32.

[9] Sun, D., Shen, L., Chen, H., Jiang, B., Jie, D., Liu., H., Yao, Y., Tang, J. "Modeling and analysis of the Thomson effect on micro-thermoelectric coolers considering interfacial and size effects" Energy, vol. 196, Apr. 2020.

[10] Simons, Rober. "Estimating Parallel Plate-fin Heat Sink Pressure Drop." *Electronics Cooling*, May 1, 2003. [Available online at https://www.electronics-cooling.com/2003/05/estimating-parallel-plate-fin-heat-sink-pressure-drop/#:~:text=Heat%20sink%20pressure%20drop%20curves,exhibit%20a%20higher%20pressure%20drop]

[11] "A psychrometric chart in English units - temperature ranging 20°F to 120°F." *The Engineering Toolbox*, 2004, [Available online at https://www.engineeringtoolbox.com/psychrometric-chart-d_816.html]

[12] EdgeStar CWD1550S-1. *CA Compact Appliance*, 2020, [Available online at https://www.compactappliance.com/edgestar-2-cu-ft-ventless-washer-dryer-combo-silver/CWD1550.html#manualsRow]

[13] "ENERGY STAR Market & Industry Scoping Report Residential Clothes Dryers." U.S. Environmental Protection Agency, November 2011.

[14] "Premium Wool Dryer Balls" *Cat Cave Co.*, 2021, [Available online at https://catcaveco.com/collections/core-wool/products/premium-wool-dryer-balls]

[15] "How Hot Should a Dryer Get?" *How Hot Should a Dryer Get? - Signs of Overheating | Home Warranty of America*, [Available online at www.hwahomewarranty.com/learning-center/homeowners/how-hot-should-a-dryer-get#:~:text=Your%20dryer%20uses%20heat%20to,to%20start%20steaming%20and%20evaporating]

[16] "Instantly Compare Electric Rates Offered by Local Providers." *Electric Choice*, [Available online at www.electricchoice.com/electricity-prices-by-state/]

[17] Laird CP2-127-10-L1-W4.5 TEC [Available online at
https://www.lairdthermal.com/products/thermoelectric-cooler-modules/peltier-cp-series/CP2-127-10-L1-W4.5]

Appendix A: Project Design Specification

Design Project: **The Drier Dryer '21**

Team: Dry Guys	Date: April 3, 2021	Revision: #4

Datum description: Dryer without attachment

ELEMENTS/ REQUIREMENTS		PARAMETERS	
	UNITS	DATUM	TARGET - RANGE
PERFORMANCE			
Time to Steady-State	secs	N/A	60-180
TEC Cold Side Temperature	°C	N/A	<-8
Incoming Air Temperature Decrease Across Cold Side	°C	N/A	>4
Incoming Air Temperature Increase Across Hot Side	°C	N/A	>4
Static Pressure (Head Loss)	ft	11-17 (Allowable)	7-9
Power	W	2000-6000	400-600
Applicable Force (Top)	lbs	N/A	75-100
Allowable Unit Rotation	deg	N/A	0-90
Unit Length	ft	3-4	2-3
Unit Width	ft	3-4	0.8-1.0
Energy Efficiency Improvement	%	0	20-25
Cycle Time Improvement	%	0	20-25
Lifespan	years	N/A	5-6
Range of Expected Ambient Relative Humidity	%	50-100	50-100
Relative Humidity of Air after passing Cold Side	%	N/A	100
Relative Humidity of Air after passing Hot Side	%	N/A	20-30
Length of Attached Ductwork	ft	N/A	2-3
Temperature of Air Inside Dryer	°C	125-145	52-63
Inlet Duct Diameter	in	4	4
Allowable Heat Sink Thermal Resistance	°C/W	N/A	0.1-0.2
Speed of Intake Airflow	m/s	4-7	4-5
SAFETY			
Temperature of Outer Casing	°C	N/A	1-43
Time to Shut Down	secs	N/A	2-3

Clearance from Dryer	inches	N/A	0-2
COST			
Manufacturing Cost	USD	350	165
Retail Cost	USD	450-1500	150-250
Savings per Dryer Load	USD	N/A	0.10-11
Savings per Year	USD	N/A	30-33
Time for System to Pay for Itself in Savings	years	N/A	5-6
USABILITY			
Time to Install	minutes	N/A	30-60
Maintenance Requirement (Changing Water Collector)	Changes/ Year	0	3

Appendix B: Hand Calculations

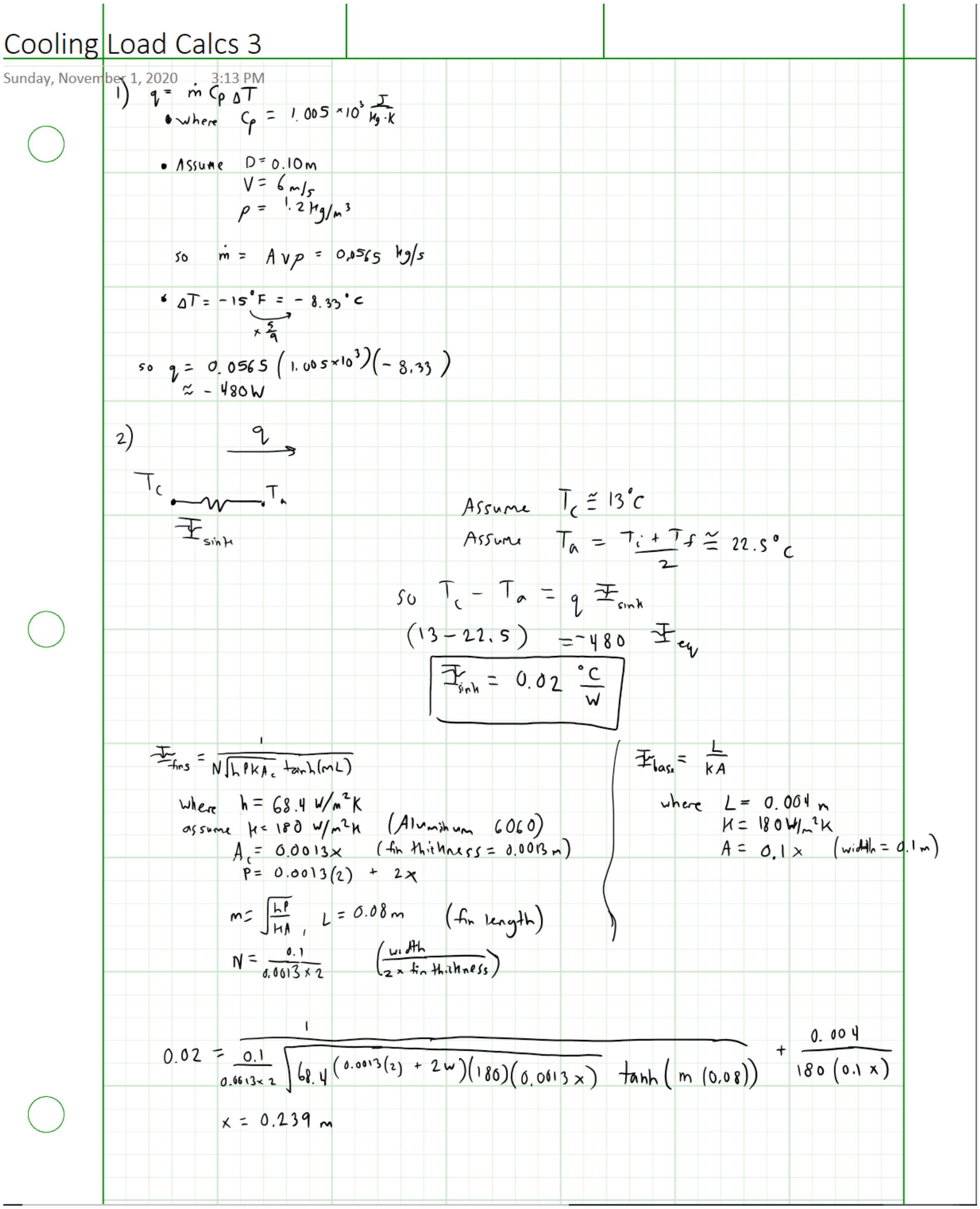

Figure B.1: (1) Cooling load calcs resulting in a 480W load. (2) Thermal resistance required for a 9°C drop at 480W of cooling. Results in a 0.02°C/W requirement. This is accompanied by a calculation of the approximate length of the heat sink that can meet this thermal resistance.

Pressure Loss

Saturday, November 7, 2020 1:55 PM

$f = 0.06$

$h_f = \frac{L}{D}\frac{V^2}{2g} f$ where $D = 0.1\,m$, $g = 9.81\,m/s^2$, $V = 6\,m/s$ } Assume all duct is of same material & diameter

- For typical dryer:

  $L_{allow} \cong 35\,ft \simeq 10\,m$

  so $h_f = \frac{10}{0.1} \cdot \frac{6^2}{2(9.81)}(0.06)$

  $= 11\,m$ (max head allowed)

  & $\Delta P_{allow} = 0.0981(11)(0.0013) \times 10^5 = 140.3\,Pa$

  ↳ SG of air

- For the proposed attachment:

  $L \cong 10\,ft \cong 3\,m$

  so $h_f = \frac{3}{0.1} \cdot \frac{6^2}{2(9.81)}(0.06)$

  $= 3.3\,m$ (head of attachment)

  & $\Delta P = 0.0981(3.3)(0.0013) \times 10^5 = 42.1\,Pa$

- Add minor losses: 2 elbows downstream of dryer & 4 upstream (90°)

  $K = 0.30$ for 4 in diameter, flanged

  $h_m = \sum \frac{V^2}{2g} K$

  $= 4 \times \left(\frac{6^2}{2(9.81)}\right) 0.30$

  $= 2.2\,m$

  & $\Delta P = .0981(2.2)(0.0013) \times 10^5 = 28.1\,Pa$

- Remaining downstream allowable length:

  $h_{remaining} = h_{allow} - h_{attachment} - h_{minor} - h_{hs}$

  $= 11 - 2.2 - 3.3 - 2.22(2) = 1.06$

  so $1.06 = \frac{L}{0.1}\frac{6^2}{2(9.81)}(0.06)$

  $L_{remaining} = 1\,m = 3.28\,ft$

- Heat sink:

  $\Delta P = \left(K_c + 4 f_{app} \cdot \frac{L}{D_h} + K_e\right)\rho \frac{V^2}{2}$

  $= \left(K_c + 4(0.06) \cdot \frac{0.288}{0.1} + K_e\right)(1.2)\left(\frac{6^2}{2}\right)$

  - $K_c = 0.42\left(1 - \left(1 - \frac{N t_f}{W}\right)^2\right)$
    $= 0.42(1 - 0.63^2)$ @ $N = 35$, $t_f = 0.002\,m$, $W = 188\,mm$
    ≈ 0.2545

  - $K_e = \left(1 - \left(1 - \frac{N t_f}{W}\right)^2\right)^2$
    $= 0.3673$

  so $\Delta P = \left(0.2545 + 4(0.06) \cdot \frac{0.288}{0.1} + 0.3673\right)1.2\left(\frac{6^2}{2}\right)$

  $= 28.36\,Pa$

  $h_{hs} = 2.22\,m$ per heat sink

Figure B.2: Pressure drop calculations used to determine if supplemental fans were necessary. The pressure loss was found to exceed the head produced by the built-in fan.

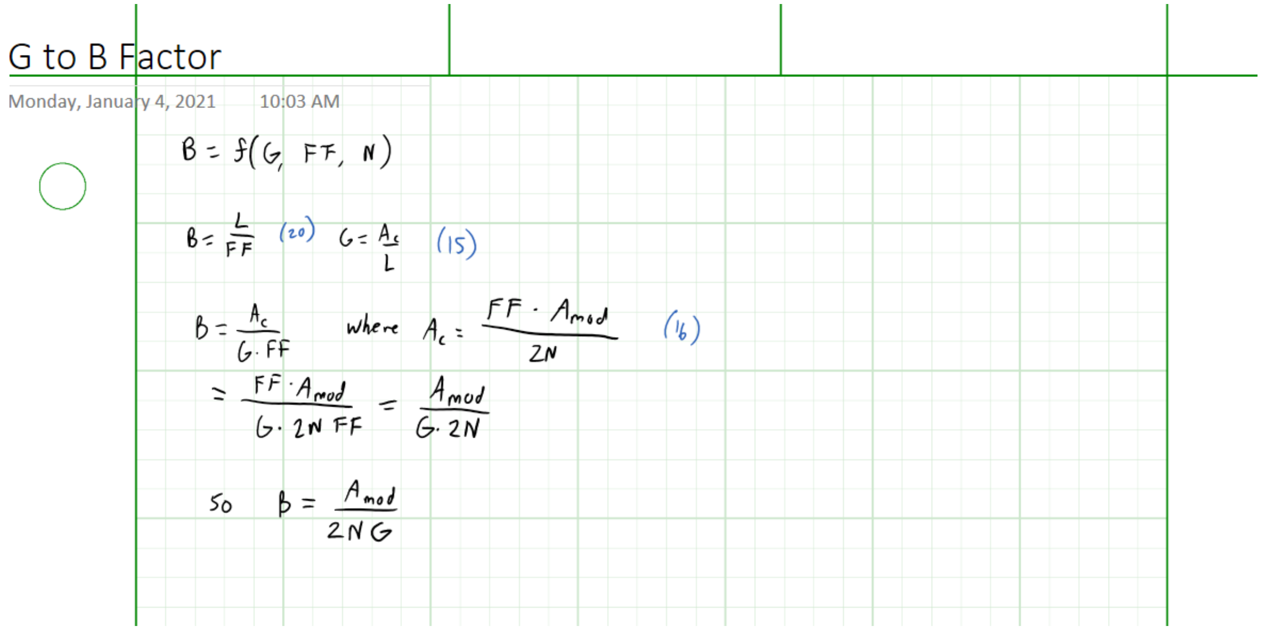

Figure B.3: Conversion of G factor to B factor used to computational estimate the voltage and current requirements for the TEC to run at maximum temperature difference [6].

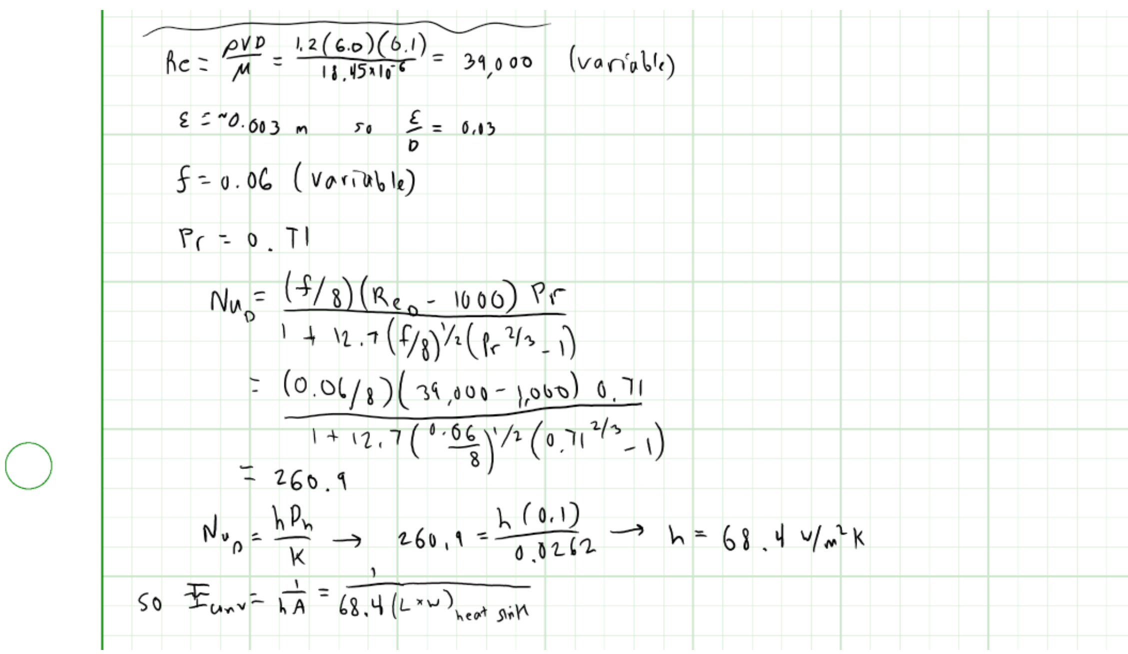

Figure B.4: Reynolds number of the flow through the dryer exhaust and the resulting convective heat transfer coefficient for turbulent flow.

Appendix C: Prototype Drawings

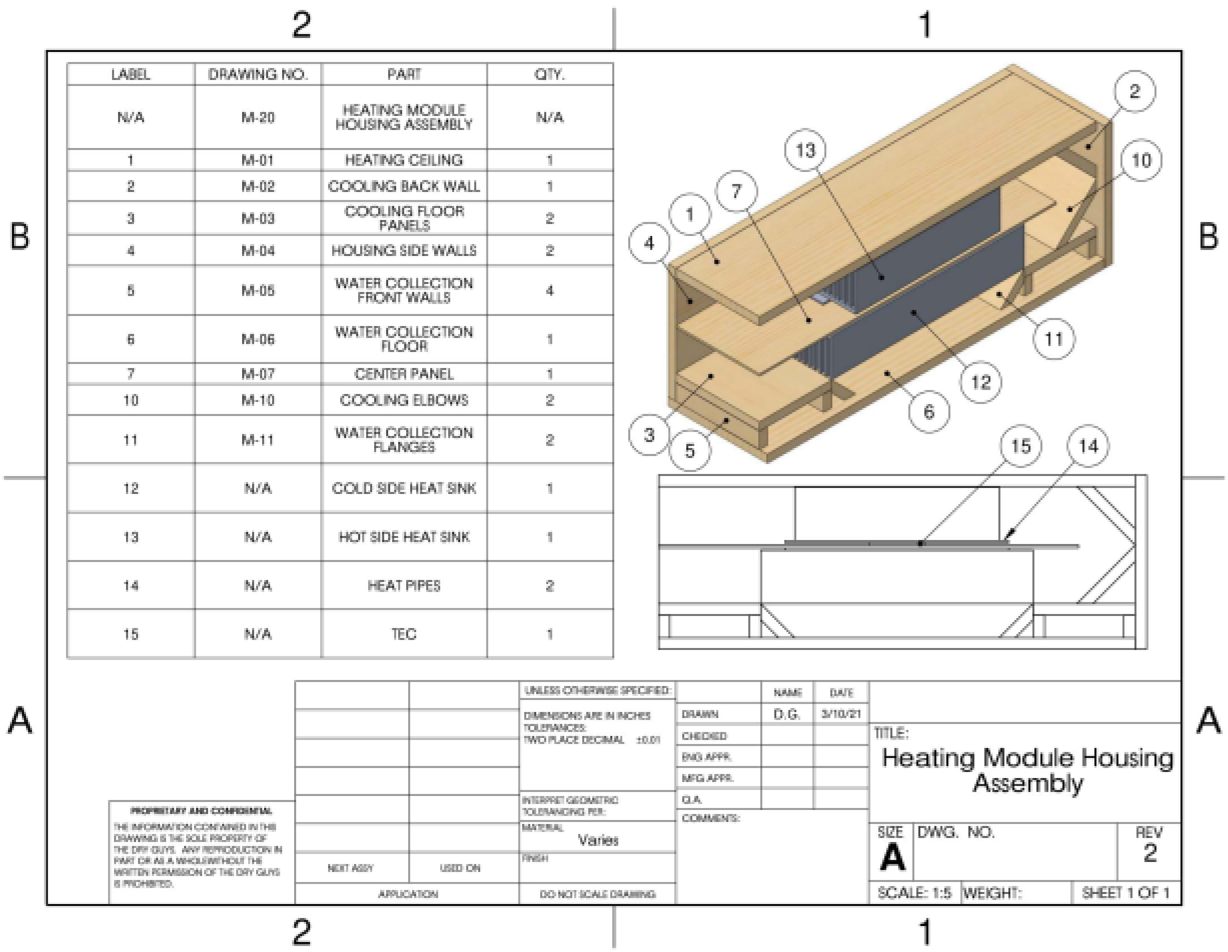

LABEL	DRAWING NO.	PART	QTY.
N/A	M-20	HEATING MODULE HOUSING ASSEMBLY	N/A
1	M-01	HEATING CEILING	1
2	M-02	COOLING BACK WALL	1
3	M-03	COOLING FLOOR PANELS	2
4	M-04	HOUSING SIDE WALLS	2
5	M-05	WATER COLLECTION FRONT WALLS	4
6	M-06	WATER COLLECTION FLOOR	1
7	M-07	CENTER PANEL	1
10	M-10	COOLING ELBOWS	2
11	M-11	WATER COLLECTION FLANGES	2
12	N/A	COLD SIDE HEAT SINK	1
13	N/A	HOT SIDE HEAT SINK	1
14	N/A	HEAT PIPES	2
15	N/A	TEC	1

Figure C.1: Prototype Assembly Drawing

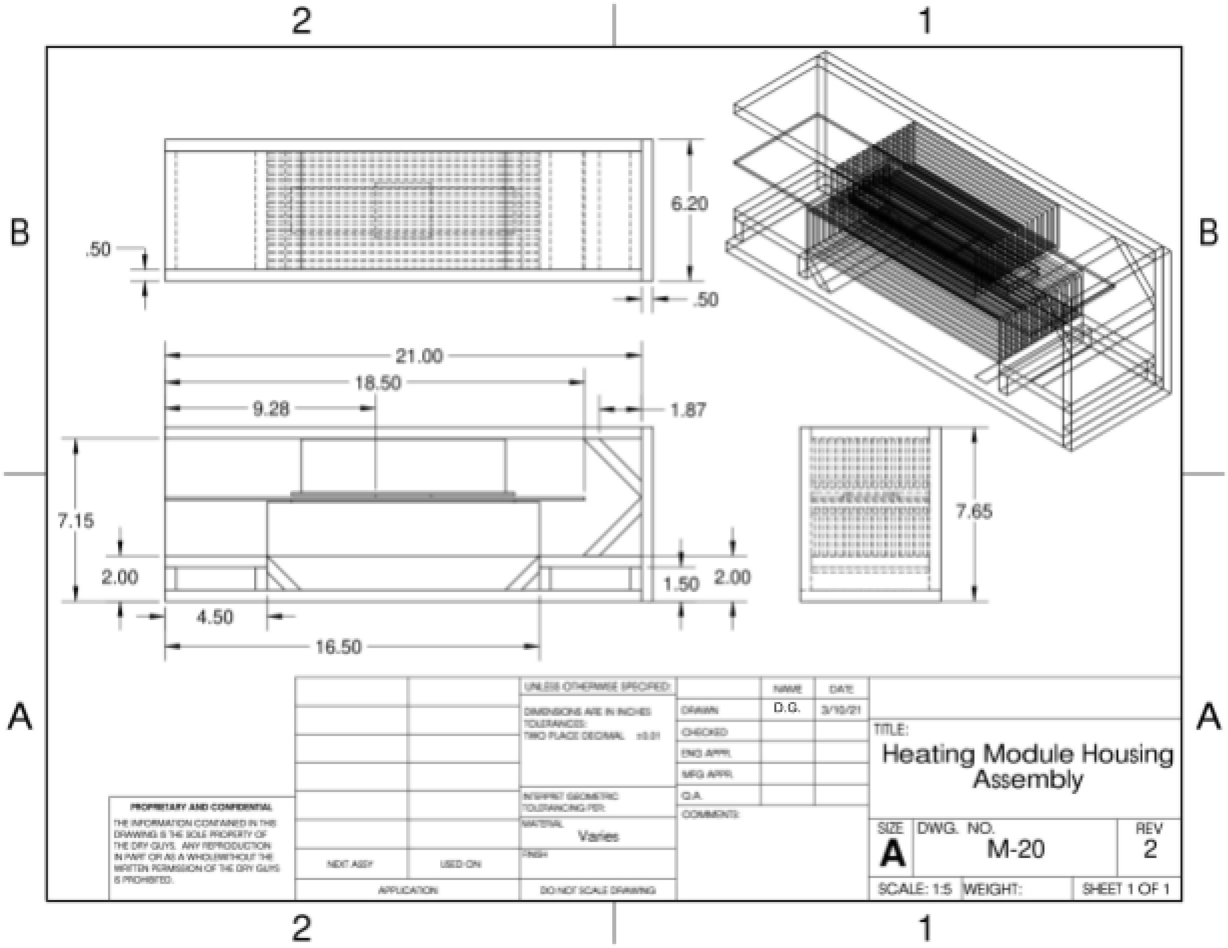

Figure C.2: Prototype Dimension Drawing

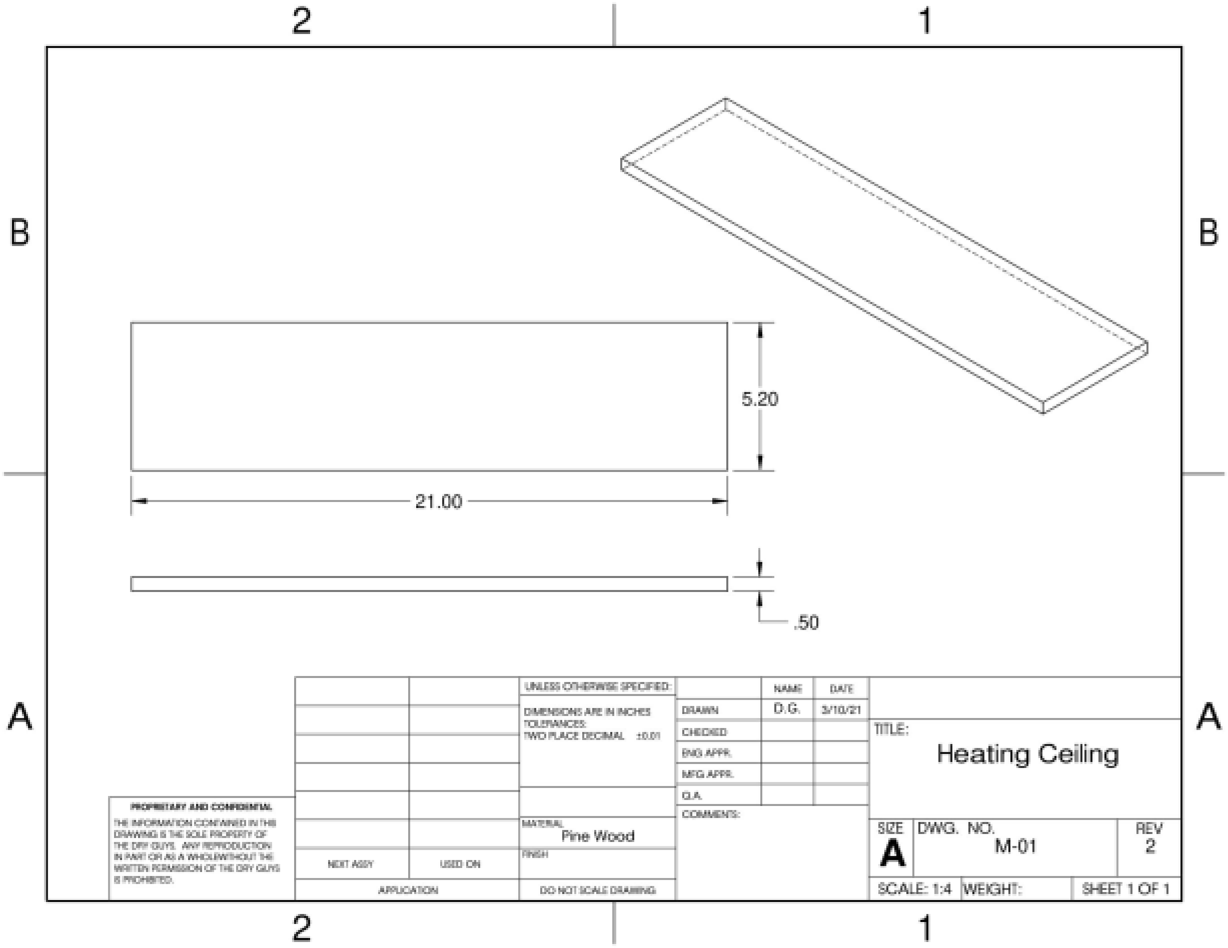

Figure C.3: Prototype Ceiling Drawing

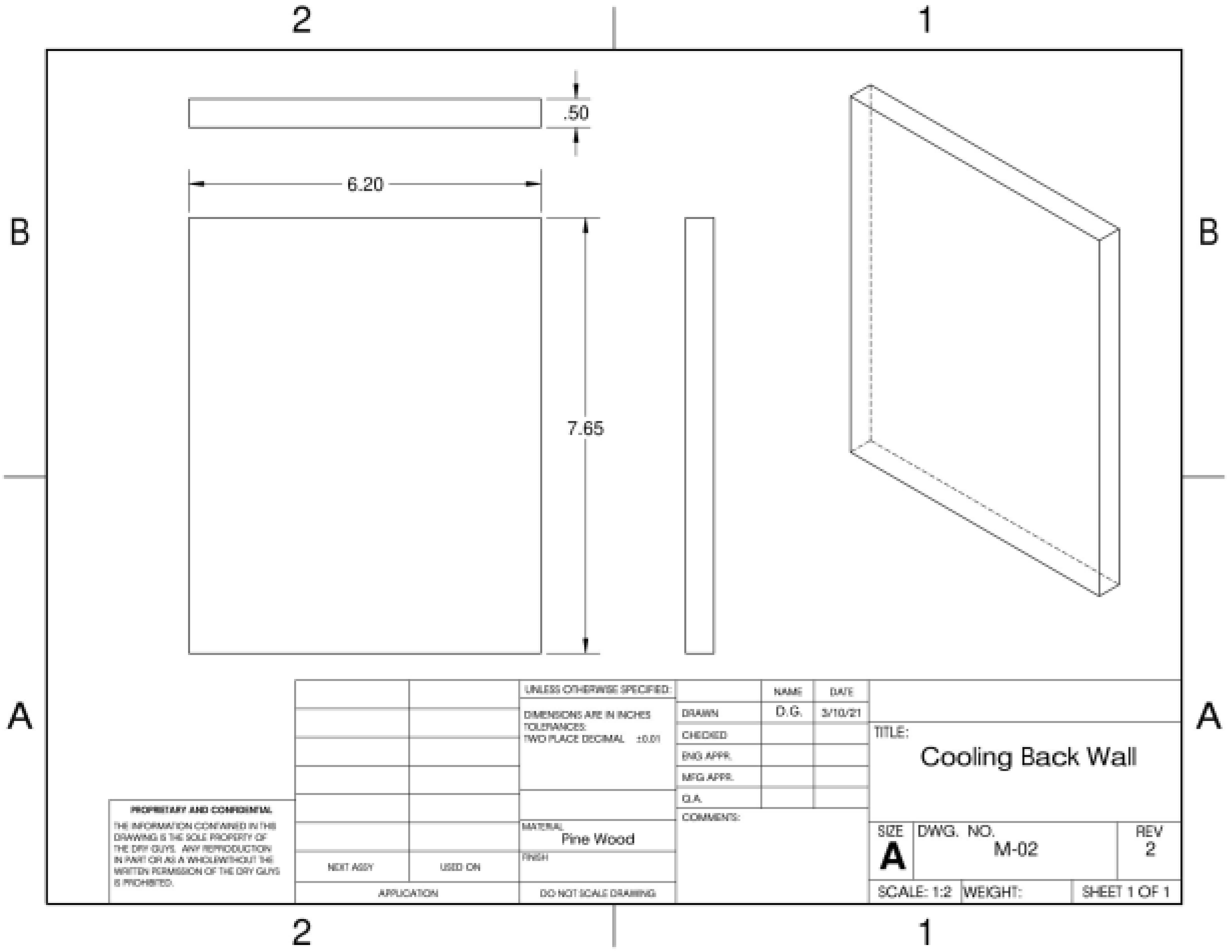

Figure C.4: Prototype Back Wall Drawing

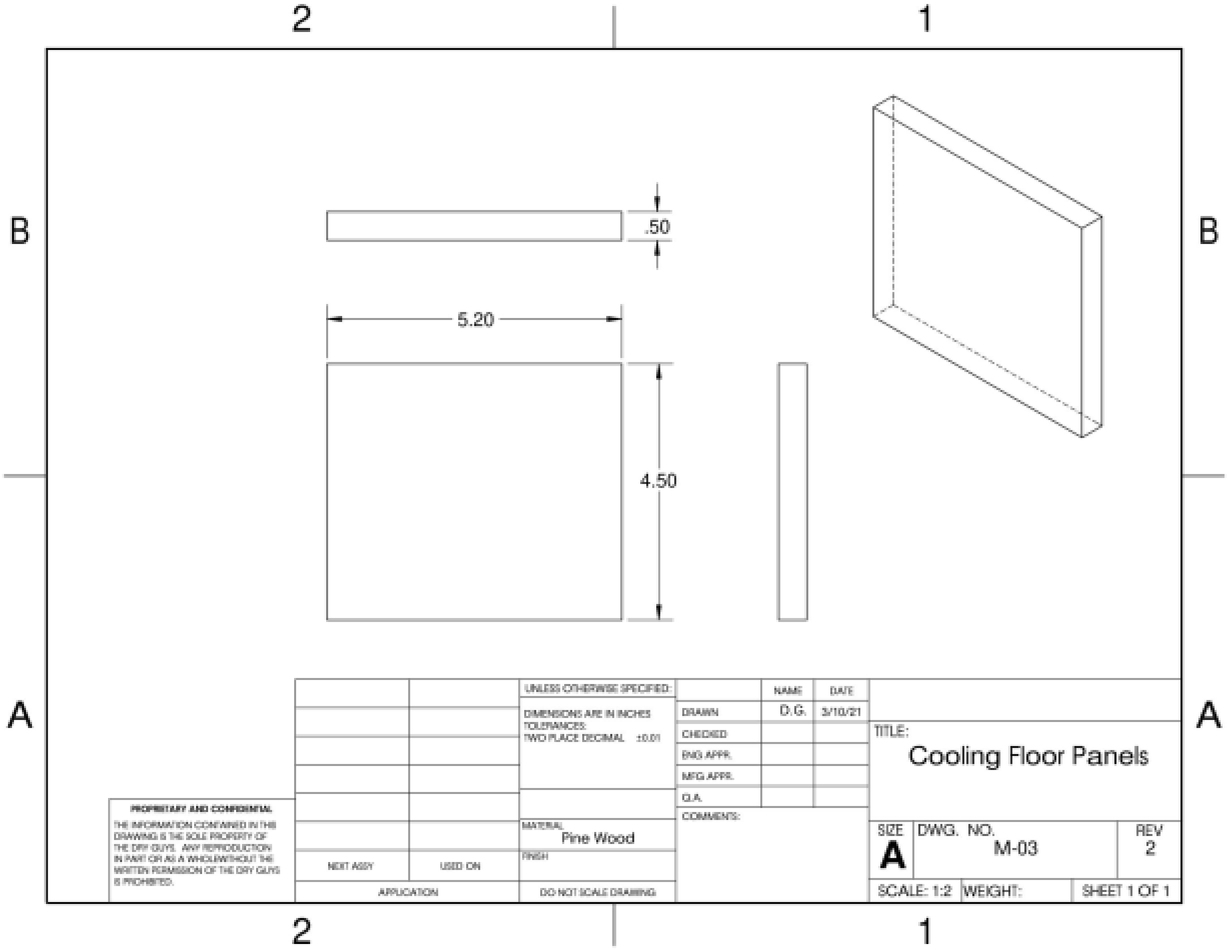

Figure C.5: Prototype Floor Panel Drawing

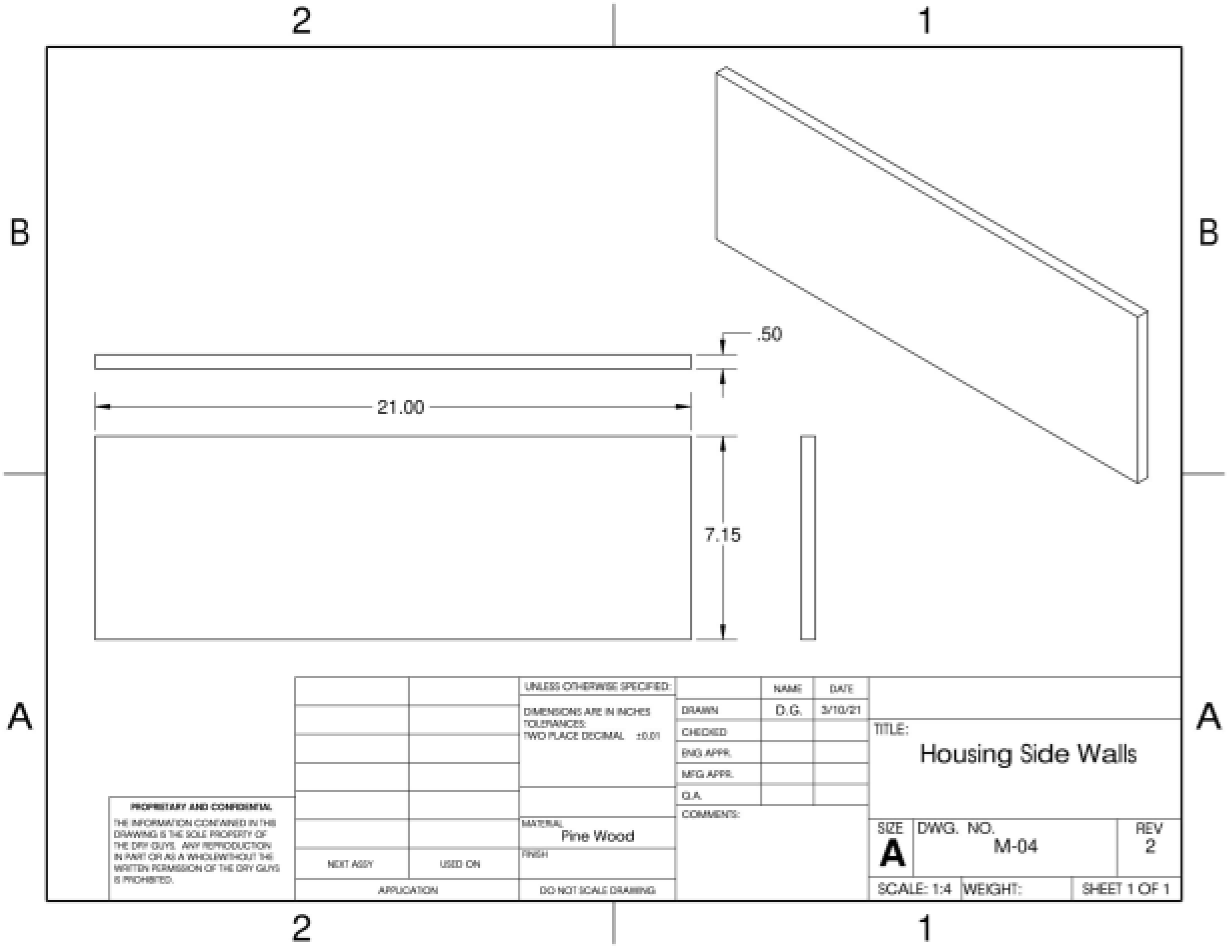

Figure C.6: Prototype Side Wall Drawing

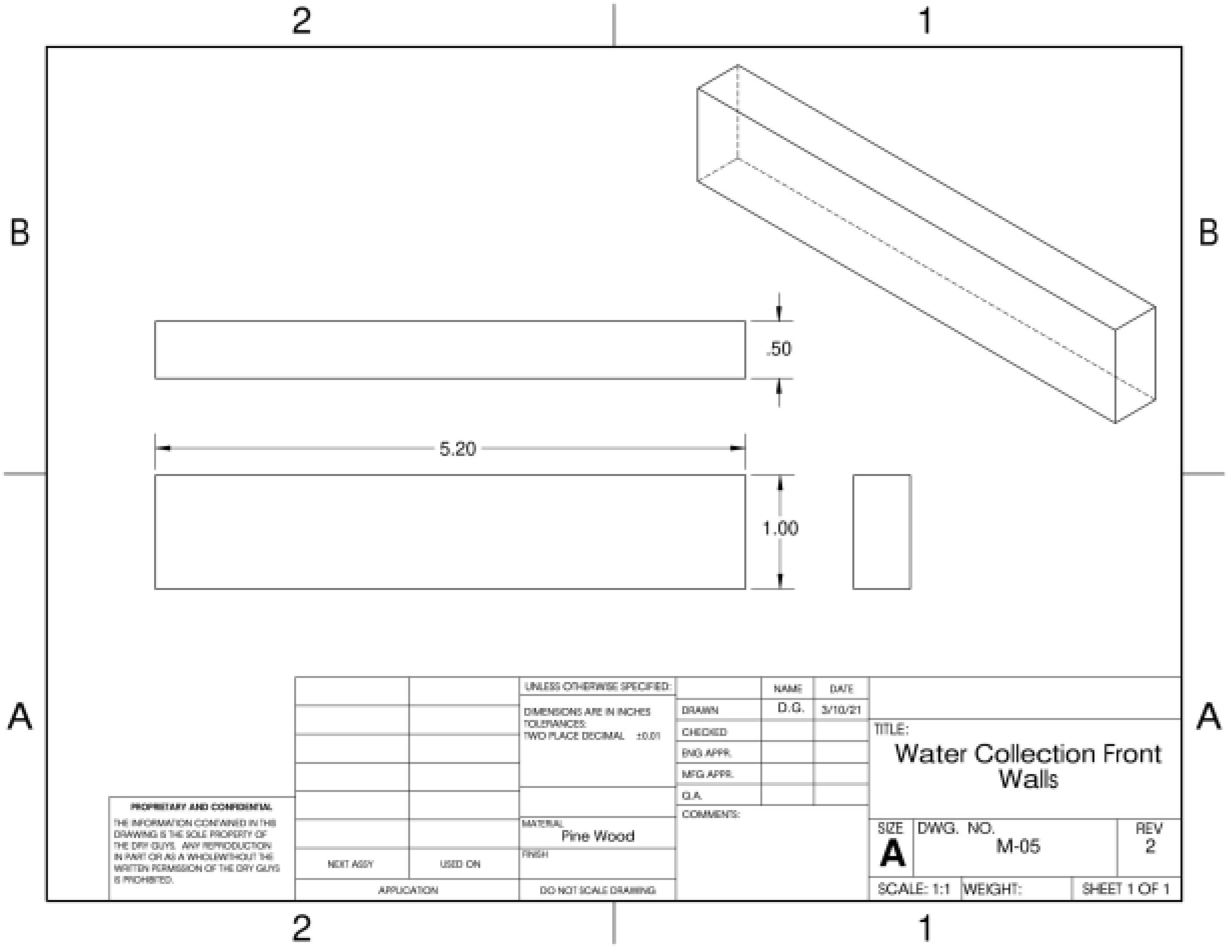

Figure C.7: Water Collection Front Wall Drawing

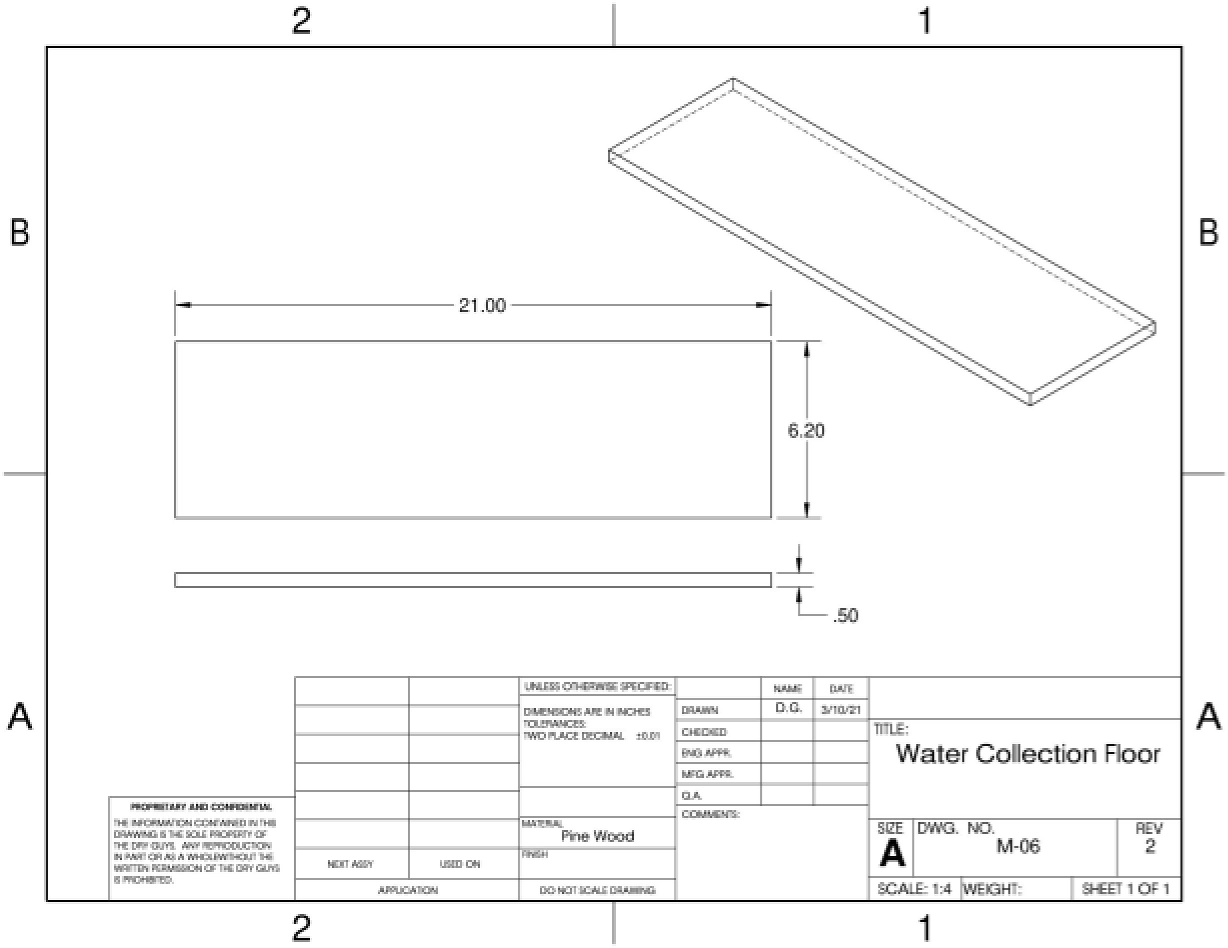

Figure C.8: Water Collection Floor Drawing

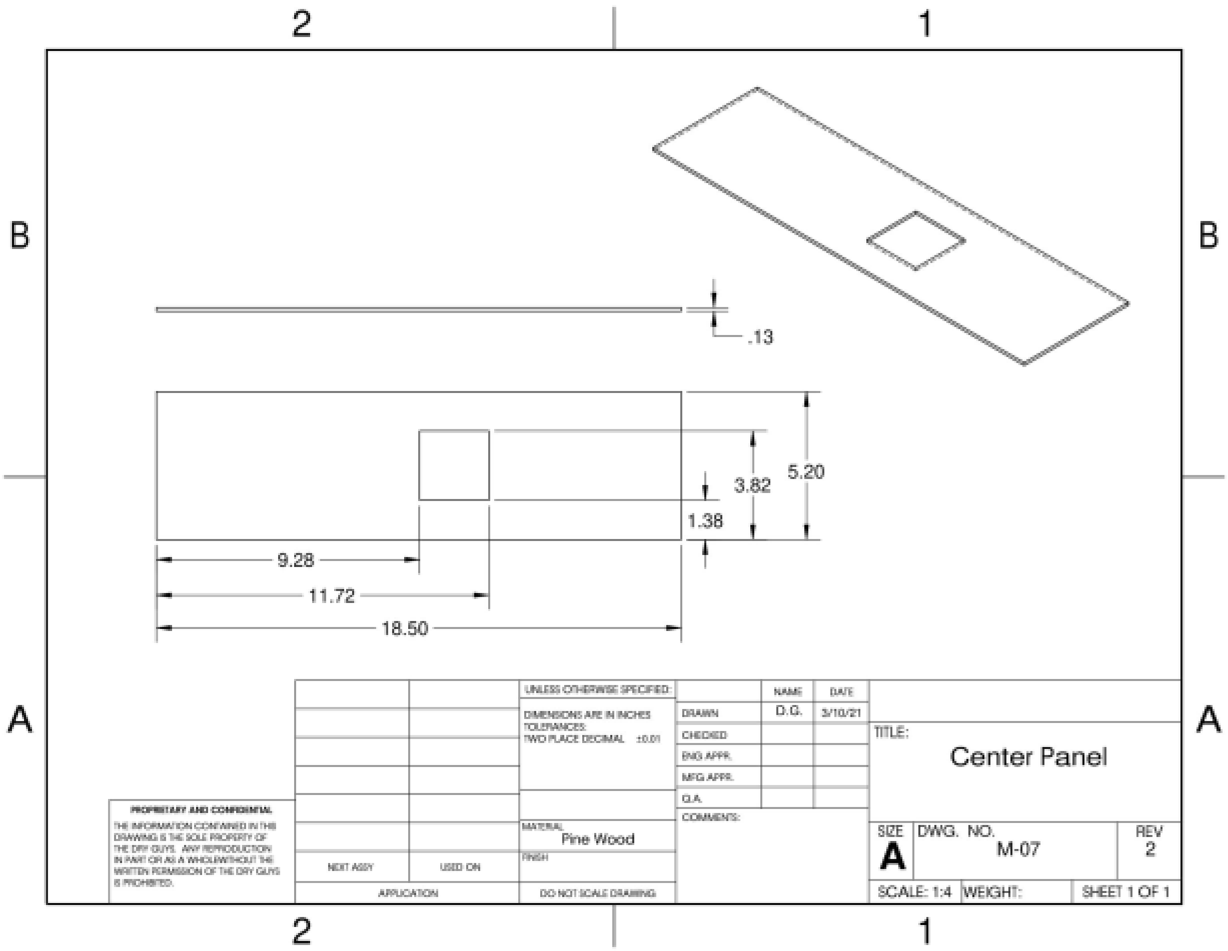

Figure C.9: Prototype Center Panel Drawing

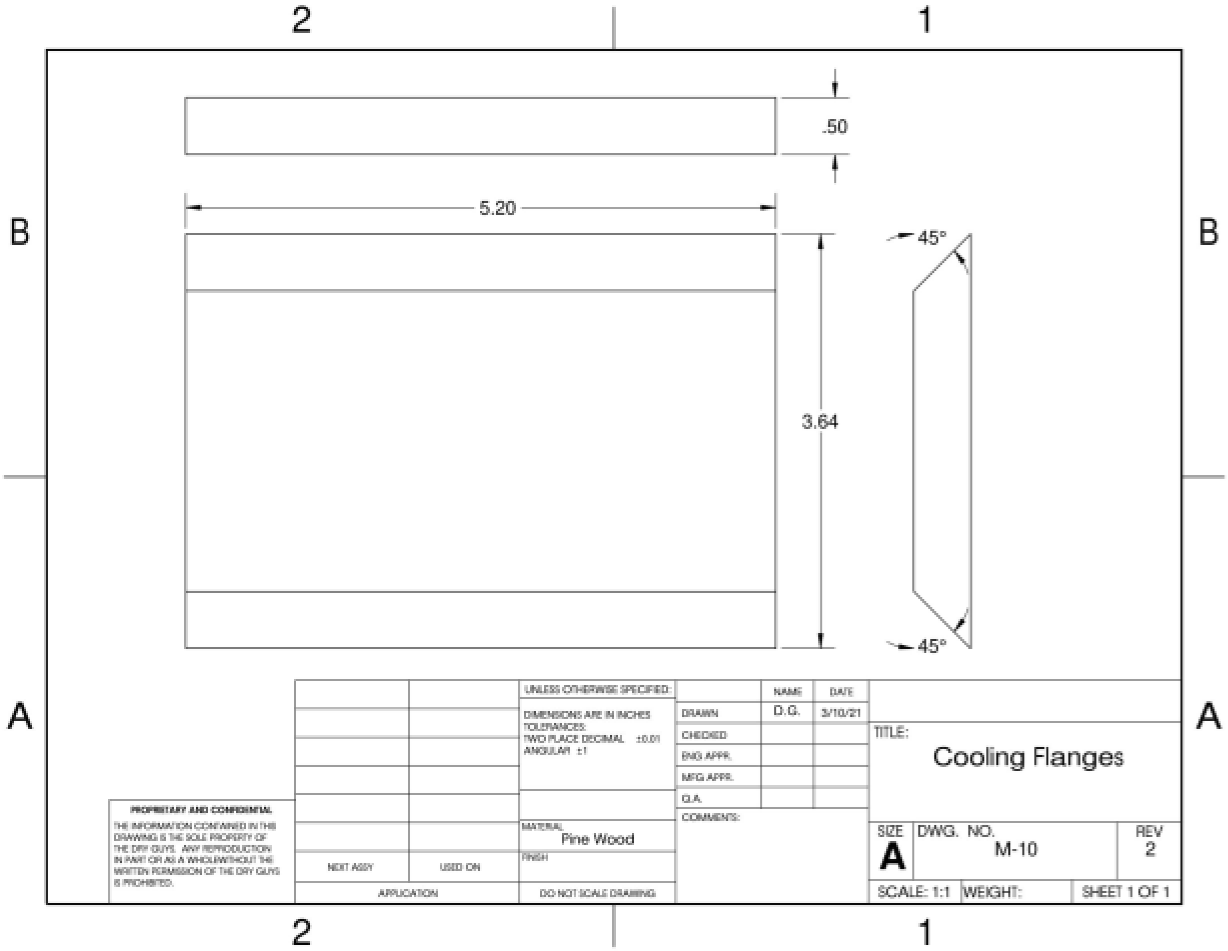

Figure C.10: Prototype Flange Drawing

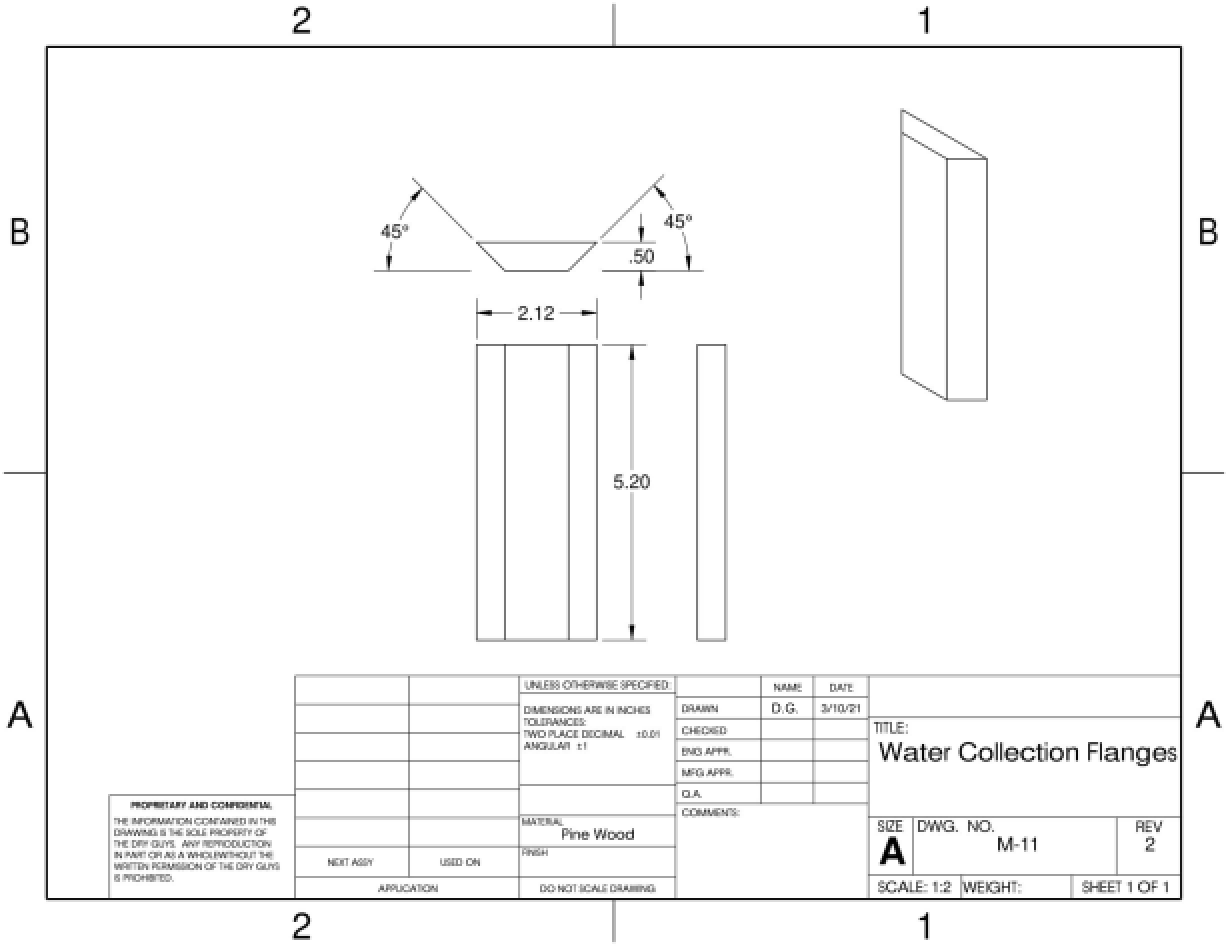

Figure C.11: Water Collection Flange Drawing

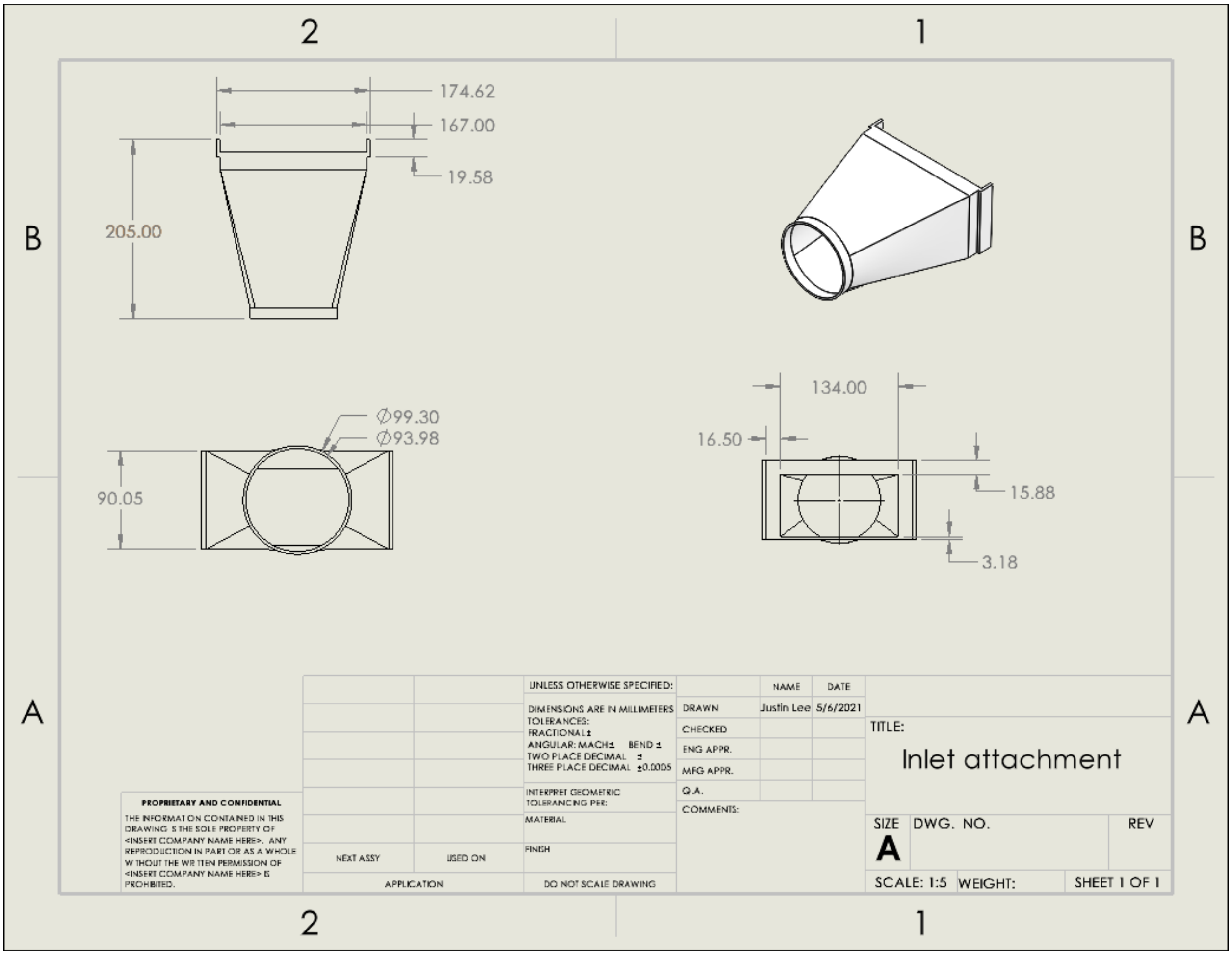

Figure C.12: Dryer attachment subsystem

Appendix D: MATLAB Code

```
clear all
clc

% Defining range of ambient conditions and corresponding vapor pressures
T_room = [22; 24; 26; 28; 30; 32; 34];
RH_room = [70 75 80 85 90 95 100];
T_dry = 55;
Psat_room = 0.6108.*exp((17.27.*T_room)./(T_room+237.3));
Pact_room = (RH_room.*Psat_room)./100;
Psat_dry = 0.6108*exp((17.27*T_dry)/(T_dry+237.3));

% Defining temperature difference the system can provide and vapor
% pressures of the treated air
Td_sys5 = T_room - 11;
RH_sys5 = [50 50 50 50 50 50 50];
Psat_sys5 = 0.6108*exp((17.27.*T_room)./(T_room+237.3));
Pact_sys5 = (RH_sys5.*Psat_sys5)/100;

dP_norm = Psat_dry - Pact_room;

% Increase in efficiency:
dP_sys5 = Psat_dry - Pact_sys5;
efficiency5 = (dP_sys5 - dP_norm)./dP_norm;

% For a drying cycle that would typically take one hour,
%money savings (in cents) is approximately:
costsavings5 = 131*efficiency5 - 1.708;
costsavings5 = costsavings5';

% Plotting the net cost savings results on a 3D graph
surf(T_room,RH_room,costsavings5)
colormap hsv;
title('Net Cost Savings for a 5°C Temperature Decrease');
xlabel('Temperature [°C]')
ylabel('Relative Humidity [%]')
zlabel('Net Cost Savings [cents]')
xticks([22 24 26 28 30 32 34]);
xticklabels({'22','24','26','28','30','32','34',});
ax = gca;
ax.FontSize = 35;
```

Figure D.1: MATLAB code generating cost savings analysis for a given performance of a TEC and its power input.

Cooling Load: Constant Heat Removal

```
L_s = 2.5/12; %side length of duct (ft)
deltaT = -20; %desired change in air temperature (deltaT = Tf - Ti)
 (F)
Cp = 0.241; %specific heat of air (BTU/(lb*F))
V = [15: 0.1: 25]; %measured velocity of air (ft/s)
D = [0.31: 0.01: 0.36]; %measured diameter of duct (ft)
D = 0.33; %test
A_TEC = 2.5/12*2.5/12; %surface area of thermoelectric module (ft^2)
p = 0.0745; %density of air (lbm/ft^3) at 70F

L = sqrt(A_TEC);
P = 4*L_s;
A_duct = L_s^2;

A_duct_meas = pi*D^2/4;
Q = V*A_duct_meas;
m_dot = Q*p;

q = -4*A_TEC*m_dot*Cp*deltaT / (P*L);
q_watts = q*1055.1; %convert BTU/s to watts

plot(Q, q_watts)
hold on;
xlabel("Volumetric Flow Rate [ft^3/s]")
ylabel("Required Cooling Load [Watts]")

% for i=1:size(D, 2)
%     A_duct_meas = pi*D(i)^2/4;
%     Q = V*A_duct_meas;
%     m_dot = Q*p;
%
%     q = 4*A_TEC*m_dot*Cp*deltaT / (P*L);
%     q_watts = q*1055.1; %convert BTU/s to watts
%
%     plot(Q, q_watts)
%     hold on;
% end
```

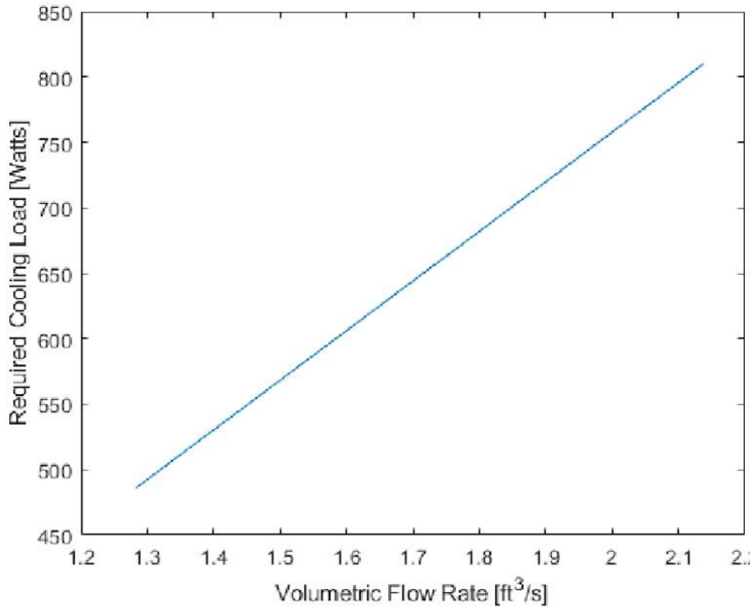

Cooling Load: Constant Tc

```
deltaT = -8.33; %desired change in air temperature (deltaT = Tf - Ti)
 (C)
Cp = 1.005E3; %specific heat of air (J/(kg*K))
V = 6; %measured velocity of air (m/s)
D = 0.1; %diameter of duct (m)
p = 1.2; %density of air (kg/m^3)

A_duct_meas = pi*D^2/4; %duct cross-sectional area (m^2)
Q = V*A_duct_meas; %volumetric flow rate (m^3/s)
m_dot = Q*p; %mass flow rate (kg/s)

q = m_dot*Cp*deltaT %Watts

Tc = 9; %temp of cold side of TEC (C)
Ta = 22.5; %average temp of air across the heat sink (C)
I_eq = (Tc-Ta)/q;

syms x; %length of heat sink

%fins
base_width = 0.1323;
fin_thickness = 0.0015; %(m)
H = 0.05; %fin height (m)
```

```
h = 68.4; %convective heat transfer coefficient (W/(m^2*K))
k = 180; %thermal conducitivity of aluminum 6060 (W/(m*K))
Ac_fins = fin_thickness*x;
P_fins = 0.0013*2+2*x;
m = sqrt(h*P_fins/(k*Ac_fins));
N = base_width/(fin_thickness*2);
I_fins = 1/(N*sqrt(h*P_fins*k*Ac_fins)*tanh(m*H)); %Thermal Resistance
 of fins as a fxn of x (length of heat sink)

%base
H_base = 0.005; %base height (m)
A_base = base_width*x;
I_base = H_base/(k*A_base);

HS_Length = vpasolve(I_base + I_fins == I_eq, x, [0 inf])
```

q =

-473.4057

HS_Length =

0.16808175663949082114555159624106

Test Thermal Resistance of heat sink

```
h = 68.4;

fin_thickness = 0.00254;
H = 0.05969; %1 in
N = 20;
k = 210; %AL 603
L = 0.2286; %1 ft
base_width = .13233;
H_base = .0056;

P_fins = 2*H + L*fin_thickness;
Ac_fins = fin_thickness*L;
m = sqrt(h*P_fins/(k*Ac_fins));

I_fins = 1/(N*sqrt(h*P_fins*k*Ac_fins)*tanh(m*H));

A_base = base_width*L;

I_base = H_base/(k*A_base);

%Spreading Resistance
S2_W = 0.1323; %width of HS-1
S2 = 0.3048; %length of HS-1
S1 = 0.035; %average length of TEC
```

```
t = 0.0056; %height of HS-1 base
h_eff = 68.4; %convective heat transfer coefficient from speed of air
 powered by dryer fan
%k = 200; %thermal conductivity of aluminum
k = 2000; %thermal condudctivity of layer of heat pipes

r1 = sqrt(S1*S1/pi());
r2 = sqrt(S2_W*S2/pi());
epsilon = r1/r2;
tau = t/r2;
Bi = h_eff*r2/k;
lambda = pi() + 1/(epsilon*sqrt(pi()));
phi = (tanh(lambda*tau)+lambda/Bi)/(1+lambda/Bi*tanh(lambda*tau));
YYmax = epsilon*tau/sqrt(pi())+1/(sqrt(pi()))*(1-epsilon)*phi;

Rsp = YYmax/(k*r1*sqrt(pi()));
%-----------------------------

I_eq = I_fins + I_base + Rsp


I_eq =

    0.1328
```

Published with MATLAB® R2020a

Figure D.2: MATLAB algorithms for the cooling load (calculated using two different methods), and a calculator for the thermal resistance of a heat sink given a number of fins, material, and dimensions.

Reynolds Number & Convective Heat Transfer Coefficient

```
p = 1.2; %density of air [kg/m^3]
V = 12.0; %speed of air [m/s]
D = 0.1524; %diameter of duct [m] (6 in.)
u = 18.45E-6; %viscosity of air [Pa*s]

Re = p*V*D/u;

e = 0.003; %duct roughness
f = 0.06; %friction factor
Pr = 0.71; %Prandtls Number
k = 0.0262; %thermal conductivity of air [W/(m^2*K)]

Nu_D = (f/8*(Re-1000)*Pr)/(1+12.7*(f/8)^(1/2)*(Pr^(2/3)-1));

h = Nu_D*k/D
```

```
h =

  139.2353
```

Published with MATLAB® R2020a

Figure D.3: MATLAB algorithm for calculating Reynolds number of a flow and the corresponding convective heat transfer coefficient (this algorithm can only be used for turbulent flow).

Table of Contents

Scenario 1 - pre-chosen heat sink

```
S2_W = 0.1323; %width of HS-1
S2 = 0.3048; %length of HS-1
S1 = 0.035; %average length of TEC
t = 0.0056; %height of HS-1 base
h_eff = 68.4; %convective heat transfer coefficient from speed of air
 powered by dryer fan
k = 200; %thermal conductivity of aluminum

r1 = sqrt(S1*S1/pi());
r2 = sqrt(S2_W*S2/pi());
epsilon = r1/r2;
tau = t/r2;
Bi = h_eff*r2/k;
lambda = pi() + 1/(epsilon*sqrt(pi()));
phi = (tanh(lambda*tau)+lambda/Bi)/(1+lambda/Bi*tanh(lambda*tau));
YYmax = epsilon*tau/sqrt(pi())+1/(sqrt(pi()))*(1-epsilon)*phi;

Rsp = YYmax/(k*r1*sqrt(pi()))


Rsp =

    0.2149
```

Generalized for varying heat sink length

```
S2_W = 0.1323; %width of HS-1
S2 = [0.035: 0.001: 0.305]; %length of HS-1
S1 = 0.035; %average length of TEC
t = 0.0056; %height of HS-1 base
h_eff = 68.4; %convective heat transfer coefficient from speed of air
 powered by dryer fan
%k = 200; %thermal conductivity of aluminum
k = 2000; %thermal condudctivity of layer of heat pipes

r1 = sqrt(S1*S1/pi());
r2 = sqrt(S2_W*S2/pi());
epsilon = r1./r2;
tau = t./r2;
Bi = h_eff*r2/k;
lambda = pi() + 1./(epsilon*sqrt(pi()));
```

```
phi = (tanh(lambda.*tau)+lambda./Bi)./(1+lambda./
Bi.*tanh(lambda.*tau));
YYmax = epsilon.*tau/sqrt(pi())+1/(sqrt(pi()))*(1-epsilon).*phi;

Rsp = YYmax/(k*r1*sqrt(pi()));

plot(S2, Rsp)
xlabel('Heat Sink Length [m]');
ylabel('Spreading Resistance [C/W]');
```

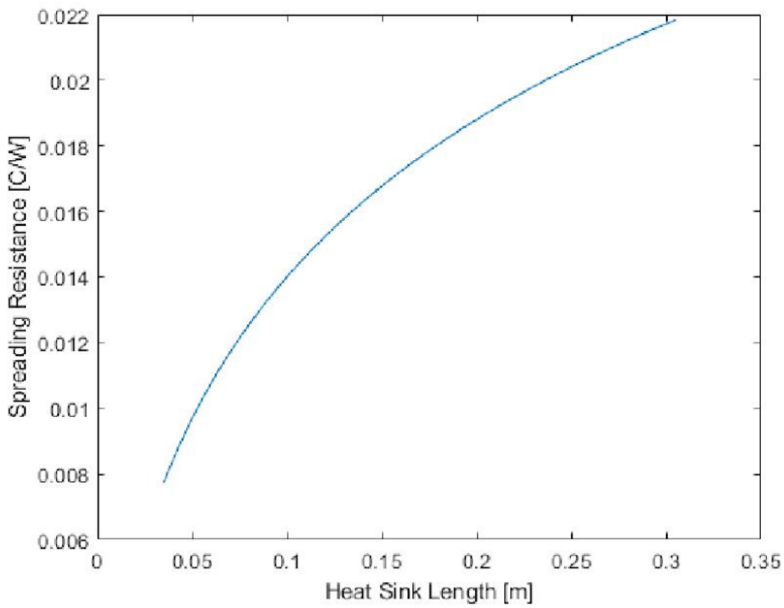

Generalized for varying number of TECs

```
num_TEC = [1: 10]
S2_W = 0.1323; %width of HS-1
S2 = 0.3048./num_TEC; %length of HS-1
S1 = 0.035; %average length of TEC
t = 0.0056; %height of HS-1 base
h_eff = 68.4; %convective heat transfer coefficient from speed of air
 powered by dryer fan
k = 200; %thermal conductivity of aluminum

r1 = sqrt(S1*S1/pi());
r2 = sqrt(S2_W*S2/pi());
epsilon = r1./r2;
tau = t./r2;
Bi = h_eff*r2/k;
```

```
lambda = pi() + 1./(epsilon*sqrt(pi()));
phi = (tanh(lambda.*tau)+lambda./Bi)./(1+lambda./
Bi.*tanh(lambda.*tau));
YYmax = epsilon.*tau/sqrt(pi())+1/(sqrt(pi()))*(1-epsilon).*phi;

Rsp = YYmax/(k*r1*sqrt(pi()));

plot(num_TEC, Rsp)
xlabel('Number of TECs');
ylabel('Spreading Resistance [C/W]');
```

```
num_TEC =

     1     2     3     4     5     6     7     8     9    10
```

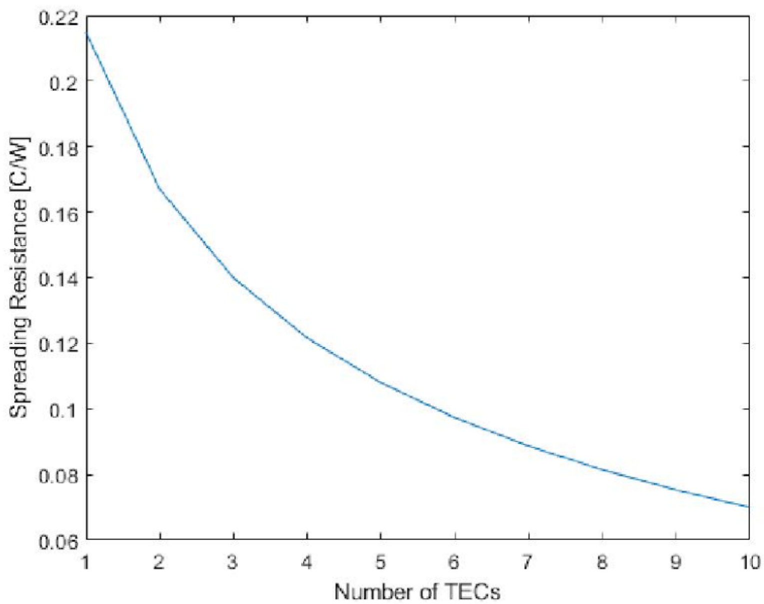

Published with MATLAB® R2020a

Figure D.4: MATLAB spreading resistance calculator for a given heat sink and TEC dimensions. In addition, this relationship is generalized to a heat sink of varying length and considering the use of multiple equally-spaced TECs on one heat sink.

Appendix E: First Page of Relevant Patents

US007347009B2

(12) **United States Patent**
Ahn et al.

(10) **Patent No.: US 7,347,009 B2**
(45) **Date of Patent: Mar. 25, 2008**

(54) **CLOTHES DRYER WITH A DEHUMIDIFIER**

(75) Inventors: **Seung Phyo Ahn**, Gyeongsangnam-Do (KR); **Jung Wook Moon**, Gyeongsangnam-Do (KR); **Dae Woong Kim**, Gyeongsangnam-Do (KR); **Seung Myun Baek**, Gyeongsangnam-Do (KR); **Byeong Jo Ryoo**, Gyeongsangnam-Do (KR)

(73) Assignee: **LG Electronics Inc.**, Seoul (KR)

(*) Notice: Subject to any disclaimer, the term of this patent is extended or adjusted under 35 U.S.C. 154(b) by 0 days.

(21) Appl. No.: **11/292,313**

(22) Filed: **Dec. 2, 2005**

(65) **Prior Publication Data**

US 2006/0117593 A1 Jun. 8, 2006

(30) **Foreign Application Priority Data**

Dec. 7, 2004 (KR) 10-2004-0102567

(51) **Int. Cl.**
F26B 7/00 (2006.01)

(52) **U.S. Cl.** **34/607**

(58) **Field of Classification Search** 34/513, 34/607

See application file for complete search history.

(56) **References Cited**

U.S. PATENT DOCUMENTS

2,752,694	A *	7/1956	McCormick	34/60
7,036,243	B2 *	5/2006	Doh et al.	34/595
2005/0246920	A1 *	11/2005	Yabuuchi et al.	34/515

* cited by examiner

Primary Examiner—S. Gravini
(74) *Attorney, Agent, or Firm*—Ked & Associates LLP

(57) **ABSTRACT**

A clothes dryer with a dehumidifier is disclosed. The clothes dryer includes a cabinet, a drying container rotatably installed in the cabinet, a driving unit for supplying a rotational force to the drying container, a first air passage connected to a side of the drying container and including a first heat exchanger, a second air passage connected to another side of the drying container and the outer side of the cabinet, and a third air passage including a second heat exchanger for dehumidifying external air of the drying container. The clothes dryer of the present invention performs drying process and dehumidifying process, the clothes dryer can prevent room humidity from increasing.

19 Claims, 5 Drawing Sheets

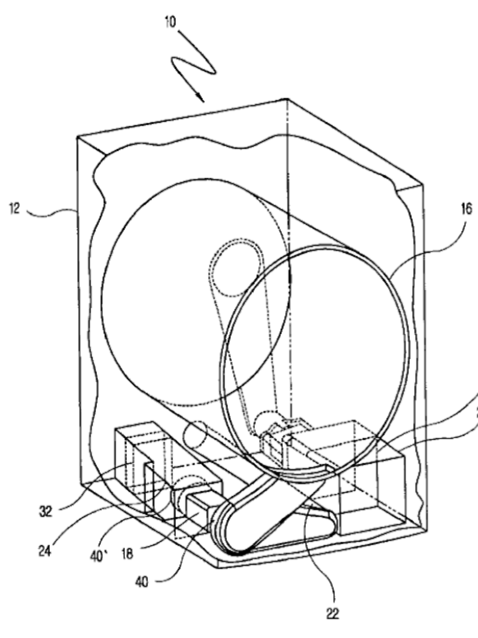

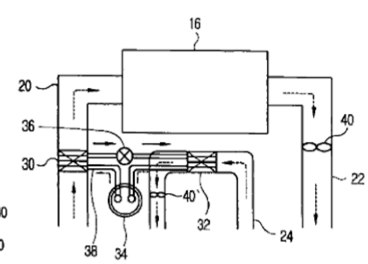

United States Patent [19]

Lanciaux

[11] **Patent Number: 4,621,438**

[45] **Date of Patent: Nov. 11, 1986**

[54] **ENERGY EFFICIENT CLOTHES DRYER**

[75] Inventor: **Francis Lanciaux,** Fort Wayne, Ind.

[73] Assignee: **Donald M. Thompson,** Glen Ellyn, Ill. ; a part interest

[21] Appl. No.: **457,528**

[22] Filed: **Jan. 13, 1983**

Related U.S. Application Data

[63] Continuation-in-part of Ser. No. 212,804, Dec. 4, 1980, abandoned.

[51] **Int. Cl.**[4] **F26B 21/06**

[52] **U.S. Cl.** **34/77;** 34/133; 34/242; 62/158; 62/228.1

[58] **Field of Search** 34/77, 89, 133, 242; 62/158, 228; 417/225, 32

[56] **References Cited**

U.S. PATENT DOCUMENTS

1,119,011	12/1914	Grosvenor	34/77
2,172,059	9/1939	Chilton	34/77
2,676,418	4/1954	Shewmon	34/77
3,190,011	6/1965	Shields	34/133
3,263,335	8/1966	Kan	34/77
3,718,982	3/1973	Deaton	34/82
3,786,649	1/1974	Kirschner	62/394
3,877,837	4/1975	Parker et al.	417/25
3,978,592	9/1976	Schuurink	34/82
4,007,546	2/1977	Sauer	34/133
4,142,375	3/1979	Abe et al.	62/158

Primary Examiner—Larry I. Schwartz
Attorney, Agent, or Firm—Edward W. Osann, Jr.

[57] **ABSTRACT**

An energy efficient heat pump dryer for clothes and other washables having a sealed rotatable clothes tumbling drum and means for circulating a stream of heated drying air in a substantially closed path through the tumbling drum. The drum is journaled upon a combined bearing and air seal means at each end. A heat pump is incorporated as the source of heat for the drying air, as a means for recirculating heat from the drying air exhausted from the tumbling drum, and as a means for removing entrained moisture from the exhausted drying air. The dryer is adapted to operate from a 110 volt household power supply and requires no air vent to the outside.

20 Claims, 26 Drawing Figures

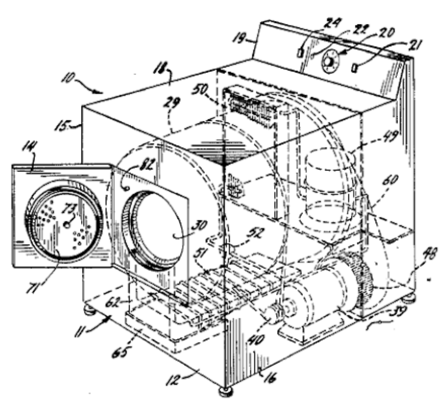

thermoelectric use of air condiitioners for dehumidifier

Abstract

The present invention collects and discharges condensed water from the heat absorbing portion and the heat absorbing portion provided with a heat sink (heat sink) and a heat dissipation fan, respectively, on both sides of the thermoelectric semiconductor element. The dehumidifier is formed by installing the dehumidifier inside the air purifier formed with the air inlet and the air outlet, and the outside air inlet through which the outside air flows into the air purifier case at the rear where the dehumidifier is installed. It can form a purge filter, sterilizer, anion generator to the inside of the outside air inlet to further enhance the air purification effect, such as to remove the moisture more contaminated air more efficiently and at the same time clean and clean It's very groundbreaking.

KR100376384B1
South Korea

Download PDF Find Prior Art Similar

Other languages: Korean

Inventor: 이용락, 허점숙

Worldwide applications

2000 KR

Application KR10-2000-0066982A events

2000-11-11 Application filed by 주식회사 티이솔루션

2000-11-11 Priority to KR10-2000-0066982A

2002-05-17 Publication of KR20020036897A

2003-03-17 Application granted

2003-03-17 Publication of KR100376384B1

Info: Patent citations (5), Cited by (14), Legal events, Similar documents, Priority and Related Applications

External links: Espacenet, Global Dossier, Discuss

Classifications

F24F5/0042 Air-conditioning systems or apparatus not covered by F24F1/00 or F24F3/00, e.g. using solar heat or combined with household units such as an oven or water heater characterised by the application of thermo-electric units or the Peltier effect

View 4 more classifications

Claims (4)

Hide Dependent

1. A heat sink 20 having a heat sink 21 formed on the thermoelectric semiconductor device 1 and a heat dissipation fan 22 on one side thereof, and a cooling sink formed under the thermoelectric semiconductor device 1. (Heat absorbing plate) 11 is provided with a heat absorbing unit 10, a dehumidifying device having a drain 30 for collecting and discharging the water condensed in the heat absorbing unit 10 to the outside, and the dehumidifying apparatus air inlet In the air purifier, characterized in that installed in the air purifier 100 formed so that the 110 and the air outlet 120 is spaced apart from each other,

   An outside air inlet 130 formed on one side of the outside of the air cleaner 100 and introducing the outside into the outside;

   The air purifier having a dehumidification device using a thermoelectric semiconductor element, characterized in that the purification filter 40 is formed inside the external air inlet 130.

   2. The method of claim 1,

      An air purifier having a dehumidification device using a thermoelectric semiconductor element, characterized in that comprises a sterilizing device (50) inside the outer air inlet (130).

3. delete

   4. The method of claim 1,

      An air purifier having a dehumidification apparatus using a thermoelectric semiconductor element, characterized in that comprising an anion generator (60) inside the outside air inlet (130).

Description

Thermoelectric use of air condiitioners for dehumidifier

The present invention is directed to an air purifier having a dehumidification device using a thermoelectric semiconductor element that the absorption and heat generation phenomenon occurs at both ends of the device by the Peltier effect when a direct current flows to the module consisting of different N-type and P-type semiconductor elements More specifically, the heat collecting portion having a heat sink (heat sink) and a heat dissipation fan on both sides of the thermoelectric semiconductor element, and the heat absorbing portion having a cooling sink (heat sink) and the water condensed in the heat absorbing portion are collected. The dehumidifier is installed in the electronic air purifier, and the polluted indoor air containing much moisture is introduced into the air purifier to remove moisture and to purify the water.

US 20050044744A1

(19) **United States**

(12) **Patent Application Publication** (10) **Pub. No.: US 2005/0044744 A1**

Tadano et al. (43) **Pub. Date: Mar. 3, 2005**

(54) **DRYING APPARATUS**

(76) Inventors: **Masaya Tadano**, Nitta-gun (JP); **Shinichi Akiyama**, Otsu-shi (JP); **Nobuo Koumoto**, Otsu-shi (JP); **Toru Kawabata**, Ora-gun (JP); **Ryoko Kubo**, Ora-gun (JP); **Hiroshi Mukaiyama**, Ora-gun (JP); **Kazuyoshi Tomochika**, Ora-gun (JP); **Koji Ono**, Ora-gun (JP)

Correspondence Address:
MCDERMOTT WILL & EMERY LLP
600 13th Street, N.W.
Washington, DC 20005-3096 (US)

(21) Appl. No.: **10/911,651**

(22) Filed: **Aug. 5, 2004**

(30) **Foreign Application Priority Data**

Aug. 7, 2003 (JP) .... JP 2003-288903
Sep. 29, 2003 (JP) .... JP 2003-337620
Sep. 29, 2003 (JP) .... JP 2003-337631

Publication Classification

(51) **Int. Cl.**[7] **F26B 3/00**
(52) **U.S. Cl.** **34/596**

(57) **ABSTRACT**

A drying apparatus having a purpose of shortening a drying time of laundry, comprising an accommodating chamber in which the laundry is accommodated, and executing a washing operation of the laundry and a drying operation after end of the washing operation in the accommodating chamber, the machine comprising: a refrigerant circuit in which a compressor, a gas cooler, an expansion valve, and an evaporator are successively connected to one another in an annular form via a piping; an air circulation path for discharging air which has exchanged heat with the gas cooler into the accommodating chamber by a blower to exchange the heat of the air passed through the accommodating chamber with the evaporator; and a control device for operating the compressor and the blower to perform the drying operation, wherein the control device starts the operation of the compressor before entering the drying operation.

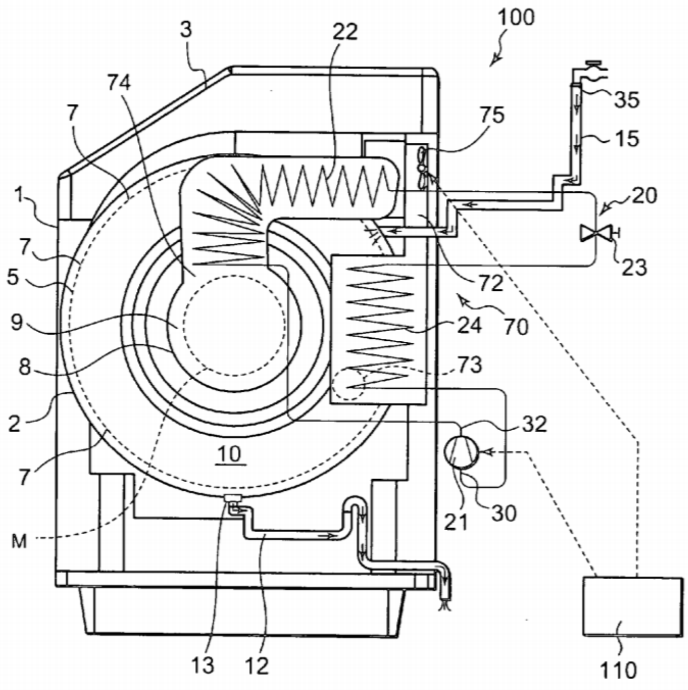

US007526879B2

(12) **United States Patent**
Bae et al.

(10) **Patent No.: US 7,526,879 B2**
(45) **Date of Patent: May 5, 2009**

(54) **DRUM WASHING MACHINE AND CLOTHES DRYER USING PELTIER THERMOELECTRIC MODULE**

(75) Inventors: **Sun Cheol Bae**, Masan-si (KR); **Ja In Koo**, Changwon-si (KR); **Jin Seok Hu**, Masan-si (KR); **Yang Hwan Kim**, Busan (KR)

(73) Assignee: **LG Electronics Inc.**, Seoul (KR)

(*) Notice: Subject to any disclaimer, the term of this patent is extended or adjusted under 35 U.S.C. 154(b) by 217 days.

(21) Appl. No.: **11/591,471**

(22) Filed: **Nov. 2, 2006**

(65) **Prior Publication Data**

US 2007/0101602 A1 May 10, 2007

(30) **Foreign Application Priority Data**

Nov. 4, 2005 (KR) 10-2005-0105595
Nov. 4, 2005 (KR) 10-2005-0105596

(51) **Int. Cl.**
F26B 21/06 (2006.01)

(52) **U.S. Cl.** **34/596**; 34/601; 34/602; 34/239

(58) **Field of Classification Search** 34/90, 34/601, 602, 239, 242, 275, 596; 68/139, 68/142; 134/26, 30
See application file for complete search history.

(56) **References Cited**

U.S. PATENT DOCUMENTS

2,660,806 A * 12/1953 Whitesel 34/77
2,676,418 A * 4/1954 Shewmon 34/77
2,779,172 A * 1/1957 Lindenblad 62/3.4
2,886,618 A * 5/1959 Goldsmid 136/204
3,036,383 A * 5/1962 Edwards 34/76
4,413,425 A * 11/1983 Candor 34/251
4,516,331 A * 5/1985 Yamauchi et al. 34/77
4,621,438 A * 11/1986 Lanciaux 34/77
5,315,765 A * 5/1994 Holst et al. 34/260
5,343,632 A * 9/1994 Dinh 34/507
5,353,519 A * 10/1994 Kanamaru et al. 34/92
5,724,750 A * 3/1998 Burress 34/267
6,088,932 A * 7/2000 Adamski et al. 34/274
6,324,771 B1 * 12/2001 McAllister et al. 34/595
6,418,728 B1 * 7/2002 Monroe 62/3.2
6,877,248 B1 * 4/2005 Cross et al. 34/275
7,222,439 B2 * 5/2007 Paintner 34/73
2004/0117919 A1 * 6/2004 Conrad et al. 8/137
2006/0137214 A1 * 6/2006 Achenbach 34/468
2006/0168840 A1 * 8/2006 Paintner 34/131
2006/0225468 A1 * 10/2006 Hong 68/20
2008/0078099 A1 * 4/2008 Schulz et al. 34/470
2008/0206455 A1 * 8/2008 Sonobe et al. 427/162

* cited by examiner

Primary Examiner—S. Gravini
(74) *Attorney, Agent, or Firm*—Birch, Stewart, Kolasch & Birch, LLP

(57) **ABSTRACT**

A drum washing machine and a clothes dryer equipped with a thermoelectric module are disclosed. The thermoelectric module includes a heat absorption side and a heat dissipation side which absorbs and dissipates heat at a junction between two dissimilar metals depending on direction of current flow through the junction. The heat absorption side is disposed at a hot air flowing passage. Accordingly, the drying apparatus can increase energy efficiency with minor structural modification and becomes environmentally friendly unlike a conventional drying apparatus using a heat pump.

10 Claims, 10 Drawing Sheets

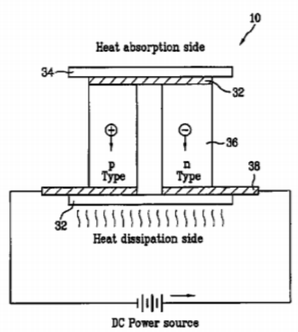

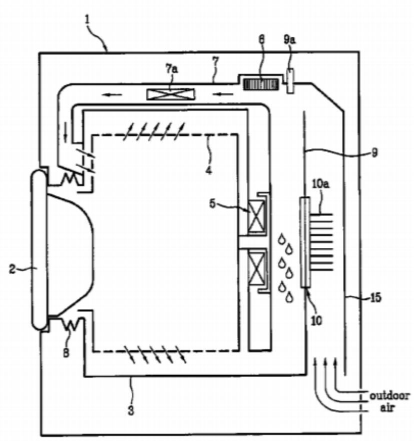

Appendix F: SDC Slides

SANTA CLARA UNIVERSITY
School of Engineering

The Drier Dryer

The Dry Guys:
Josh Sunada, Daniel Anderson, Justin Lee, Thomas Morey
Mechanical Engineering Department
Advisor: Dr. Hohyun Lee

Santa Clara University

Clothes Dryer Background

- Hot and humid areas suffer extended drying times
- Reduce cycle time by dehumidifying incoming dryer air

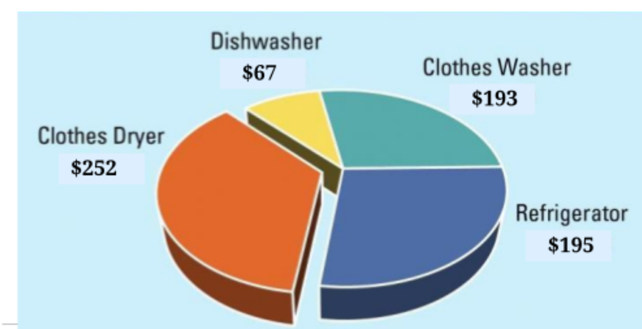

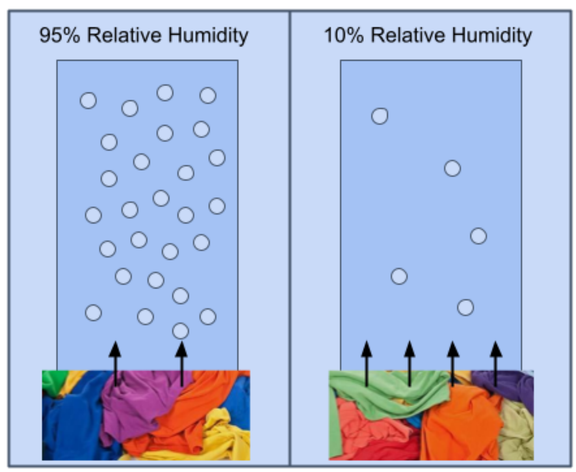

*Cost based on average Hilo, Hi electricity rate in 2020, $0.3276/kWh

Santa Clara University

Project Goals

- Reduce temperature to remove humidity
- Provide ~9¢ savings per dryer cycle
- Cost-effective to run at 1.85 kPa vapor pressure

Santa Clara University

Moisture and Cooling Requirements

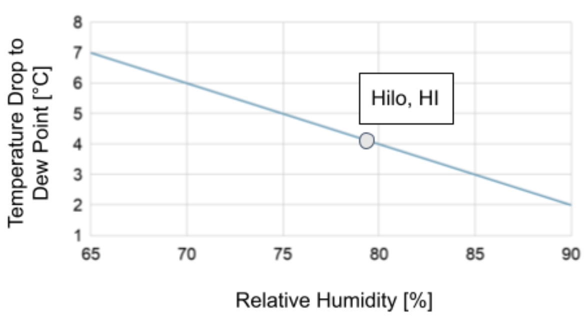

- The required temperature drop depends on relative humidity
- In Hilo, HI a 4°C temperature drop is required
- Implement a thermoelectric module (TEC)

Santa Clara University

Peltier Cooler

- Voltage creates a temperature difference
- Hot side dissipation
- Rejects and absorbs heat

(https://protosupplies.com/product/tec1-12706-thermoelectric-peltier-cooling-device/)

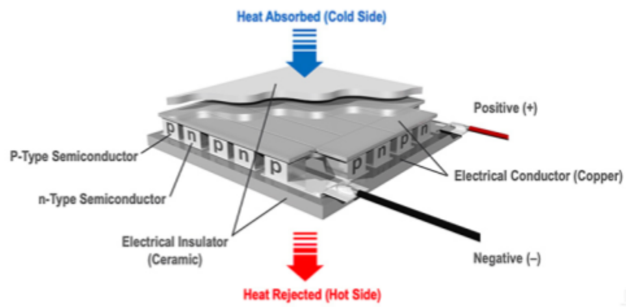

(https://www.medicaldesignandoutsourcing.com/thermoelectric-cooler-solutions-for-medical-applications/)

Santa Clara University

Design Approach - Peltier Module

- Two heat sinks for air to flow through
- Dehumidify incoming air
- Find ideal voltage for cooler

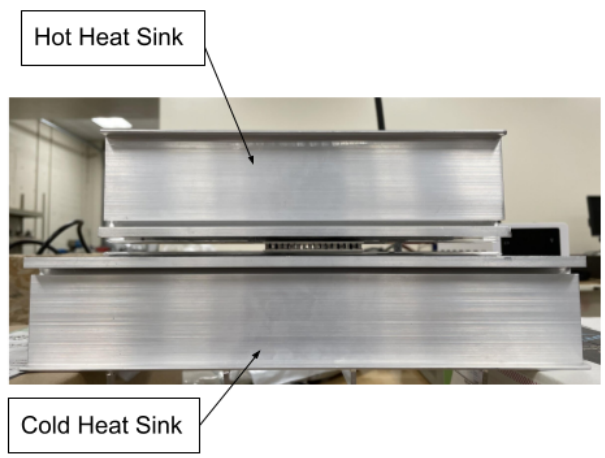

Santa Clara University

Attachment Design - Subsystems

Subsystems:

1) Heating module
2) Water collection system
3) Dryer attachment system

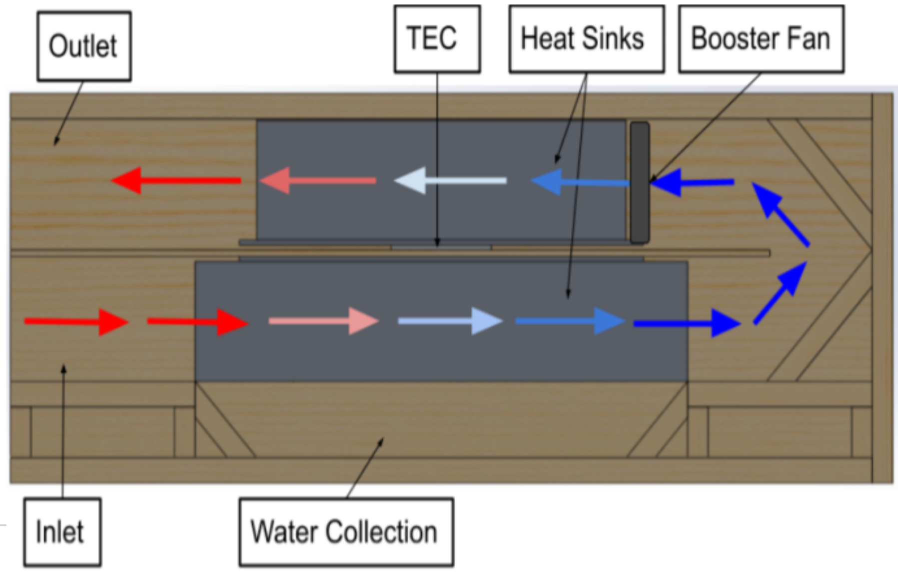

Projected Savings - Overview

- "Efficiency" measured by money savings
- Efficiency increase is proportional to vapor pressure difference
- Net savings graphs produced for various scenarios

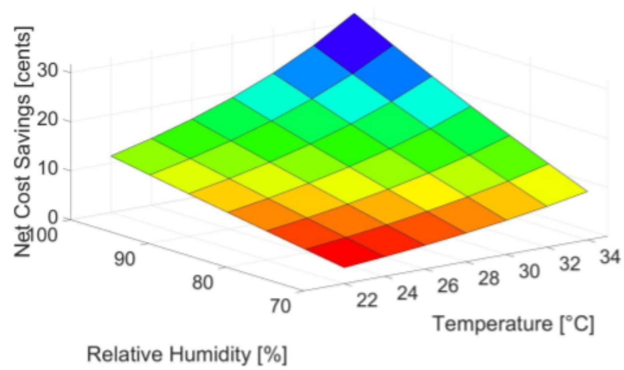

Santa Clara University

Projected Savings - Various Conditions

Note: Hawaii cost of electricity used for calculations (32.76¢ per kWh)

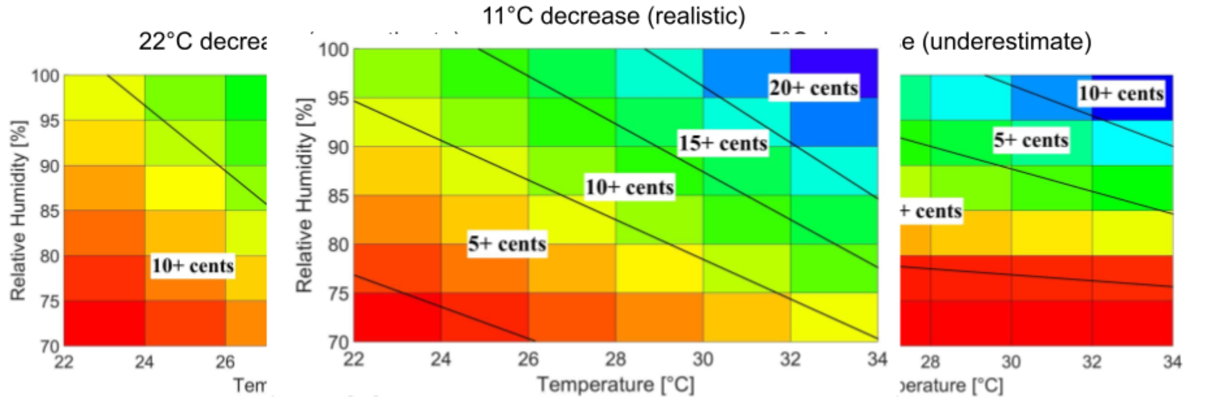

Santa Clara University

Prototype Construction

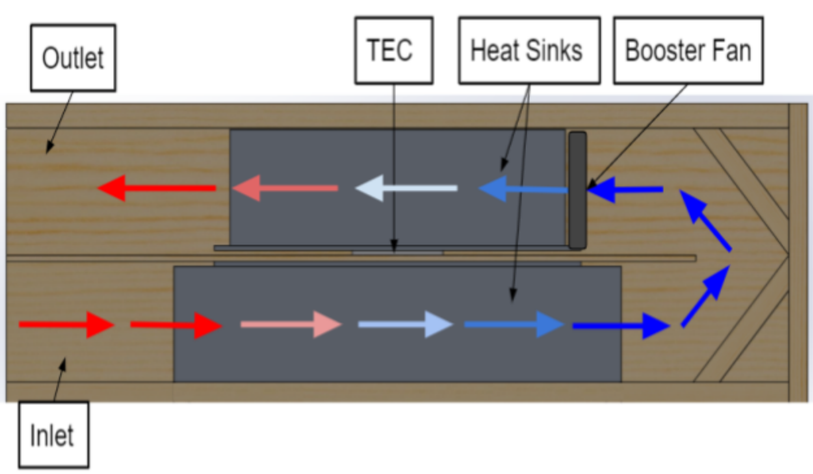

Testing Setup

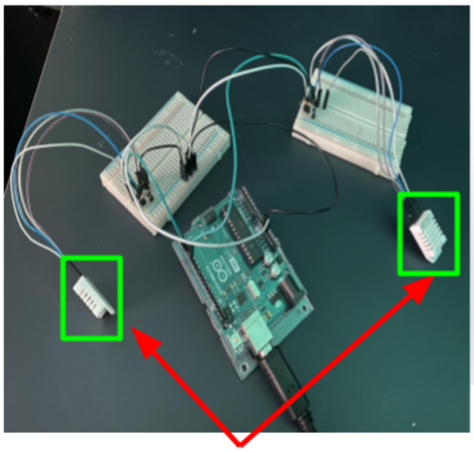

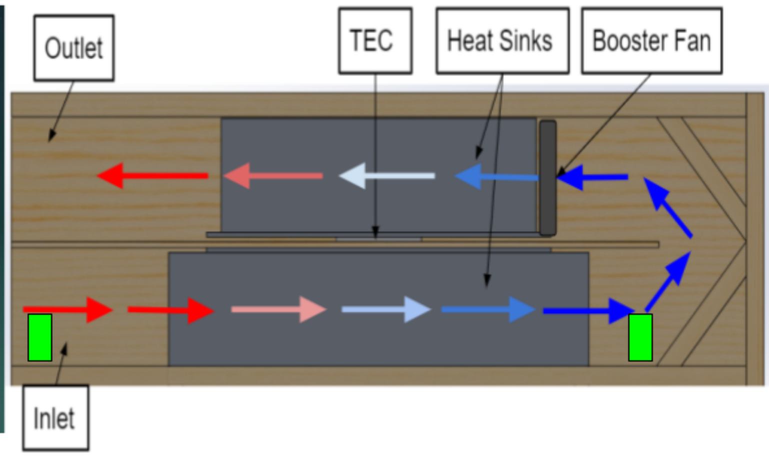

DHT22 temperature and humidity sensors

Santa Clara University

First Prototype Test Results

- Air cooled by 2 °C
- No moisture removed
- Poor ventilation, both heat sinks are warmer than expected.

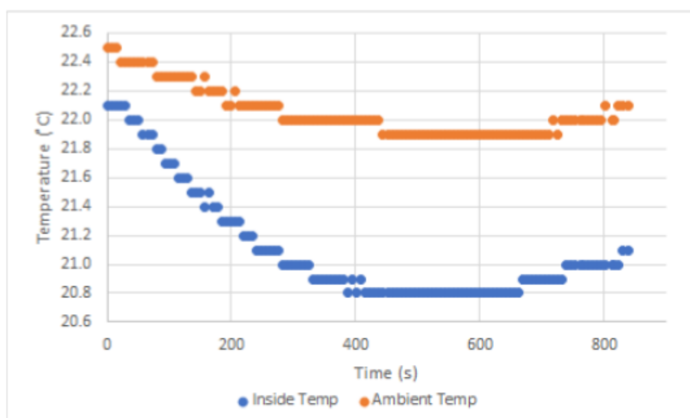

Santa Clara University

COMSOL Simulations

Feature	Heat Ratio [%]
Control	0
Flange Constriction	12
Heat Pipes	47
2 TECs	8
Flange Constriction, Heat Pipes	88
Flange Constriction, Heat Pipes, Baffle	248

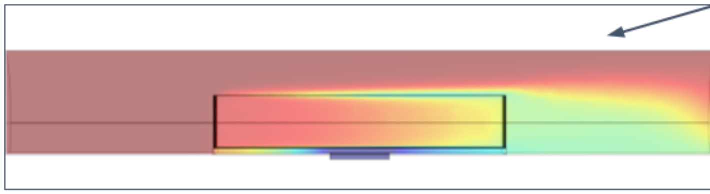

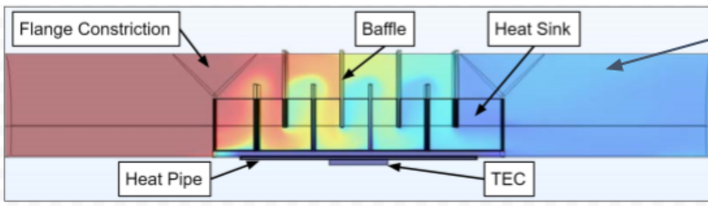

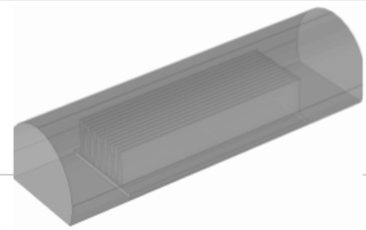

Final Design Changes

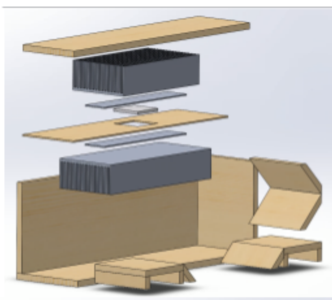

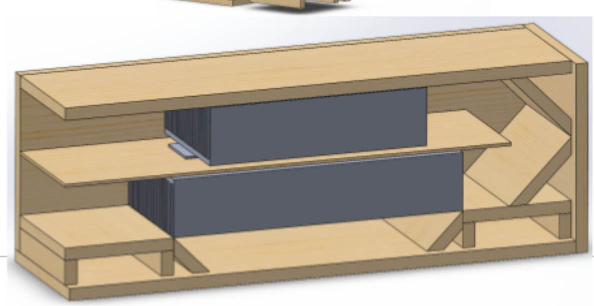

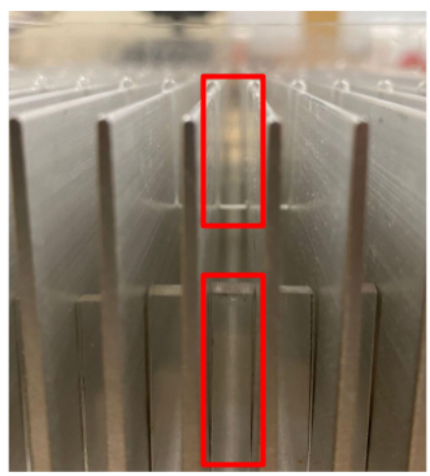

Santa Clara University

Budget

- Budget of $2000
- Manufacturing cost ~$165 if mass-produced
- Testing material costs

Prototype Materials

Category	Description	Original Cost	Bulk Cost
Housing	Wood	$ 9.20	$ 9.20
	Water Collection Tray	$ 1.89	$ 1.89
	Misc. (screws, glue, thermal paste)	$ 10.00	$ 10.00
Heating Module	Moisture Fabric and Insulation	$ 10.00	$ 10.00
	TEC	$ 85.11	$ 57.15
	Heat Sinks (2)	$ 169.68	$ 10.00
	Heat Pipes (2)	$ 107.35	$ 67.22
	TOTAL	$ 393.23	$ 165.46

Santa Clara University

Future Plans

- Improve TEC performance and airflow and begin testing with dryer
- If successful, submit patent and market product

Santa Clara University

Acknowledgements

The Dry Guys would like to thank the following for their selfless assistance to our project:

- Santa Clara University
- Professor Rodney Broome
- Matthew Blanco & Beverly Dutra
- Anne Hunter
- Dr. Timothy Hight, Dr. Tony Restivo, Dr. Vlad Ivashyn

Santa Clara University

Appendix G: Full Purchase List

Category	Description	Cost	Date of Purchase
Prototype Material	Heat Sinks	$169.68	1/11/2021
	Peltier Cooler	$85.11	3/1/2021
	Wood	$40.47	3/3/2021
	Construction Screws	$8.68	3/3/2021
	Thermal Paste	$39.85	1/19/2021
	Heat Pipes	$107.35	2/3/2021
	Wicking Fabric	$14.97	3/1/2021
	Wood Glue	$10.99	4/7/2021
Testing Material	Peltier Coolers (5)	$372.46	1/27/2021-4/28/2021
	Anemometer+Batteries	$23.80	10/19/2020-4/7/2021
	Probe Thermometer 1	$21.77	10/17/2020
	Probe Thermometer 2	$15.10	3/16/2021
	DC Power Supply	$59.94	1/13/2021
	Tempi.fi Humidity Sensor	$43.59	11/8/2020
	Small Booster Fans	$32.35	4/7/2021-4/23/2021
	Humidifier	$49.99	1/8/2021
	Large Booster Fan	$32.99	1/13/2021
	Arduino Board +DHT22 sensors+batteries and wiring	$138.76	2/1/2021-2/26/2021
Construction Material	4 in. x 8 ft. Flexible Duct	$10.84	11/7/2021
	6 in. x 8 ft. Semi-Rigid Flexible Duct	$15.66	11/21/2021
	Wire Kit	$14.49	1/8/2021

	Insulation Material	$11.82	3/3/2021
	Foil Seal	$27.22	3/3/2021
	6 in. x 25 ft, Flexible Aluminum Foil Duct	$24.86	1/16/2021
	Craft Magnets	$5.99	3/1/2021
	Plastic Water Tray	$1.87	3/16/2021

Appendix H: SCU Frugal House Dryer Pictures

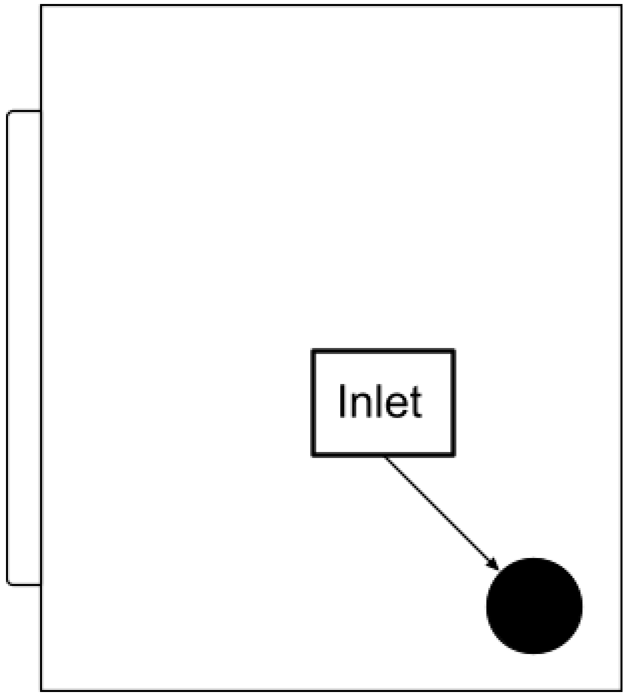

Figure H.1: Sketch of the side of the dryer (both sides).

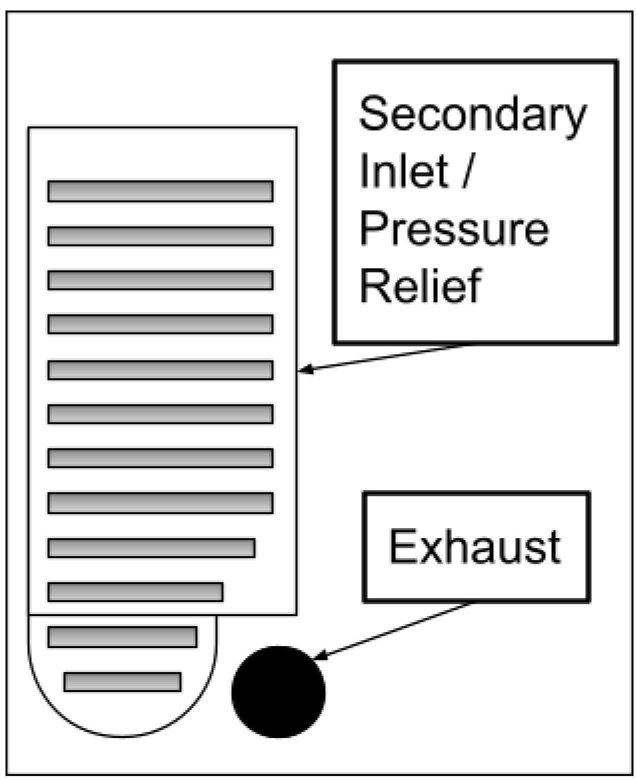

Figure H.2: Sketch of the back of the dryer.

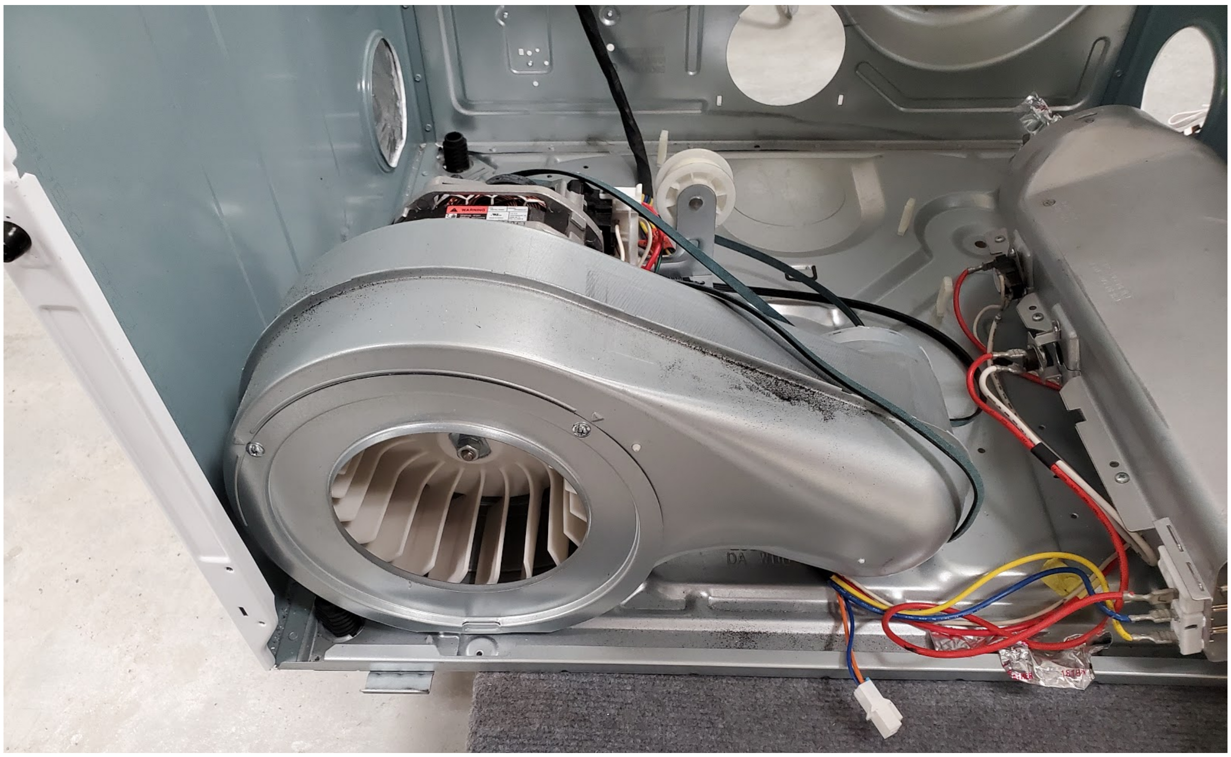

Figure H.3: Built-in dryer fan.

Figure H.4: Built-in dryer heater.

Figure H.5: Exterior side view.

Figure H.6: Front view and tumbler band.

Figure H.7: Front wiring.